JUSTUS-LIEBIG-UNIVERSITÄT GIESSEN

Justus Liebig University Giessen

MTA2/NuRD as a Regulator of NF-ƙB Signalling in Lung Cancer Progression

Inaugural Dissertation
submitted to the
Faculty of Veterinary Medicine or Faculty of Medicine
in partial fulfilment of the requirements
for the PhD-Degree
of the Faculties of Veterinary Medicine and Medicine
of the Justus Liebig University Giessen

by

Nefertiti El-Nikhely

of

Alexandria, Egypt

Giessen 2016

From **Max Planck Institute for Heart and Lung Research**
Department of Lung Development and Remodelling

Director/Chairman: Prof. Dr. med. Werner Seeger

First Supervisor and Committee Member: Prof. Dr. med. Werner Seeger
Co-Supervisor and Committee Member: Prof. Dr. Reinhard Dammann
Date of Doctoral Defence: 01.02.2017

Dedication

To my mom & To my dad

To whom I owe everything I am or ever will be.

Table of contents

Table of contents

List of Figures

Table of contents

List of Tables

List of Abbreviations

ADC	Adenocarcinoma
ATII	Alveolar type II cells
ATM kinase	ataxia telangiectasia mutated kinase
BADJ	Bronchioalveolar duct junction
BAH	Bromo-adjacent homology
BASCs	Bronchioalveolar stem cells
BSA	Bovine serum albumin
C/EBP	CCAAT/enhancer binding protein
CBP	CREB binding protein
CC	Coiled coil
CCSP	Clara cells specific cell marker protein
CHD4	Chromodomain-helicase-DNA-binding protein
DAPI	4',6-diamidino-2-phenylindole
DDB2	Damaged DNA-binding 2 protein
DLBCL	Diffuse large B-cell lymphoma
DTT	Dithiothreitol
EGFR	Epidermal growth factor receptor
ELM	Egl-27/MTA1
EMT	Epithelial-mesenchymal transition
ERK	extracellular signal-regulated kinases (MAPK)
ERα	Oestrogen receptor alpha
G-CSF	Granulocyte colony-stimulating factor
GM-CSF	Granulocyte-macrophage colony-stimulating factor
HCC	Hepatocellular carcinoma
HDAC	Histone deacetylase
HIF1α	Hypoxia-inducible factor 1 alpha
HLH	Helix-loop-helix
HPRT	Hypoxanthine phosphoribosyltransferase1
HRP	Horseradish peroxidase
ICAM	Intracellular adhesion molecule
ICC	Immunocytochemistry
IF	Immunofluorescence
IHC	Immunohistochemistry
IKK	Inhibitor of kappa B kinase
iNOS	Inducible nitric oxide synthase
IPA	Inhibitors of apoptosis
JNK	c-Jun N-terminal kinase
KRT7	Keratin 7
LCLC	Large cell lung cancer
LLC1	Lewis lung carcinoma

LPS	Lipopolysaccharide
LTßR	Lymphotoxin ß-receptor
LZ	Leucine zipper
MALT lymphoma	mucosa-associated lymphoid tissue lymphoma
MBD	Methylated-CpG-binding domain
MCP-1	Monocyte chemotactic protein 1 (CCL2)
MEKK1	Mitogen-activated protein kinase kinase kinase1 (MAP3K1)
MMP	Matrix metalloproteinase
MTA	Metastasis-associated protein
NBD	NEMO binding domain
NEMO	NF-ƙB essential modulator
NF-ƙB	Nuclear factor kappa B
NIK	NF-ƙB inducing kinase
NSCLC	Non-small-cell lung cancer
NuRD complex	Nucleosome and deacetylase remodelling complex
PCNA	Proliferating cell nuclear antigen
PHD	Plant homodomain
PI3K	Phosphoinositide 3-kinase
PKA	Protein kinase A
PKCζ	Protein kinase Cζ
PLA	Proximity ligation assay
PTEN	Phosphatase and Tensin homolog
RAF	Rapidly accelerated fibrosarcoma
RANK	Receptor activator for nuclear factor kappa B
RANTES	Regulated on activation, normal T cell expressed and secreted (CCL5)
RbAp (RBBP)	Retinoblastoma-associated protein (Retinoblastoma binding protein)
RHD	Rel homology domain
ROS	Reactive oxygen species
RSK1	Ribosomal S6 kinase 1
SAHA	Suberoylanilide hydroxamic acid
SANT	Switching defective protein 3, Adaptor 2, nuclear receptor co-repressor, transcription factor III B
SCC	Squamous cell carcinoma
SCID	Severe combined immunodeficiency
SCLC	Small cell lung cancer
SOX2	Sex determining region Y (SYR)-box 2
SPC	Surfactant protein C
STK11	Serine/threonine kinase 11
TAB1	TGF-ß activated kinase (TAK1)
TAD	Transactivation domain

TAK1	TGF-ß activated kinase
TGF-ß	Transforming growth factor beta
T_H	T-helper cells
Timp1	Tissue inhibitor of metalloproteinases 1
TKI	Tyrosine kinase inhibitor
TLR	Toll-like receptor
TNF-α	Tumour necrosis factor alpha
TRAF1	TNF Receptor-Associated Factor 1
TRD	Transcription repression domain
TTF1	Thyroid transcription factor 1
VCAM	Vascular cell adhesion molecule
VEGFR	vascular endothelial growth factor
WHO	World health organization
XIAP	X-linked inhibitor of apoptosis protein
ZF	Zinc fingers

1 Introduction

1.1 Lung Cancer

1.1.1 Statistics

According to the reports of the World Health Organization (WHO), lung cancer is leading the cancer-related death cases worldwide. Out of 8.2 million cancer deaths cases, 12% were related to lung cancer followed by liver and stomach cancer (Fig. 1.1a). Despite the enormous research conducted on lung cancer and the development of new therapies, the 5-year survival is still modest being only 5.8 % for lung cancer compared to 48% for all cancers (Fig. 1.1b)[1]. In women, lung cancer occupies the third place as a common cause of cancer incidence after breast cancer and cervical cancer and second most common cause of cancer mortality. However, in the developed countries there are no differences between both genders[2].

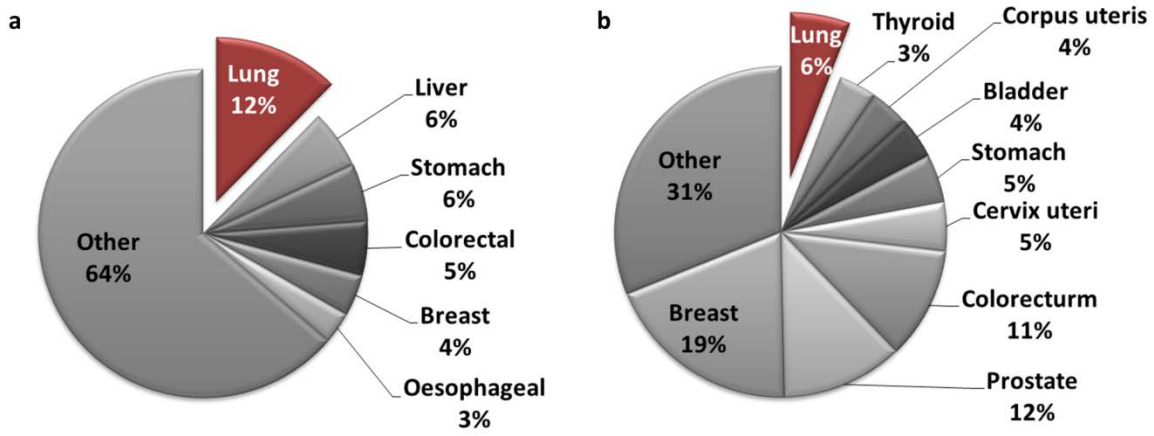

Figure 1.1 Cancer Statistics 2012. Worldwide statistics of both genders representing a) Cancer-related death cases worldwide, b) Percentage of 5-year prevalent adult cancer cases. (Adapted from WHO report, Globocan IARC, 2012)[2].

Differences in incidence, survival and deaths caused by lung cancer vary according to world region, development state, lifestyle, gender and age. Like many other cancer types, lung cancer incidence increases with increasing age probably due to accumulation of mutational changes or environmental hazards. The main challenge of lung cancer is that most cases are presented at advanced at late stage of the disease and therapy often encounters chemoresistance[2].

1.1.2 Classification of lung cancer

For pathological diagnosis, lung cancer is classified via histological and cytological approaches into small cell lung cancer (SCLC) and non-small-cell lung cancer (NSCLC), which is subdivided into adenocarcinoma (ADC), squamous cell carcinoma (SCC) and large cell lung cancer (LCLC). These are the main histologic types of lung cancer but there is continuous debate on better and more detailed classification[3]. Results of several studies the classification of tumours based on their driver mutations and not merely based on their histological types[4]. The importance of a thorough classification of lung cancer relate to the impact of cancer type on choosing the suitable therapy. Where EGFR tyrosine kinase inhibitors (TKIs) or pemetrexed-based therapy regimens are suitable for patients with ADC having EGFR mutation, patients with SCC are not eligible for these therapies[3].

NSCLC accounts for over 85% of all lung cancer cases and is predominantly represented by ADC (about 50%) and SCC (40%). Besides the morphological structure of the tumour specimen, specific biomarkers are used to identify the cancer type. ADC usually has a glandular structure and expresses thyroid transcription factor 1 (TTF1) and keratin 7 (KRT7). On the other hand, SCC expresses cytokeratin 5 and cytokeratin 6 and/or the transcription factors SRY-box 2 (SOX2) and p63[5]. Table 1.1 illustrates main features of ADC and SCC.

Table 1.1 Main characteristics of lung adenocarcinoma and squamous cell carcinoma[6, 7].

	Adenocarcinoma (ADC)	**Squamous Cell Carcinoma (SCC)**
Origin	distal airways, alveolar type II cells	proximal airways in the vicinity of pseudostratified columnar epithelium of tracheal and upper airways
Biomarkers	TTF1 (NKX2-1), KRT7	Cytokeratin 5, Cytokeratin 6, SOX2, p63
Common mutations	*KRAS, BRAF, EGFR, HER2, MET, FGFR1, FGFR2*	*DDR2, FGFR1, FGFR2, FGFR3*, Several genes in PI3K pathway

ADCs originate from secretory alveolar type II (ATII) cells and thus develop in distal airways, whereas SCCs form in proximal airways in the trachea and upper bronchial epithelium. SCLC on the other hand arises from neuroendocrine cells and is considered the most aggressive form[6]. The cell of origin of lung cancer assumingly determines the tumour type, at least from studies in murine models with specific genetic alterations in respective

cells[8]. Cancer-initiating cells often known as cancer stem cells were identified in the lung in the bronchioalveolar duct junction (BADJ). This region harbours a cell population expressing both Clara cell marker (CCSP) and ATII cell marker, surfactant protein C (SPC), along with possessing stem cell markers like Sca-1 and CD34. They were termed BASCs, bronchioalveolar stem cells[8]. Recently, Xu *et al.* provided evidence that ATII cells are the cell of origin of lung adenocarcinoma using a mouse model with K-Ras mutation[9].

With increasing data on the molecular changes identified within resected tumour samples, many studies plead for the integration of genomic information into cancer classification, especially for the metastatic cancers of unknown primary origin[10].

1.1.3 Aetiology of lung cancer

The lung is a unique organ with multicellular diversity making lung cancer a multifaceted disease. Several environmental factors were reported to affect the incidence of lung cancer including air pollution and occupational hazards. Cigarette smoke is on the top of this list and was reported in correlation with SCC rather than ADC. However, 10% of lung cancer cases occur in patients with no smoking history[11]. This indicates that there are other predispositions for lung cancer development.

Increasing evidence support the impact of genetic susceptibility on increasing cancer risk. Compared to many cancer types, lung cancer was reported to show high mutational burden assumingly due to exposure to carcinogens as air pollutant and cigarette smoke[7]. Nevertheless, ADC patients with no smoking history often show mutations of EGFR gene and thus respond to TKIs though they develop resistance. On the other hand, smokers frequently develop *KRAS* mutations and do not respond to TKI therapy. In a genome-wide study on 188 primary lung ADC samples, a set of 26 genes was identified with a high rate of mutations in tumour suppressor genes (*TP53*, *CDKN2A*, and *STK11*) as well as known oncogenes (*KRAS*, *EGFR* and *NRAS*). It is worth mentioning that EGFR and KRAS mutations were mutually exclusive[12].

1.1.4 Oncogenes *KRAS* and *C-RAF*

KRAS mutations were detected in about 30% of ADC cases[13]. Most mutations of *KRAS* identified in smokers are transversions (G →T or G→ C) in a single amino acid in codon 12. KRAS belongs to the RAS oncogene family together with HRAS and NRAS, which are small GTPases serving in the mitogenic cascade (Fig. 1.2). The signalling is then mediated through a series of kinases forming the RAF/MEK/ERK cascade[14]. An interesting study conducted by Blasco *et al*. using *K-Ras*$^{+/G12V}$ mice concluded that the elimination of both Erk1 and Erk2 is required to block tumour development, whereas deletion of B-Raf showed no significant effects on tumour development. Instead, C-Raf expression was essential to mediate K-Ras signalling and form tumours[15].

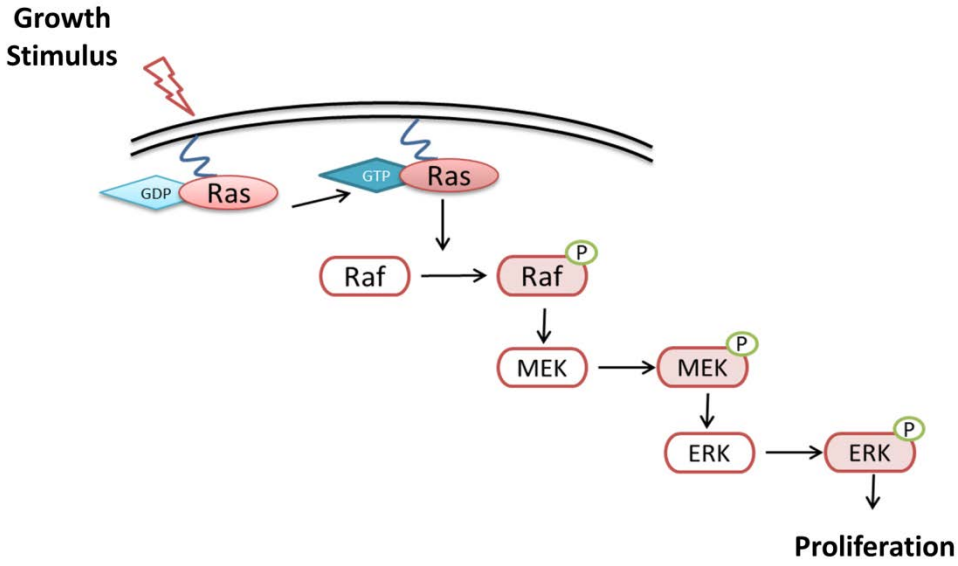

Figure 1.2 RAF signalling pathway. Schematic representation of the Raf signalling through the extracellular signal-regulated kinase (ERK)/mitogen-activated protein kinase (MAPK) cascade. Growth stimuli to the cell activate Ras protein which then activates C-RAF inducing sequential downstream phosphorylation steps. At the end of the cascade phosphorylated ERK can phosphorylate both nuclear and cytosolic targets resulting in proliferation (Adapted from Meister *et al*., 2013)[14].

More than two decades ago Rapp and colleagues identified C-RAF as the mammalian homologue of v-raf oncogene[16]. The name RAF derives from the ability of the viral homologue to induce rapidly accelerated fibrosarcomas in mice[17]. Several studies followed showing the role of C-RAF in lung development and carcinogenesis. Though activation mutations in C-RAF were reported, e.g. E478K, S427G and I448V, their significance still has to be established as they were rarely reported in human cancers. However, targeting C-Raf

overexpression in the lung demonstrated transforming potential. Rapp *et al*. established a lung tumour mouse model with constitutively active C-RAF, termed C-Raf BxB. These mice developed benign adenomas in the lung though no metastasis was detected[18].

Sorafenib is a C-Raf kinase inhibitor that acts on wildtype C-Raf and B-Raf as well as on oncogenically activated B-Raf kinases. In addition to its antiproliferative effects, like many kinase inhibitors, sorafenib had several off target effects. Its anti-angiogenesis activity was shown to be stronger acting through the inhibition of VEGFR kinases. Furthermore, sorafenib increased apoptosis in preclinical models of hepatocellular carcinoma (HCC) and was later used clinically in a phase III trial in both HCC and renal cell carcinoma[19]. In NSCLC, sorafenib showed anti-tumour activity but was suggested only for treatment of a subset of patients and in conjunction with other inhibitors[20].

As C-Raf is relatively on the top of the mitogenic cascade it can affect many downstream signalling pathways. NF-ƙB signalling was found to be activated indirectly by C-Raf through MEKK1 which goes in line with the increased inflammatory signals observed in many cancers[21].

1.2 NF-ƙB signalling pathways & the role in cancer

1.2.1 The transcription factor family NF-ƙB

Nuclear Factor-ƙB was first discovered in 1986 by Sen and Baltimore as DNA-binding protein in B cells[22]. It was first thought to play a role only as a regulator of ƙB light chain expression. Meanwhile, intense research showed that NF-ƙB is expressed ubiquitously in almost all cell types and that it is a pleiotropic transcription factor having its specific NF-ƙB binding sites at the promoters of a wide range of genes[23, 24].

In mammals, NF-ƙB transcription factor family consists of five proteins which form various combinations of homo- and heterodimers with each other. They all share a conserved 300 amino acids long Rel homology domain (RHD) at their amino terminal. RHD is required for their dimerization, nuclear translocation, DNA binding and interaction with IƙB proteins. The carboxyl end of the RHD is thought to be responsible for dimerization and interaction with IƙBs, whereas its amino terminal part facilitates the binding of NF-ƙB transcription factors to specific NF-ƙB consensus sequence (5'-GGGpuNNPyPyCC-3') present in the promoter region of various regulated genes[25].

Three members of the family, RelA (p65), RelB and c-Rel (also known as Rel), have a transactivation domain (TAD) at their carboxyl terminal. The other two members, p105 (NF-ƙB1) and p100 (NF-ƙB2), lack such domain but instead have a sequence of 5-7 ankyrin repeat motifs at their carboxyl terminal. They are precursors for p50 and p52, respectively, which can bind actively to the DNA. Due the presence of ankyrin repeat motifs, p100 and p105 are also considered inhibitors of ƙBs as they block the interaction with the DNA (Fig. 1.3a).

NF-ƙB activation is a relatively rapid process, as in the unstimulated state, the transcription factor dimers are sequestered in the cytoplasm being bound to IƙB proteins. IƙBs are a family of 5 members, with IƙBα, IƙBβ and IƙBε being the most studied members. The C-terminal portions of p105 and p100 were historically termed IƙBγ and IkBδ, respectively. BCL-3 is an unconventional IƙB protein as it contains a transactivation domain to interact with the DNA and mediate transcriptional activity[26]. It was reported that IƙB proteins suppress NF-ƙB activity not just by masking the nuclear localization signal (NLS) and preventing binding to the DNA but also by facilitating the nuclear export of NF-ƙB active dimers[26, 27].

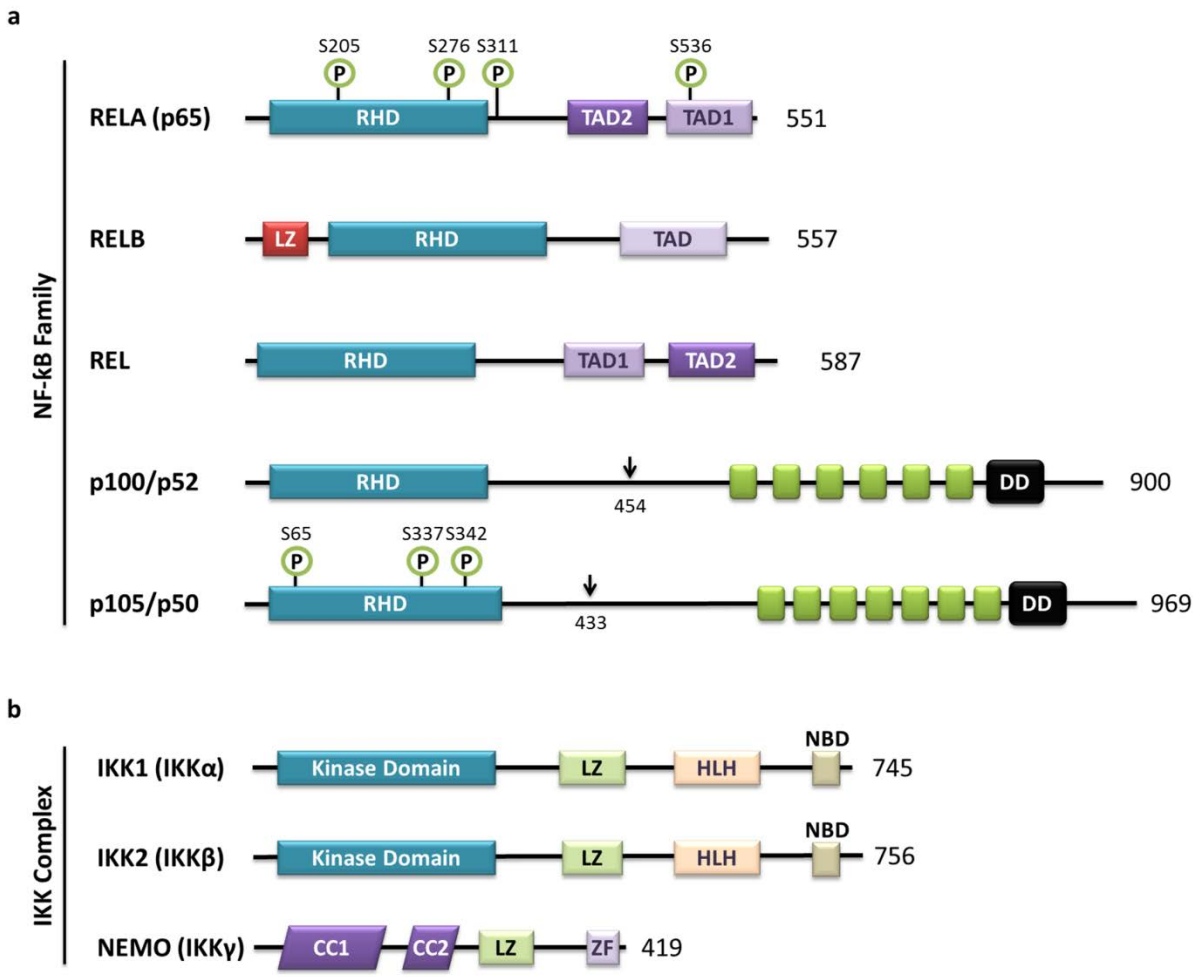

Figure 1.3 Members of the NF-kB transcription factor family. a) NF-kB subunits, RELA (p65), RELB and REL have rel homology domains (RHD) at the N-terminal which is important for dimerization and DNA binding. At the C-terminal transactivation domains (TAD) mediate transcriptional activity. NF-kB1 (p105) and NF-kB2 (p100) possess only RHD in addition to Ankyrin repeats (green boxes) that allow their function as IkB proteins. p105 and p100 are proteolytically processed (at black arrow) to generate p50 and p52, respectively. Main phosphorylation sites of RelA (p65) and p50 are indicated by a green circle with P. b) IKK complex consists of IKK1 and IKK2 with kinase domain whereas NEMO lacks enzymatic activity. They interact with NEMO via their NBD (NEMO binding domain. LZ (leucine zipper); HLH (helis-loop-helix); CC (Coiled coil); ZF (zinc finger). (Adapted from Oeckinghaus and Ghosh[25], Perkins[28] and Hoesel and Schmid[26]).

Within this transcriptional system different NF-kB members show specificity by preferential binding to specific DNA-binding consensus sequences as summarized in Table 1.2[29]. Hence, distinct dimers can activate certain target genes. This preferential control is also stimulus dependent and activates different signalling pathways.

Table 1.2 NF-ƙB subunits and their binding sites [30, 31]

NF-ƙB subunit	DNA-binding consensus sequence
General	5'-GGGpuNNPyPyCC-3' or 5'- GGG-ATTTCC-3'
RelA/p65	GGGGTATTTCCC
p50	GGG-AT--CCC
c-Rel	GGGGTATTTCC
RelB	GGGGTATTTCC
p52	GGGGTATTTCC

1.2.2 Canonical and non-canonical pathways

Activation of NF-ƙB is mediated by inhibitory ƙB kinases (IKKs), IKK1 and IKK2 also known as IKKα and IKKβ, respectively. IKKγ is a regulatory subunit commonly known as NEMO (NF-ƙB essential modulator) which lacks kinase activity but is required for the formation of the complex. The kinases IKK1 and IKK2 contain a kinase domain at the amino terminal, a leucine zipper to allow dimerization of the kinases and helix-loop-helix domain supporting the kinase activity (Fig 1.3b). The complex is activated by phosphorylation at two serine residues; Ser177 and Ser181 for IKK2 and Ser176 and Ser180 for IKK1. Several upstream kinases can activate the IKK complex, e.g. NIK (NF-ƙB inducing kinase), TAK1 (TGFβ-activating kinase 1), MEKK1 and MEKK3. In addition, mutual autophosphorylation within the IKK dimers can be initiated in response to stimulus or proximity-induced conformational changes mediated by NEMO[32].

The canonical NF-ƙB signalling pathway is triggered by inflammatory cytokines, e.g. TNFα, pathogen-associated molecules, e.g. LPS, antigen receptors, and Toll-like receptors (TLRs). The trimeric complex of IKK1, IKK2 and NEMO phosphorylates IƙBα so that ubiquitin binds to the inhibitor and is degraded by the proteosomal machinery freeing p50/p65 for nuclear translocation. On the other hand, the non-canonical or alternative NF-ƙB activation pathway is activated by other receptors including lymphotoxin β-receptor (LTβR), receptor activator for nuclear factor kappa B (RANK) and CD40. This activation is mediated via NIK which mainly phosphorylates IKK1 dimer. Subsequently, p100 is either partially digested into p52 or ubiquitinated for degradation. Generation of p52 often encourages the dimerization with RelB to target a distinct set of genes (Fig. 1.4). Finally, atypical activation pathways exist

in response to genotoxic stress where ATM kinase activates IKK complex leading to the ubiquitination of NEMO[26].

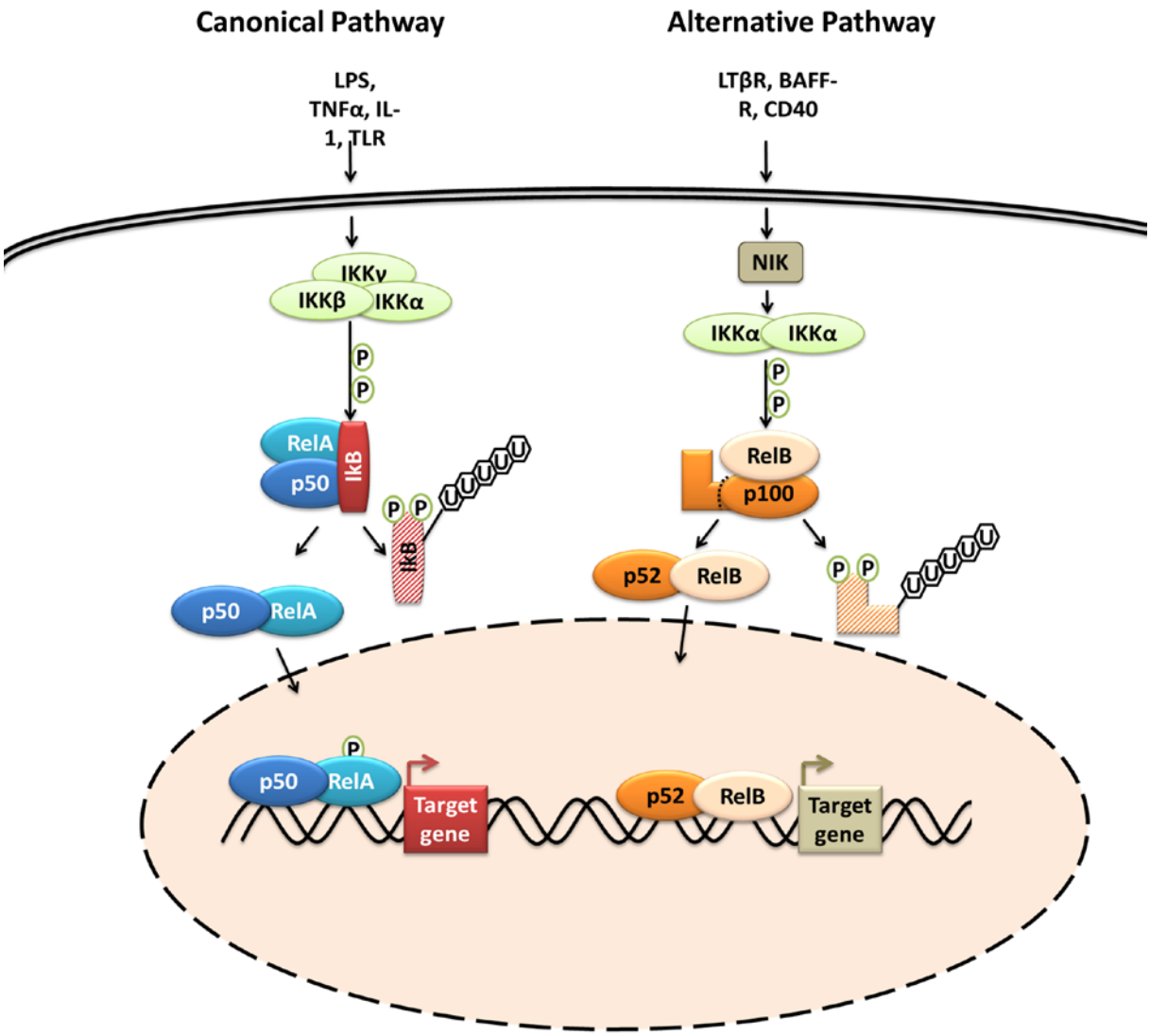

Figure 1.4 NF-ƙB signalling pathways. In the canonical pathway, stimuli lead to the phosphorylation of IKK complex which phosphorylated IƙBα. This is followed by ubiquitin mediated degradation of IƙB and release of p50/RelA to translocate to the nucleus. In the non-canonical alternative pathway, IKK1 dimer is phosphorylated by NIK and consequently phosphorylates p100 to be partially proteasomally degraded releasing p52/RelB to the nucleus. (Adapted from Jost *et al.*, 2007)[33].

1.2.3 Posttranslational modifications of NF-ƙB subunits

Owing to its seminal role in various biological processes, NF-ƙB is tightly regulated at different levels. Besides the regulatory IƙB proteins, NF-ƙB subunits themselves are directly regulated by posttranslational modifications. Phosphorylation of RelA/p65 was reported both in the RHD at five sites (Ser205, Thr254, Ser276, Ser281, and Ser311) as well as in the TAD at seven residues (Thr435, Ser468, Thr505, Ser529, Ser535, Ser536, and Ser547)[34]. Depending on the stimulus and modification site, NF-ƙB transcriptional activity is regulated by a different mechanism. The p50 subunit also undergoes posttranslational modifications. Hou *et al.* identified three serine residues (Ser65, Ser337, and Ser342) in the RHD that are phosphorylated to regulate the ability of p50 to bind to the DNA[35]. Table 1.3 summarizes the role of the main modifications on p50 and RelA/p65.

Table 1.3 Main posttranslational modifications of NF-kB subunits and their significance

NF-kB subunit	Site/Location	Mediated by	Effect	Reference
RelA/p65				
Phosphorylation	S205, S281/RHD	Several kinases	• Regulate subcellular localization • Not required for IκBα binding	Hochrainer *et al*., 2007[36]
	S276/RHD	Protein kinase A, MSK1	• Critical for the interaction with c-activators • PKA phosphorylation enhances recruitment of p300 and CBP • Decreases HDAC1 affinity for p65	Yang et al., 2003[37]
	S311/RHD vicinity	Protein kinase Cζ (PKCζ)	• Essential for the interaction with CBP • Needed for the recruitment of RNA polymerase II to target gene promoters • Mediated by TNFα	Duran, *et al.*, 2003[38] Hochrainer *et al*., 2013[34]
	S529/TAD	Casein kinase II		Yang et al., 2003[37]
	S536/TAD	IKK2, TAK1-TAB1	Increases interaction with p300 for acetylation at K310	Yang et al., 2003[37]
		Ribosomal S6 kinase 1 (RSK1)	Stimulated by p53	Bohuslav *et al.*, 2004[39]
Acetylation	K122, K123		Reduce DNA binding but facilitate p65-IκBα interaction	Hochrainer *et al*., 2007[36]
	K218, K221	p300 & deacetylated by HDAC3	• They impair p65-IκBα interaction and thus nuclear export • HDAC3 terminates NF-κB and allows nuclear export of p65-IκBα	
p50				
Phosphorylation	S20	DNA-dependent protein kinase	Increases DNA binding as seen on *VCAM1* promoter	Ju *et al.*, 2010[40]
	S65, S337, S342	Protein kinase A	Increases DNA binding but doesn't affect dimerization	Hou *et al.*, 2003[35]
Acetylation				
	K431, K440, K441	p300	Potentiates interaction of p50/p65 upon TNFα or LPS stimulation to sustain activity	Deng *et al.*, 2003[41] Deng *et al.*, 2003[42] Furia *et al.*, 2002[43]

1.3 NF-kB cellular functions

Activation of NF-kB results in the active transcription of many genes playing a role in vital biological processes. Many of the pleiotropic functions of NF-kB were correlated to neoplastic transformation.

1.3.1 NF-kB in immune and inflammatory responses

Different genes involved in both innate and adaptive immune response are target genes of NF-kB, e.g. *IL1*, *IL6*, *IL8*, *TNFα, GM-CSF, G-CSF, MCP1,* and *RANTES*. Selective deletion of IKK2 in murine lung epithelial cells resulted in delayed Th17 and B cell responses and thus delayed fungal clearance in a model of pneumocystis[44]. In a study on patients with severe combined immunodeficiency (SCID), patients carried a loss of function mutation in IKK2 gene which was reflected in the presence of almost naïve T cells and the lack of regulatory T cells. Their isolated immune cell failed to respond to stimulation by cytokines and mitogens[45]. Even a developmental function for NF-kB signalling was identified in the maturation of T-lymphocytes[46].

1.3.2 NF-kB and cell cycle regulation and apoptosis

Cell growth is regulated by different signalling pathways including NF-kB. Entry into the S phase of the cell cycle is activated by G1 cyclins, especially by cyclin D family. NF-kB directly binds to the kB site on the cyclin D1 promoter leading to its transcriptional activation. Besides it activated c-myc encouraging the entry into the cell cycle[47].

NF-kB also plays a role in cell survival and escape from programmed cell death. It induces the expression of several anti-apoptotic proteins involved in the intrinsic death signalling pathway like Bcl-2 family, members of the inhibitors of apoptosis (IAP) family, p53, and suppresses JNK by inducing JNK inhibitors such as XIAP. It was shown that mouse embryonic fibroblasts lacking IKK2 showed increased cell death and stabilized p53 in response to chemotherapeutic agents corroborating to the role of NF-kB in drug resistance[48]. Furthermore, deletion of RelA in fibroblasts sensitizes cells to TNF-α induced apoptosis[49].

1.3.3 NF-ƙB in cell adhesion and angiogenesis

The role of NF-ƙB outranges proliferation to encourage cell mobility and angiogenesis. NF-ƙB induces the expression of various cell adhesion molecules, e.g. matrix metalloproteinases (MMP2 and MMP9), vascular cell adhesion molecule (VCAM-1), and intracellular cell adhesion molecule (ICAM-1). The target genes scope of NF-ƙB also covers diverse genes regulating endothelial cell growth, vasodilation via inducible nitric oxide synthase (iNOS) and angiogenesis via vascular endothelial growth factor (VEGF)[47].

1.4 IKK2 and NF-ƙB in lung carcinogenesis

On account of the aforementioned cellular functions of NF-ƙB in cell proliferation, promotion of migration and invasion as well as inhibition of apoptosis, it is not surprising that NF-ƙB plays a significant role in cancer development. Though few genetic alterations were detected amongst the NF-ƙB family, several mutations were detected in their upstream activators. Besides, the contribution of an inflammatory microenvironment to tumour progression made inflammation the seventh hallmark of cancer[50].

1.4.1 Expression of NF-ƙB in different cancer types

NF-ƙB activation was observed in lymphoid malignancies as well as in most solid tumours. NF-ƙB activation was reported in MALT lymphomas, diffuse large B-cell lymphoma (DLBCL), and multiple myeloma. Other lymphoid cancers resulting from viral tumour viruses, like Epstein-Barr virus, Kaposi Sarcoma-associated herpes virus or human T-cell lymphoma virus, also reveal NF-ƙB activation[51, 52].

In some cancer types, presence of persistent inflammation paves the road to tumorigenesis, a concept termed cancer-related inflammation[53]. Vlantis *et al.* showed in a mouse model that persistent genetic activation of NF-ƙB signalling in intestinal epithelial cells is sufficient to induce intestinal tumours[54]. In another colitis-associated cancer model, Greten *et al.* show that deletion of IKK2 in both epithelial and myeloid cells could diminish tumour formation[55].

In prostate cancer, activation of NF-ƙB was correlated with tumour progression as well as with chemoresistance[51]. Hypoxic prostate cancer cells, which are resistant to therapy, express higher levels of IL-8 as a result of NF-ƙB activation and thus promote cell survival[56].

In lung cancer, it was shown that in tumours with PTEN inactivation, NF-ƙB promotes cell invasiveness and anchorage-independent growth mediated via PI3K/AKT pathway[57]. Glioblastoma tumours often show a deletion of *NFKBIA* which is mutually exclusive with *EGFR* amplification[58]. Activation of NF-ƙB was also observed in head and neck squamous cell carcinoma and was correlated with metastasis[59], in hepatocellular carcinoma[51] and in breast cancer by promoting tumour-initiating cells[60].

1.4.2 Targeting NF-ƙB for cancer therapy

It is well established that NF-ƙB promotes proliferation and survival of cancer cells, supports angiogenesis and thus metastasis, evades adaptive immunity and alters responses to chemotherapy. Thus, cancer-related inflammation is an appealing target for novel therapeutic strategies and even diagnosis[61].

The benefits of targeting NF-ƙB were observed in several cancers either using NF-ƙB inhibitors solely or in combination with other therapies. In multiple myeloma, there is often activating mutation in NIK which mainly activates the alternative NF-ƙB pathway. Selective NIK inhibitors were selectively toxic for cells with such mutations. Combination therapy of NIK inhibitors and other chemotherapeutic agents provide a promising therapeutic strategy for multiple myeloma[62].

Targeting NF-ƙB sensitizes cancer cells to chemotherapy in NSCLC[63] and in breast cancer[64]. Combined treatment of lung cancer cell lines with SAHA, an HDAC inhibitor, and Bay11-7085, a selective IKK2 inhibitor, was more effective than either drugs alone[65]. In support with these data, Bay11-7085 increases the therapeutic effectiveness of bortezomib, a proteasome inhibitor, in ovarian cancer[66]. These studies emphasize the importance of acquiring more insight into the regulation of NF-ƙB.

1.5 Epigenetic control via NuRD complex in lung cancer

The nucleosome and remodelling deacetylase complex was first discovered in 1998 in different species. It is a chromatin remodelling complex having important roles in chromatin assembly, transcription, and genomic stability. Initially, it was called Mi-2 complex but now the common name is NuRD complex[67].

1.5.1 Members of the NuRD complex

The NuRD complex comprises mainly six core subunits; of which only two possess enzymatic activity and the rest act as scaffold proteins and facilitate the interaction between the complex members, transcription factors and the DNA. Chromodomain-helicase-DNA-binding protein 3 and 4 (CHD3 and CHD4, also known as Mi-2α and Mi-2β, respectively) have ATPase activity to unwind the chromatin so that it is accessible to histone deacetylase 1 and 2 (HDAC1 and HDAC2). The other structural proteins are metastasis-associated protein 1, 2 and 3 (MTA1, MT2, MTA3), retinoblastoma binding proteins 4 and 7 (RBBP4 and RBBP7, also known as RbAp46 and RbAp48, respectively), methylated CpG-binding protein 2 and 3 (MBD2 and MBD3) and GATAD2a (p66α) or GATAD2b (p66β)[68, 69] (Fig. 1.5). According to Smits *et al*. who studied the stoichiometry of the NuRD complex, the complex comprises one subunit of CHD3 or CHD4, one HDAC1 or HDAC2, three subunits of MTA1/2/3, one MBD2 or MBD3, six RbAp46/48, and two GATAD2a/b[67].

CHD3 and CHD4, the Mi-2 protein homologues, were first identified as an autoantigen in dermatopolymyositis. They have a molecular mass of 220kDa and their ATPase activity is stimulated by chromatin rather than by naked DNA or histones. Through their PHD domains they bind to H3 tails. By releasing energy from ATP, they mediate chromosome remodelling making DNA more accessible to HDACs and to RNA polymerases[69].

HDAC1 and HDAC2 are members of class I histone deacetylases. They are 55kDa in size and share 83% sequence homology, which is reflected in their redundant functionality. Owing to their deacetylation activity they were related to transcriptional repression especially of genes involved in cell proliferation. However, knockdown of HDAC1 or HDAC2 lead to the downregulation of several genes indicating a dual role in gene regulation[70, 71].

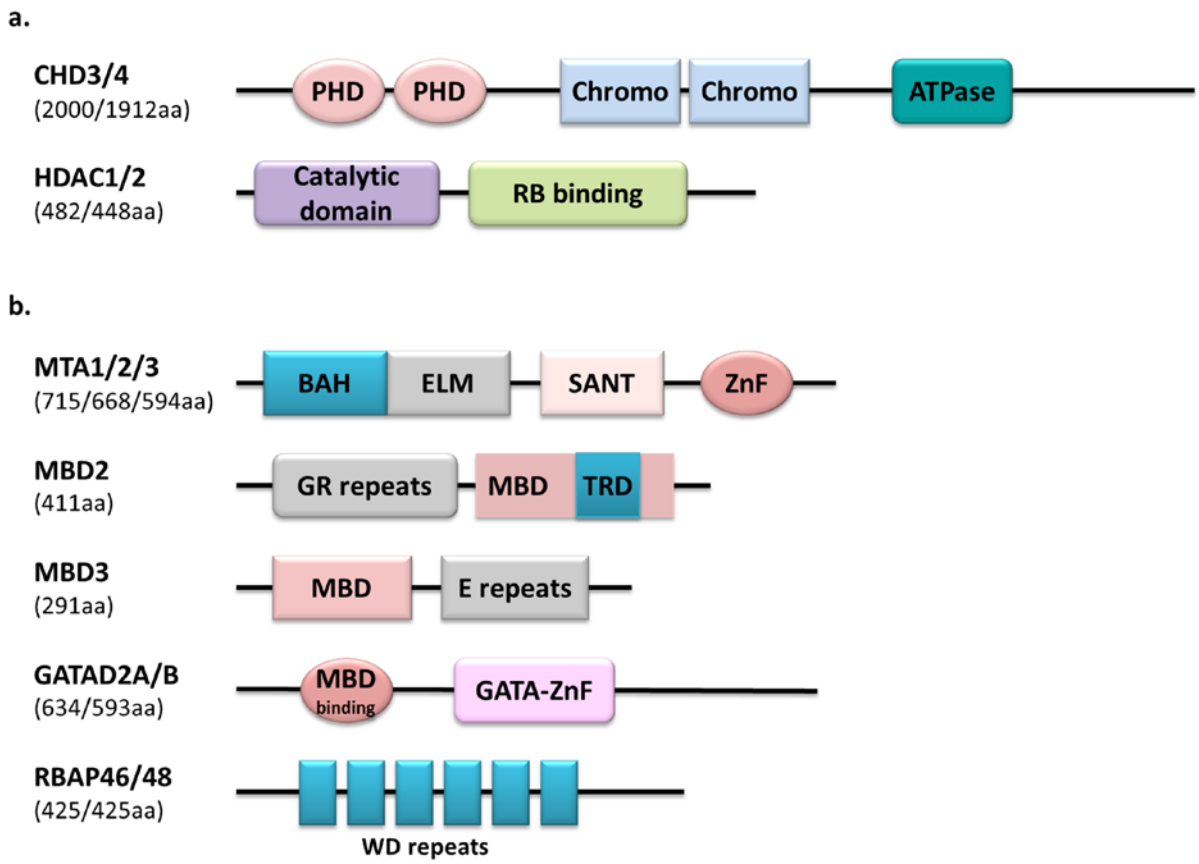

Figure 1.5 Core components of the NuRD complex. Schematic representation of a) enzymatic subunits CHD3/4 (chromodoamin-helicase-DNA-binding protein) and HDAC1/2 (histone deacetylase) and b) structural subunits MTA1/2/3 (metastasis-associated proteins), MBD2/3 (methyl-CpG-binding domain), GATAD2A/B (GATA zinc finger domain containing 2A/B) and RBAP46/68 (retinoblastoma associated protein) showing their respective protein domains. BAH (bromo-adjacent homology); Chromo (chromatin organization modifier); ELM (Egl-27 and MTA1 homology); E repeats (poly glutamate); GR repeats (glycine-arginine rich region); PHD (plant homodomain); RB binding (binding domain to RbAp proteins); SANT (Switching-defective protein 3, Adaptor 2, nuclear receptor co-repressor, transcription factor IIIB); TRD (transcription repression domain); WD repeats (repeats of WD40); ZnF (zinc finger).(Adapted from Torchy *et al*., 2015; Allen *et al*., 2013; and from Lai *et al*., 2011)[68, 69, 71]

MTA family comprises three members where MTA1 and MTA2 are more functionally related than MTA3. Their molecular masses are 80, 70 and 65kDa for MTA1, MTA2 and MTA3, respectively. They lack intrinsic enzymatic activity but they contribute to the assembly and stabilization of the NuRD complex via their different domains. Though the exact functional roles of their domains are not fully elucidated yet, some functional roles are assumed from similar proteins. The BAH domain is involved in protein-protein interactions, whereas SANT and ELM were reported to interact with HDACs wrapping around their catalytic domain. In addition, SANT domain interacts with unmodified histone tails. The zinc finger GATA-like domain could be responsible for direct interaction with the DNA[72, 73].

MBD2 and MBD3 are the smallest subunit of the NuRD complex (43 and 33kDa, respectively). MBD2 has a transcription repression domain (TRD) and binds mainly to methylated CpG islands at transcription start sites, whereas MBD3 binds to unmethylated DNA suggesting a role in active transcription[74].

Retinoblastoma-associated proteins RbAp46 and RbAp48 are mainly responsible for protein-protein interaction through their WD40 protein repeats. These are a structure motif of 40 amino acids forming a ß-propeller conformation for recognition at protein-protein or protein-DNA interfaces. GATAD2 proteins were shown to interact and co-localize with MBD2 and MBD3. It is reported that other subunits could also bind and interact with the NuRD complex depending on the biological context[71].

1.5.2 Biology and function of NuRD complex in cancer

Initially, the function of the NuRD complex was related only to transcription repression. However, there is increasing evidence of its role both as repressor and gene activator. In cancer, the NuRD complex was recruited by oncogenes as TWIST to suppress E-cadherin and thus drive the cells into epithelial-mesenchymal transition (EMT)[69]. Another mechanism is by altering tumour suppressor genes which are often methylated in cancer. The NuRD complex was found to be recruited to these sites mediating further silencing of the tumour suppressor genes.

Moreover, the NuRD complex can directly interact with other proteins and transcription factors, e.g. HIF1α and p53. In breast cancer MTA1 recruits HDAC1 to acetylated HIF1α thus leading to its stabilization. HIF1α stabilization activates various genes promoting angiogenesis and metastasis[68, 71]. In case of p53, the NuRD complex deacetylates p53 leading to its inactivation and cells are driven to uncontrolled cell growth and resistance to apoptosis[75].

1.5.3 MTA2/NuRD in cancer

MTA1 was first characterized in rat mammary adenocarcinoma. Despite their structural similarity, MTA1 and MTA2 vary functionally from MTA3. In DLBCLs MTA3 mediates BCL-6-dependent repression of genes associated with plasma cell differentiation. In addition, MTA3 is induced by oestrogen and is a transcriptional target of oestrogen receptor (ERα). However, it is highly expressed in normal ducts to maintain healthy differentiated epithelial phenotype

by repressing *SNAI1*, a transcription factor promoting EMT. MTA3 also represses Wnt4 and subsequent Wnt target gene expression in mammary epithelial cells[76].

On the contrary, MTA1 and MTA2 correlate with cancer progression and poor prognosis in different cancer types including breast cancer, colorectal cancer, gastric cancer, hepatocellular carcinoma and lung cancer. In lung cancer, Liu *et al*. showed that nuclear MTA2 correlates with lung cancer cell proliferation, tumour size, and lymph node metastasis making it a potential candidate for molecular staging[77]. Besides, MTA2 overexpression was correlated with tumour progression and poor prognosis in a study conducted on patients with oesophageal squamous cell carcinoma[78].

At this stage it is worth mentioning that MTA1 and MTA2 localize primarily in the nucleus though cytoplasmic localization was also detected. In embryonic studies MTA1 was mainly identified in the cytoplasm indicating its role in embryogenesis whereas adult cells show nuclear localization indicating a shift in its functional role to adult cell regulation[79].

The role of the NuRD complex and its members in the outcome of cancer is gaining attention yet it requires deep functional insight to elucidate its differential regulation in different cellular contexts. Being a major epigenetic regulator, further investigations are required to delineate the interaction of the NuRD complex with transcription factors.

1.6 NF-ĸB and epigenetic control

NF-ĸB is capable of mediating a plethora of effects within the cell which makes its intricate control a necessity. Increasing evidence show the epigenetic regulation of NF-ĸB especially in the context of tumorigenesis.

Several reports provide evidence of the interaction of NF-ĸB and the chromatin remodelling machinery. Akirin, which regulates NF-ĸB-dependent transcription, mediates the interaction between NF-ĸB and SWI/SNF complexes resulting in the regulation of several genes related to the innate immune response. IĸB-ζ forms a complex including p50 and SWI/SNF together with Akirin2 and upon stimulation the complex is recruited to the promoter of certain genes, e.g. *Il6* and *Il12b* to activate them[80].

In breast cancer, NF-ĸB regulation was recently linked to damaged DNA-binding 2 protein (DDB2), which is a negative regulator of migration and invasion. Overexpression of DDB2 decreases invasiveness and metastasis via reduction of MMP9 levels. Therefore, metastatic breast tumour cells lacked DDB2 expression compared to their non-metastatic counterparts. Strikingly, DDB2 induced IĸBα expression which consequently decreased NF-ĸB activity[81].

Additionally, members of NF-ĸB family can act themselves as epigenetic regulators of NF-ĸB-dependent gene activation. The homodimer of p50 interacts with HDAC1 to inhibit pro-inflammatory genes[82]. This mechanism was also reported in LPS tolerance[83]. A study in acute myeloid leukaemia suggests that C/EBP displaces HDACs from p50 homodimers and thus driving the activation of anti-apoptotic genes[84].

Hitherto, the epigenetic regulation of NF-ĸB is an intriguing conundrum that requires more investigation. Unravelling the underlying mechanisms and the contributing complexes regulating NF-ĸB in cancer would aid in the development of novel but specific therapeutic modalities.

2 Aims

The role of NF-ƙB in lung cancer showed puzzling effects despite extensive studies indicating the need for further efforts to elucidate the molecular activation and regulation of NF-ƙB.

The aim of the following work is to study the role of NF-ƙB signalling via IKK2 in the pathogenesis of lung adenocarcinoma and to study the epigenetic control of NF-ƙB through MTA2/NuRD complex.

The study aimed at investigating the role of IKK2/NF-ƙB in lung tumour development by:

- Comparison of different cancer cell lines for NF-ƙB expression and activity
- Studying the effect of LPS and TNFα as stimuli
- Testing of IKK2 inhibitors
- Generation of compound transgenic mice with IKK2 constitutive activation or IKK2 downregulation in SpC C-Raf BxB tumour mouse model (SpC rtTA/Tet-O-IKK2^{CA}/SpC C-Raf and SpC rtTA/Tet-O-IKK2^{DN}/SpC C-Raf)
- Evaluation of tumour burden after long term induction with doxycycline for 12 months
- Investigating the changes in immune cell repertoire in compound mice
- Isolation of alveolar type II cells to study signalling changes regulated by IKK2

MTA2/NuRD hypothesized regulation of NF-ƙB is addressed by:

- Overexpressing MTA2 in cancer cell lines and assessing the NF-ƙB activity
- Studying the interaction between MTA2/NuRD complex and NF-ƙB
- Evaluating the effect of knocking down MTA2 by shRNA on tumour development in a xenograft mouse model

3 Materials and Methods

3.1 Cell biological methods & cell culture

3.1.1 Cell cultivation

Human lung adenocarcinoma cells (A549, A427, Colo699, H1650, H2122) BEAS-2B (human bronchial epithelial cells), human embryonic kidney cells (HEK293T) and mouse Lewis lung carcinoma (LLC1) were obtained from ATCC. A549 and HEK cells were cultured in DMEM medium supplemented with 10% foetal calf serum (FCS, Th. Geyer, Germany) and 1% penicillin/streptomycin (100 I.U./ml and 100µg/ml, respectively, Gibco® by Life Technologies, Germany). A427, Colo699, H1650, H2122 and LLC1 were cultured in RPMI medium supplemented with L-glutamine, 10% FCS and 1% penicillin/streptomycin. BEAS-2B cells were cultured in DMEM/F-12 (Dulbecco's Modified Eagle Medium/Ham's F-12) medium using 5% FCS, 1% penicillin/streptomycin. All cells were cultured at 37°C and 5% CO_2 (HERAcell 150i, Thermo Scientific) according to manufacturer's recommendations.

When cells reach 80-90% confluency, they were subcultured and split in a ratio of 1:3 to 1:6 depending on the density needed and cell type. Medium was aspirated, cells were washed with 1x phosphate buffered saline (1xPBS, Gibco® by Life Technologies) and incubated with 1x trypsin (Thermo Fisher, Germany) for 3-5minutes at 37°C until cells detach. To stop the trypsin activity, media with FCS or FCS alone was added to the cells and the cell suspension was collected and centrifuged at 300xg for 5minutes. Cell pellet was then resuspended in fresh media and cells were plated at the desired ratio.

For freezing purposes, cells were trypsinized and cell pellet was resuspended in freezing medium containing 10% dimethylsulfoxide (DMSO, Sigma Aldrich, USA) and 20% FCS. Cells were frozen in cryovials and stored in liquid nitrogen tank until further use.

3.1.2 Isolation of mouse alveolar type II cells

Alveolar epithelial cells were isolated as described previously with some modifications[85]. Briefly, mice were anaesthetized and lungs were perfused with 1xPBS then filled with approximately 1.5ml sterile dispase (BD Biosciences, Germany) and 0.5ml low-melting agarose (Sigma-Aldrich) via the trachea. After gelling, lungs were removed and incubated further in dispase for 40 minutes at room temperature with rotation. The trachea and

surrounding connective tissue were removed and lung tissue was minced in DMEM/2.5% HEPES with 0.01% DNase (50 µg/ml; Sigma) and incubated with shaking for further 10 minutes at 37°C. Digested tissue was washed with PBS and single cells were separated by successive filtration through 100-µm and 40-µm nylon filters and collected by centrifugation[86, 87]. To remove the immune cells, single cell suspension was incubated with CD32 (3µl/lung) and CD45 (7µl/lung) antibodies for 30 minutes at 37°C. Cell-antibodies mixture was centrifuged, resuspended in 7 ml medium and incubated with 1xPBS-pre-equilibrated streptavidin magnetic beads for 30 minutes on a rolling table. After purification of all bound cells, the supernatant containing all epithelial cells was plated on fibronectin-coated plates. Once the cells adhered to the plates, they were washed several times with 1xPBS to get rid of erythrocytes. The cells were kept in culture for maximum three days.

3.1.3 Stimulation and inhibition of NF-ƙB signalling pathway

To stimulate the classical signalling pathway of NF-ƙB, cells were treated with lipopolysaccharide LPS (Sigma Aldrich, Germany) at a concentration of 5µg/ml or 10µg/ml for 2h (or as specified) or with human recombinant tumour necrosis factor TNFα (R&D Systems, Minneapolis, USA, 210-TA) at a concentration of 10ng/ml for 30 min. For inhibition, sc-514 In-Solution (Santa Cruz, Germany) was used to selectively inhibit IKK2 at a final concentration 0f 12.5µM. Other inhibitors were also applied such as MG-132 (Merck Millipore, Darmstadt, Germany) at a concentration of 25µM, Bay 11-7085 (Cayman Chemical company, Estonia) at 10µM and parthenolide at 20µM (Cayman Chemicals).

3.1.4 Transient cell transfection

Cells were seeded in 6-well plates at a density of $3x10^5$cells/well and cultured overnight to attach. When they reached 70-80% confluency, they were transfected with the desired plasmid using TurboFect™ Transfection reagent (Thermo Fisher Scientific Inc., Germany) or Lipofectamine® 2000 (Life Technologies, Germany) for more resistant cells at a ratio of 2:1 or 3:1, respectively (amount of plasmid DNA in µg: volume of transfection reagent in µl). Transfection efficiency was checked after 24 hours and ranged from 70% -90% according to the cell line. Cells were collected 24h post-transfection for RNA isolation; and for protein isolation and functional assays 48h post-transfection.

3.1.5 Stable cell lines generation

Stable cells were generated via lentiviral transfection. First HEK293T cells were cultured until 80% confluent and then transfected with the lentiviral vector of interest together with viral packaging vector psPAX2 and envelope vector pMD2G at a ratio of 3:2:1 using TurboFect transfection reagent (Thermo Fisher Scientific Inc., Germany) and serum-free medium. Three lentiviral vectors were used: empty vector pCDH-CMV-MCS-EF1-copGFP-T2A-Puro depicted in Fig.3.1a (SBI System Biosciences, USA), IKK2-S177E-S181E, a gift from Anjana Rao (Addgene plasmid #11105)[88], cloned into the pCDH empty vector and referred to as $IKK2^{CA}$ (Fig. 3.1b).

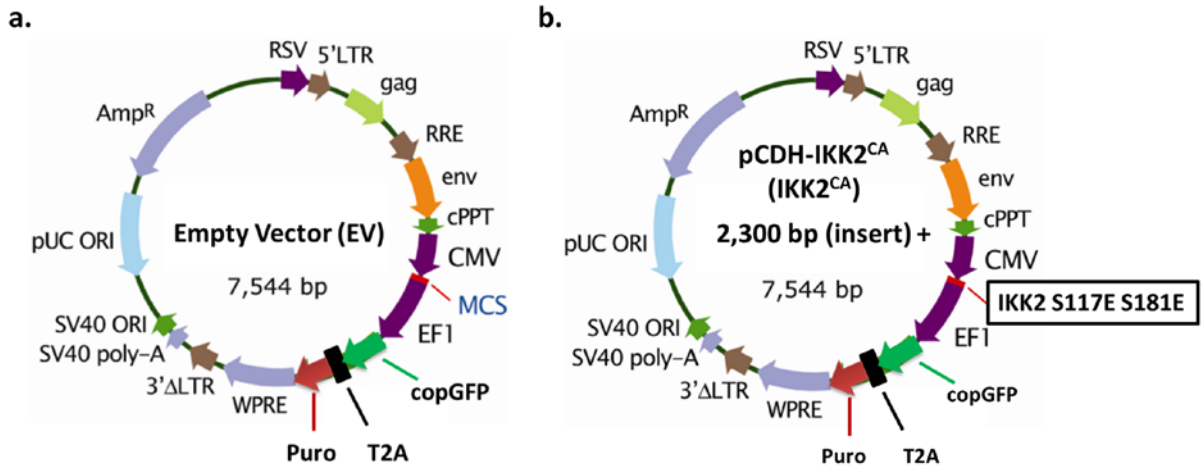

Figure 3.1 Vector map of lentiviral vectors. a) pCDH-CMV-MCS-EF1-copGFP-T2A-Puro empty vector; b) pCDH--CMV-$IKK2^{CA}$-EF1-copGFP-T2A-Puro which carries two activation mutations at S117 and S181 making IKK2 constitutively active. (Adpated and modified from SBI System Biosciences pCDH cloning and expression lentiviral vectors).

After 48h of transfection, cell medium containing the viral particles was collected, centrifuged to get rid of cell debris and then supernatant was filtered through 0.45µm-nitrocellulose filter. Viral particles were used immediately or were stored in aliquots at -80°C until further use. To transduce target cells with the lentiviral vector of interest, they were seeded in 24-well plate and cultured until 70-80% confluency. The corresponding viral particles were mixed with polybrene (Fermentas, Germany) at final concentration of 0.8µg/ml with fresh medium, incubated at room temperature for 5min and then pipetted on

top of the cells. Two days later, the transduction efficiency was estimated and positive cells were selected with puromycin at a concentration 6-8µg/ml according to the cell line.

LLC1 cells were transduced by spinoculation or spin infection. A volume of 1-2ml viral particles was added to 50 000 cells in a 50ml-Falcon tube to which 2µl polybrene (stock is 10mg/ml) was added. The mixture was mixed well and incubated at room temperature for 5 minutes. The cells-viral particles mixture was then centrifuged at 2500rpm at 30°C for 3h, after which the supernatant was removed. Cells were resuspended in medium supplemented with 10% FCS and plated in 24-well plate. After 48h, cell selection was started by the addition of puromycin.

3.1.6 Immunocytochemistry (ICC)

Cells were seeded in 8-well chamber slides (BD BioSciences, Germany) at a density of 0.5-1x10^4 cells/ml. When confluent, the supernatant was removed and cells were washed with 1xPBS for 5 min. Then cells were fixed either with ice-cold acetone/methanol mixture (1:1) at -20°C for 30 min or with 4% PFA at room temperature for 30 min. After fixation cells were washed 3 times with 1x PBS and blocked with 5% BSA/0.1% triton X for 1h at room temperature. Primary antibodies (p50, RelA/p65 from Santa Cruz, Germany and SP-C from Millipore, Germany) were prepared at a dilution of 1:200 in the blocking solution and added to the cells overnight. After incubation, cells were washed 4 times with 1xPBS and incubated with the fluorescently conjugated secondary antibodies (anti rabbit IgG- AlexaFluor®488, AlexaFluor®555 and AlexaFluor®594, Invitrogen, Germany) at a dilution of 1:1000 for 1h protected away from the light. Cells were washed 4 times with 1xPBS and nuclei were counterstained with 4', 6-diamidino-2-phenylindole (DAPI, Life Technologies, USA) diluted 1:100 for 10 min. After a final wash with 1xPBS cells slides were mounted with Dako fluorescent mounting medium (Dako North America, Inc., USA) and examined under Leica fluorescent microscope. (Details on antibodies listed in Appendix I, Table 9.2 for primary antibodies and Table 9.4 for secondary antibodies).

3.1.7 Proximity ligation assay (PLA)

A549 cells were grown in 8-well tissue culture chamber slides (Sarstedt, Germany) and transfected with pIKK2CA, pMTA2 or shMTA2. Proximity ligation assay was performed using the Duolink® In Situ fluorescence red starter kit mouse/rabbit (OLink Bioscience, Uppsala, Sweden) according to manufacturer's protocol. Briefly, cells were fixed in ice-cold acetone/methanol mix for 20min at -20°C and permeabilized with 1xPBS containing 01% TritonX-100 for 10minutes. Duolink In Situ blocking solution was added to the chamber slides and incubated in a humidity chamber for 30min at 37°C. Primary antibodies, MTA2 (Abcam, Germay) and p-p65 (Santa Cruz, Germany), were diluted 1:200 in the provided antibody diluent solution and incubated overnight with the cells. After incubation primary antibodies were removed and slides were washed in 1x Wash Buffer A twice each for 5min. PLA probes were diluted 1:5 and added to samples to incubate in a pre-heated humidity chamber for 1h at 37°C. PLA probes were then discarded, slides washed in 1xWash Buffer A twice for 5min each and Ligation-Ligase solution was added. After incubation for 30min at 37°C, solution was removed and slides were washed twice in 1xWash Buffer A under mild agitation. The amplification-polymerase solution was prepared under light protection and incubated on the samples for 100min at 37°C. Finally, cells were washed twice in Wash Buffer B for 10min each, then once in 0.01x Wash Buffer B for 1min. After drying, slides were mounted Duolink In Situ Mounting Medium with DAPI and nail polish was used to seal the edges. Microscopic analysis followed using the Leica fluorescent microscope.

3.2 Functional assays for cells

3.2.1 Cell proliferation by BrdU incorporation

Proliferation of cells was determined using colorimetric cell proliferation ELISA BrDU kit (Roche, Germany) according to the manufacturer's protocol. Cells were seeded as 6-8 replica in 96-well plate at a density of $1x10^4$ cells/well in 100µl of full medium and cultured overnight. Medium was then removed and cells washed with 1xPBS before they were serum starved in medium without serum supplementation. After 24h of serum starvation, the medium was replaced with medium to be tested and incubated for as long as required for the stimulation or inhibition. BrdU was then added to the cells for 2-4h in serum-free medium. Cells were then fixed and BrdU incorporated in proliferating cells was detected

with antibody having horse radish peroxidase (HRP) conjugation. An HRP-substrate was added and the colour developed was measured spectrophotometrically at 370nm with reference measurement at 492nm using Tecan Infinite M200 PRO reader (Tecan Group Ltd, Switzerland). Proliferation of cells was plotted as function of absorbance at 370nm.

3.2.2 Boyden chamber migration assay

For the evaluation of the migratory capacity, the Boyden chamber migration assay[89] was performed. In 24-well companion plates (BD BioSciences, Franklin Lake, USA), a volume of 700µl of media complemented with 10% FCS was distributed into the wells. Cells were seeded on filters (8.0µm pore size; BD Falcon cell culture insert, transparent PET membrane, Corning, Inc.) at a density of 5×10^4 cells per filter in 300µl serum-free medium. Cells were incubated for 6-8 hours in the incubator at 37°C with 5% CO_2. After incubation the filters were washed with 1×PBS and dried from the inner side with a cotton swab to remove cells that haven't migrated. For fixation, filters were submersed in methanol (Roth, Germany) for 3 minutes, and stained for 10 minutes with Crystal Violet solution (Sigma-Aldrich, USA) diluted 1:10 with ddH_2O. After the final wash in ddH_2O, filters were dried, cut out from the inserts and mounted on slides with Pertex (Medite GmbH, Germany). Slides were scanned with Nanozoomer 2.0HT digital slide scanner C9600 (Hamamatsu Photonics, Japan) and the migrated cells per membrane were counted using ImageJ software.

3.2.3 Soft agar attachment-independent colony formation assay

Soft agar assay was performed to characterise LLC1 tumour cells for their ability to grow independently of anchorage. LLC1 control cells as well as LLC1 transfected with empty vector, $IKK2^{CA}$ or shMTA2 were compared. For this assay, 0.7% bottom agar was prepared by mixing 2x DMEM with sterile agar stock solution (1.8%). After plating in 6-well plates, agar was left to solidify for at least one hour. Cells were trypsinized and cell samples were prepared in 0.3% top agar at a concentration of $5x10^4$cells/ml at 42°C. Plate was left to cool down before incubating at 37°C with 5% CO2. Colony formation was monitored regularly after one week under the microscope and after 14 days of culture, images were taken with representative colonies. Images were analysed by ImageJ software for counting the number of colonies and measuring their area.

3.3 Molecular biology & biochemical methods

3.3.1 RNA isolation

For isolation of RNA from tissues, 50-100mg tissue were homogenised in 1ml Trizol (Qiagen, Germany) twice at 6500rpm for 25 seconds using Precellys® Ceramic Kit 1.4 (PEQLAB, Erlangen, Germany) and Precellys homogeniser. For RNA isolation from cells, they were first washed with PBS then were directly scraped in Trizol (1m/10cm plate). Cells or homogenized tissue were centrifuged at 12000rpm for 30min at 4°C and RNA was isolated according to manufacturer's protocol. In brief, chloroform (Sigma Aldrich, Germany) was added to the supernatant (0.2ml for each ml Trizol), mixed vigorously, incubated for 10min at room temperature and centrifuged at 12000rpm for 15min at 4°C. The upper aqueous layer was transferred to another tube and overlayed with 500µl isopropanol/ml Trizol. After gentle mixing, mixture was incubated for 10min at room temperature. To collect the precipitated RNA, mixture was centrifuged at 12000 rpm for 10 min at 4°C. The supernatant was then removed and the pellet was washed twice with 75% ethanol and then left to dry. The isolated RNA was then resuspended in an appropriate amount of DEPC-treated water and the concentration and purity of RNA were measured using NanoDrop (Peqlab Biotechnologies GmbH, Erlangen, Germany). After checking the integrity of RNA on 1% agarose gels, RNA was stored at -80°C until further use.

3.3.2 Reverse transcription for cDNA synthesis

To ensure for better purity, RNA was pre-treated by DNase (Fermentas, Germany) to eliminate possible contamination with genomic DNA. The RNA concentration was adjusted to 100ng/µl and 800ng of RNA in total were used per sample. The DNase treatment was performed using a master mix as described in Table 3.1 and incubated for 30min at 37°C. To stop the enzymatic action of DNase, 1µl of EDTA was added to each sample and incubated for further 10min at 65°C.

Table 3.1 DNase Treatment of RNA

Component	Volume (µl)	Incubation Conditions
DNase Buffer	1	
RNase Inhibitor	0.33	30 min at 37°C
DNase	1	
EDTA	1	10 min at 65°C

RNA was then transcribed to cDNA with Oligo-dT primers using ImProm-II™ Reverse Transcription System (Promega, Madison, USA) according to the suppliers' recommendation. A volume of 8µl RNA (100ng/µl) were mixed with 2µl oligomers and incubated for 6min at 70°C. After cooling, 30µl of the master mix described in Table 3.2 were added and incubated in the thermocycler. The High Capacity cDNA Reverse Transcription Kits (Applied Biosystems, USA) was also applied for cDNA synthesis. The synthesized cDNA was diluted 1:3 before proceeding with qPCR.

Table 3.2 Master mix for cDNA synthesis using ImProm-II™ Reverse Transcription System

Component	Final Concentration	Volume (µl)
ImProm-II™ 5x reaction buffer	1x	8
$MgCl_2$ (25mM)	5mM	4
dNTP Mix (10mM)	0.5m	2
RNasin® ribonuclease inhibitor	0.5U	1
ImProm-II™ reverse transcriptase (RT)	1U	2
Nuclease free water		13
Total		30

3.3.3 Quantitative real time polymerase chain reaction (qRT PCR)

The Real Time-qPCR reaction mixture was prepared using iQ™ SYBR Green Supermix (Bio-Rad, Germany) according to manufacturer's recommendations (Table 3.3). Exon spanning primers were designed to produce an amplicon size varying from 100-200bp.

Appendix II, Table 9.5 and Table 9.6 list all primers used, their sequence and the corresponding annealing temperature.

Table 3.3 Reaction mixture for qPCR

Component	Volume (µl)
iQ™ SYBR® Green Supermix (2x)	10
Forward primer (10mM)	0.5
Reverse primer (10mM)	0.5
Nuclease free water	7
cDNA template	2
Total	20

Master mixture and cDNA template were pipetted into non-skirted 96-well plates and the reaction was run in Mx3000P qPCR system using the reaction conditions described in Table 3.4. Data were analysed with the MxPro2000 software and the level of mRNA expression was represented as ΔCt values (Ct value of the housekeeping gene – Ct value of the gene of interest). The data were normalized to the expression of *HPRT* (hypoxanthine phosphoribosyltransferase1) as housekeeping gene.

Table 3.4 Reaction conditions for qPCR programme

Temperature	Time	Number of Cycles
95°C	3 min	1
95°C	15 sec	40
58°C or 60°C	20 sec	
95°C	1 min	1
55°C	30 sec	1
95°C	30sec	1

3.3.4 Protein isolation

Tissue was homogenised as for RNA with Precellys ceramic kit. Cells or tissue were ruptured using RIPA buffer (Chem Cruz, Santa Cruz Biotechnology, Inc) supplemented with protease inhibitor (Santa Cruz, Germany) and phosphatase inhibitors (PMSF as 1mM final concentration and sodium orthovanadate as 0.2mM final concentration). For 100mg tissue 500µl RIPA buffer was used; for cells 150µl RIPA buffer was used for 10cm-plate and 70µl RIPA buffer for one well of a 6-well plate. Cell suspension or homogenized tissue were incubated for 10 minutes at 4°C then centrifuged at 12000rpm for 30min at 4°C. The supernatant was collected and stored at -80°C until further use.

For isolation of cytoplasmic and nuclear protein fractions, NE-PER™ Nuclear and Cytoplasmic Extraction Kit (Thermo Scientific™, Germany) was used following the manufacturer's instruction. Both fractions were collected and stored at -80°C until further use.

The protein content was quantified by a modified Lowry assay using DC™ Protein Assay (Bio-Rad, Munich, Germany). Different concentrations of bovine serum albumin (BSA, BioRad, USA) were used as a protein standard ranging from 0.125-2µg/µl. Samples from tissues were diluted 1:10 and those from cells were diluted 1:5 to be in the range of the standard. The developed blue colour was measured at 750nm using Tecan Infinite M200 PRO microplate reader (Tecan Group Ltd, Switzerland).

3.3.5 Co-Immunoprecipitation (Co-IP)

Protein was isolated as described above section 2.2.3 and 500µg protein were diluted to 1µg/µl protein in Co-IP buffer (or modified cell lysis buffer) and incubated with 1µg antibody or IgG control for 3h or overnight at 4°C with rotation. After equilibration of protein A-agarose beads (GE Healthcare, Germany) in modified cell lysis buffer, 30µl beads were added to each protein/antibody sample. Samples were incubated with the beads for 3h at 4°C. The protein fraction pulled down by the antibody and beads were collected by centrifugation at 14000rpm for 10min at 4°C. The supernatant was collected to check for unbound proteins and the protein pellet was washed twice with RIPA buffer, twice with Co-IP buffer and once with 1xPBS. Finally the pellet was resuspended in approximately 50µl of 2xSDS sample application buffer and prepared for western blotting. As control, 10% input was used as

positive control and IgG control of the respective species was used as negative control (Buffers used are listed in Appendix III, Table 9.10).

3.3.6 Western blotting

Protein samples were mixed with 5x SDS sample application buffer and boiled for 3-5min and then loaded on 10% SDS PAGE gels. After the run, gels were electrophoretically transferred to nitrocellulose membranes and blocked in either 5% non-fat milk in TBS(T) or in 5% BSA in TBS(T) for 1h at room temperature with agitation. After incubation with the primary antibody overnight at 4°C, membranes were washed three times in TBS(T) and then incubated with the corresponding secondary HRP-coupled antibody for 1h. The SuperSignal™ West Femto Chemiluminescent Substrate (Thermo Fisher Scientific, Inc., Germany) was added after washing the membranes and development was done using ImageQuant™ LAS 4000 Version 1.2 (GE healthcare Life Sciences, Germany). (Antibodies used and the corresponding conditions are listed in Appendix I, Table 9.1. Buffers used are listed in Appendix III, Table 9.11).

3.3.7 Chromatin Immunoprecipitation

Cells were seeded in 10cm plates, treated and cultured until confluency. Formaldehyde was added to a final concentration of 1% for 10min at room temperature to crosslink protein and DNA. Glycine was then added at a final concentration of 125mM for 5min to quench formaldehyde. All further steps were carried out on ice. Crosslinked cells were washed three times with cold 1xPBS and collected by scraping. To lyse the cells, they were incubated with cold L1 lysis buffer supplemented with protease and phosphatase inhibitors and 2mM DTT for 5min. Lysed cells were centrifuged at 3000rp for 5min to separate the supernatant with the cytoplasmic fraction and the chromatin in the pellet. Cell nuclei were then resuspended with L2 nuclear resuspension buffer supplemented with protease and phosphatase inhibitors and 2mM DTT.

The chromatin was then sonicated using Bioruptor® Next gen (Diagenode, Belgium) for 16 cycles for A549 cells at 90% power. After centrifugation at maximum speed for 10min, the supernatant containing the chromatin solution was collected, diluted with DB-dilution buffer supplemented with protease and phosphatase inhibitors and then incubated with 80µl protein A or G agarose beads conjugated with salmon sperm DNA for 1h at 4°C with rotation.

The supernatant DNA-protein precleared sample was collected after centrifugation at 1000xg for 3min and distributed into equal amounts to be incubated overnight at 4°C with 2µg of antibody or IgG in a final volume of 1.8ml. From the DNA-protein sample 10-20% were stored as input control. After incubation with the antibodies of interest, 30µl agarose beads were added and incubation was continued for further 2h. Supernatant was removed by centrifugation and kept to check for proper binding and the remaining agarose beads with bound DNA-protein moiety were washed with 800µl of low salt washing buffer, then high salt washing buffer, then LiCl washing buffer and finally twice with TE buffer (Buffers used are listed in Appendix III, Table 9.9).

To de-crosslink and elute the DNA, 100µl of freshly prepared DNA elution buffer was added to the beads together with 0.5µl RNase A (1mg/ml, Fermentas, Germany) and incubated at 37°C on thermo-shaker (900rpm) for 2h. To digest the protein 5µl of 10mg/ml proteinase K (Sigma Aldrich, Germany) was added to the beads and incubated at 56°C for 2h with shaking. Finally NaCl was added to a final concentration of 0.2M and incubated overnight at 65°C. Samples were then centrifuged for 1min and the supernatant collected and the DNA content in it was purified with QIAquick PCR purification kit (Qiagen, Germany) according to the manufacturer's instruction. Finally, DNA was diluted 1:4 with water and used for qPCR. (Primers used for ChIP assay and their sequences are listed in Appendix II, Table 9.8).

3.3.8 Fractionation of nuclear lysate by sucrose gradient

H1650 cells were cultured in 15cm-culture plates, two for each condition. After treatment with LPS and TNFα for 6h, cells were washed twice with 1xPBS. Cells were collected by scraping and subsequent centrifugation. Using 2ml of hypotonic lysis buffer complemented with protease and phosphatase inhibitors, cell pellets were lysed by vortexing and incubation on ice for 10-15min followed by centrifugation. The pellet which is the nuclear fractions was lysed by 450µl native nuclear lysis buffer.

A sucrose gradient was prepared by mixing 1ml of 5%, 13.75%, 22.5%, 31.25% and 44% of sucrose. Tubes were incubated overnight at 4°C to form a continuous gradient. Carefully the nuclear samples were overlayed on top of the sucrose gradient and centrifuged at 375000rpm for 16h30min. After centrifugation, the plastic tubes were gently pierced from

the bottom to collect 500µl fractions. The proteins collected were then examined by immunoblotting (Buffers used are listed in Appendix III, Table 9.10).

3.3.9 Cloning of pCDH-IKK2^{CA}

The plasmid containing IKK-2 S177E S181E (short pIKK2^{CA}) was a gift from Anjana Rao (Addgene plasmid #11105)[88]. Using PCR cloning, XbaI and BamH1 restriction sites were introduced to the amplified IKK2^{CA} sequence. Both the empty lentiviral vector pCDH-CMV-MCS-EF1-copGFP-T2A-Puro (short pCDH) (Fig. 3.1) and the modified purified IKK2^{CA} sequence were digested with XbaI and BamH1 restriction enzymes to have matching cohesive ends. The digested fractions were run on 1% agarose gel and the correct bands (2300bp for IKK2^{CA} and 7544bp for pCDH) were excised and purified from the gel using Gene Elute^{TM} gel extraction kit (Sigma Aldrich, Germany). Both vector and insert were mixed at a ratio of 1:3 and ligated overnight at 16°C using T4 DNA ligase (New England Biolabs, Germany).

The ligation product was checked on agarose gel and used to transform *DH5α E. coli* competent cells (New England Biolabs, Germany). Transformed bacteria were cultured on ampicillin plates (100µg/ml) for selection. Selected colonies were cultured in 3ml LB broth containing ampicillin and the plasmids were purified using Plasmid Mini Kit (Qiagen, Germany) or peqGold Plamsid Miniprep (Peqlab). Plasmids were screened by double restriction digestion, by qualitative PCR followed by agarose gel electrophoresis, and by sequencing. The clone with the correct plasmid was cultured overnight in maxi LB cultures supplemented by ampicillin at 37°C. Plasmid was then purified using NucleoBond Extra Maxi kit (Machery-Nagel GmbH, Germany).

3.4 Activity assays

3.4.1 NF-Gluciferase reporter assay

Cells were seeded in 48-well plates and cultured until they reached 70-80% confluency. Then they were transfected with NF-Gluc plasmid, a kind gift from Dr. Bakhos A. Tannous[90]. This plasmid has a reporter system expressing the secreted *Gaussia* luciferase (Gluc) under NF-ƙB responsive promoter elements. After 24h or 48h, 50µl of the cell-free conditioned medium was collected and activity was assayed by adding equal volume of 20µM of stabilized colenterazine substrate (p.j.k. GmbH, Germany) and measuring photon count using Infinite® 200 PRO microplate reader (Tecan, Switzerland).

3.4.2 NF-ƙB activity assay

NF-kB p65 transcription Factor assay kit (ab133112, Abcam, Germany) was used to measure NF-ƙB activity in the isolated nuclear extracts. This ELISA-based assay measures the binding of p65 present in the nuclear samples to NF-ƙB-specific double stranded DNA sequence containing NF-ƙB response elements immobilized on the ELISA plate. Nuclear extracts were added to the ELISA plate and incubated overnight. The plate was washed and incubated with antibody against p65. After incubation with the HRP-conjugated secondary antibody, substrate was added and absorbance was measured at 450nm using Infinite® 200 PRO microplate reader (Tecan, Switzerland).

3.4.3 HDACs activity assay

Epigenase™ HDAC activity/inhibition direct colorimetric assay kit (Epigentek, USA) was used to determine HDAC activity in nuclear extracts of cells or in whole cell lysate. An amount of 10µg protein was added per well, which are coated with acetylated histone HDAC substrate. The deacetylated products were detected with a specific antibody conjugated with HRP and measured spectrophotometrically at 450nm.

3.5 Histological techniques

3.5.1 Haematoxylin & Eosin staining (H&E staining)

Paraffin sections were cut with 0.3µm thickness and were stained with haematoxylin and eosin (H&E) using standard protocols. Briefly, sections were deparaffinised and hydrated by heating at 60°C for 1h and then by passing the slide through a series of three times of xylol, followed by a decreasing concentration of ethanol from 99,6% till 70%. After washing shortly in water, sections were incubated in Mayer's hematoxylin (AppliChem, Darmstadt, Germany) for 20min, washed shortly under running water to get rid of excess dye and then incubated with Eosin Y (AppliChem, Darmstadt, Germany). Slides were then washed briefly in water then rehydrated in a series of increasing ethanol concentration and then 3 times in xylol each for 10min. Finally slides were mounted with Pertex (Medite GmbH, Germany) and sections were scanned with Nanozoomer 2.0HT digital slide scanner C9600.

3.5.2 Immunohistochemistry (IHC)

Mouse lungs were dissected and fixed with 4% paraformaldehyde in 1xPBS overnight at 4°C. The tissue samples were rinsed in 1xPBS, dehydrated, and then embedded in paraffin blocks. Three-micrometer tissue sections were deparaffinized, rehydrated in graded series of alcohol. For antigen retrieval, sections were cooked in 10mM citrate buffer for 20 minutes, then kept warm for further 10min or they were treated with Trypsin or EDTA according to the antibody. Endogenous peroxidase activity was quenched with methanol containing 3% H_2O_2. Non-specific binding was blocked with 5% of specific serum or 10% BSA for 1 hour. After blocking, sections were incubated with primary antibodies overnight at 4°C. Immunohistochemistry was performed using the following antibodies at the indicated dilutions: CD11b (1:100), CD3 (1:200) and MTA2 (1:200). Following primary antibody incubation, sections were incubated with the corresponding secondary antibodies of the ImmPRESS peroxidase reagent kit (Vector Laboratories, USA) for 60 minutes at room temperature then sections were developed with DAB or NovaRed (Vector Laboratories). Sections were then counterstained with hematoxylin solution, Gill Nr.1 (Sigma Aldrich, USA) or methylgreen (Vector Laboratories Inc, Burlingame, USA) and mounted with Pertex after dehydration. Finally, slides were scanned with Nanozoomer 2.0HT digital slide scanner C9600 (Hamamatsu Photonics, Japan). Negative controls included the omission of the

primary antibody. (Detailed information on the primary antibodies used is listed in Appendix I, Table 9.9).

3.5.3 Immunofluorescence

For immunofluorescence, tissue sections were hydrated and incubated with trypsin for 10 min for antigen retrieval or with citrate for 30min. Then, tissues were blocked in 5% BSA with 0.1% Triton-X in PBS for 1h at RT, to avoid unspecific binding of the antibodies. The following primary antibodies were used: p-p65 (Ser311), p65, MMP9, C-Raf, PCNA, MTA2 and IKK2 all diluted 1:200. After incubation with the primary antibodies at 4°C overnight, slides were incubated with the corresponding Alexa Fluor®-labelled secondary antibodies (Invitrogen, Molecular Probes, Invitrogen, Paisley, UK) at a dilution of 1:1000, counterstained with 4,6-diamidino-2-phenylindole (DAPI, Life Technologies, USA) and mounted with Dako fluorescent mounting media (Dako, North America, Inc., USA). Quantification of total fluorescent intensity was carried out by computer-aided image analysis using ImageJ software. (Detailed information on the primary antibodies used and the corresponding conditions is listed in Appendix I, Table 9.9).

3.6 Animal experiments

Wildtype C57Bl/6J animals were purchased from Charles River Laboratories (Sulzfeld, Germany) and transgenic animals were provided by Prof. Ulf Rapp. Animals were kept in individually ventilated cages (IVC) in a pathogen-free environment and were handled in accordance with the European Union commission on Laboratory animals. Animal study proposals were approved by the Regierungspräsidium Giessen, the local regulatory authorities for animal research in Hessen, Germany (Animal proposals B2/233 and B2/1026).

3.6.1 Transgenic animal model

SpC C-Raf BxB

SpC C-Raf BxB transgenic mice were maintained as hemizygotes in the C57 BL/6 mouse strain background. They express a truncated C-Raf -lacking the regulatory domain- under the control of the surfactant protein C (SPC) promoter. This leads to lung-targeted expression of C-Raf BxB in alveolar type II cells leading to the formation of lung adenomas as early as 3 months of age[18]. Polymerase chain reaction was used to secure the transgenic status as described in section 3.6.3.

Tet-O-IKK2^{CA} and Tet-O-IKK2^{DN}

Mice were developed by Wirth T group (Ulm University, Germany). The mice carry either a constitutively active form of IKK2 with activating mutations at S177E and S181E (referred to as Tet-O-IKK2^{CA} or short IKK2^{CA}), or they carry a down-regulated form of IKK2 with mutation at D145N (referred to as Tet-O-IKK2^{DN} or short IKK2^{DN})[91]. As such the mice don't show any phenotype.

3.6.2 Breeding and Induction

Tet-O-IKK2^{CA} and Tet-O-IKK2^{DN} were cross bred with SpC rtTA mice to obtain ATII-specific IKK2 changes, referred to as SpC rtTA/Tet-O-IKK2^{CA} (short SPC/IKK2^{CA}) or SpC rtTA/Tet-O-IKK2^{DN} (short SPC/IKK2^{DN}), respectively. The double transgenic mice were induced by doxycycline (Fagron, USA) supplemented in food (725mg/kg). Transgene induction started at week 5 postnatal after complete lung development.

For the generation of compound triple transgenic mice, SpC C-Raf BxB mice (referred to as BxB) were cross bred with SpC rtTA/Tet-O-IKK2^{CA} or SpC rtTA/Tet-O-IKK2^{DN} to generate

SpC rtTA/Tet-O-IKK2^{CA}/SpC C-Raf BxB (short: SPC/IKK2^{CA}/BXB) and SpC rtTA/Tet-O-IKK2^{DN}/SpC C-Raf BxB (short: SPC/IKK2^{DN}/BXB), respectively. Transgenes were expressed conditionally in ATII cells upon feeding the mice with food supplemented by doxycycline. Induction of compound mice was for 50-56 weeks.

3.6.3 Genotyping

Mice were genotyped via tail tip samples of pups. Tails were lysed in 190µl of tail lysis buffer (50mM EDTA pH8, 50 mM Tris pH 8, 0.5% SDS) supplemented with 10µl proteinase K (10mg/ml; Sigma Aldrich, Germany) and incubated at 56°C for 4h or overnight. After incubation and complete lysis of tail tissue, the samples were centrifuged for 15 minutes at maximum speed at 4°C. Then samples were diluted 1:10 before using as a DNA template for PCR using the master mix described in Table 3.5. Primers used for genotyping are listed in Appendix II, Table 9.7.

Table 3.5 Reaction master mix for genotyping PCR

Component	Volume (µl)
Taq buffer 10x	3
dNTP (10mM)	3
Forward primer (10mM)	0.3
Reverse primer (10mM)	0.3
Taq Polymerase	0.3
Nuclease free water	21.1
cDNA template	2
Total	30

3.6.4 Subcutaneous xenograft (autochthonous) model

Mice were injected subcutaneously with 3x10^6 cells in 0.2ml PBS into their hind flank. Tumours were measured every 4 days using an external digital caliper to measure the greatest longitudinal diameter (length) and the greatest transverse diameter (width). The tumour volume was calculated by the modified ellipsoidal formula[92].

$$Tumour\ Volume\ (mm^3) = \frac{1}{2}\ (Length\ x\ Width^2)$$

The whole body weight of the mice was also monitored every 4 days throughout the experiment. Mice were sacrificed after 21 days and lungs and subcutaneous tumours were isolated to quantify expression on both protein and RNA level.

3.6.5 Magnetic resonance imaging of the lung

Mice were anaesthetized with 1.5% isofluorane and placed abdominally inside the coil of a magnetic field. The abdominal area of mice was scanned using respiratory-gated UTE-3D sequence with a repetition time of 8.0ms, echo time of 20µs, slice thickness/interslice distance: 0.39/0.39mm, field of view 2.50x2.70x5.00cm^3 and a matrix of 128/128/128. Images were analysed in axial view using ImageJ software. The heart ventricles in the upper part of the images were used to normalize each image[93].

3.6.6 Lung compliance

Lung compliance was measured by FlexiVent (SCIREQ, emka Technologies, France) which is a computer-controlled research ventilator for small animals. After anesthetization, mice were connected to FlexiVent via the trachea and ventilated with a tidal volume of 10ml/kg at a frequency of 150breaths/min and a positive end-expiratory pressure of 3cm H_2O. Three perturbations were performed in the following order: deep inflation v7.0; an 8s broadband perturbation (primewave-8); pressure-volume loops including stepwise inflation and deflation of 1ml of air (PVs-V). The three perturbations were performed and recorded. The inspiratory capacity (IC) was obtained through the perturbation of deep inflation v7.0. A forced oscillation perturbation, primewave-8, was applied to calculate the resulting impedance data as tissue damping or tissue resistance (G), tissue elastance (H) and tissue hysteresivity (G/H = η). PV-loops were generated to obtain static compliance (Cst)[94]. After finishing the measurements mice were then used for further analysis and tissue collection.

3.7 Statistical analysis

Statistical analyses were performed with GraphPad Prism 5 Software (GraphPad Software, Inc.). Student's *t* test (two-tailed) was used to compare two groups. When more than two groups were compared, differences among the groups were determined by one-way ANOVA with Tukey's posttest for unpaired non-parametric variables. Outliers were identified using ROUT with Q=1%. Data are expressed mean ± SEM; statistical significance was set at $p \leq 0.05$. Significance level is noted as follows: * $p \leq 0.05$, ** $p \leq 0.01$, ***$p \leq 0.001$, ****$p \leq 0.0001$.

4 Results

4.1 NF-ƙB is increased in cancer cells

NF-ƙB is a major inflammatory pathway that is activated both via intrinsic and extrinsic factors[50]. In order to check for the NF-ƙB pathway in lung cancer, several lung cancer cell lines (A549, Colo699, H1650, and H2122) were analysed for their basal expression of p50 and p65 (referred to as *NFKB1* and *RELA,* respectively). By comparing them with BEAS-2B (B2B) cells as control cells, which are normal but immortalized human bronchial epithelial cells, A549, Colo699, H1650 cell lines showed increased levels of both NF-ƙB genes whereas H2122 showed only higher expression of *NFkB1* (Fig. 4.1a). However, after LPS (5 µg/ml) stimulation for 2h, all cell lines showed higher level of activation as measured with target genes *MMP9* and *FN1* (Fig 4.1b). *NFKB1* and *RELA* are also target genes for NF-ƙB canonical signalling which are responsible for positive feedback activation sustaining the activity of NF-ƙB. The extent of activation varied between cell lines depending on the target gene selected and on the exposure time to stimulus.

In the canonical NF-ƙB pathway, LPS and TNFα are both classical external stimulants of NF-ƙB. Cells were transfected with NF-Gluc vector, a reporter plasmid expressing Gaussia luciferase under the response elements of NF-ƙB then 24h later they were treated with stimulants for 24h. The activity was checked in the medium as Gaussia luciferase is secreted (Fig. 4.2a). Increased luciferase activity was observed upon stimulation in all cell lines (BEAS-2B, A549, Colo699, H1650 und H2122) where TNFα showed stronger effects than LPS except in H2122 cell line. Another major response to stimulation is the nuclear translocation of the heterodimer p50/p65. Immunocytochemistry of H2122 stimulated with LPS (for 1h and 6h) and TNFα (for 30 minutes and 6h) showed stronger nuclear p50 and p65 after stimulation compared to the unstimulated control (Fig. 4.2b).

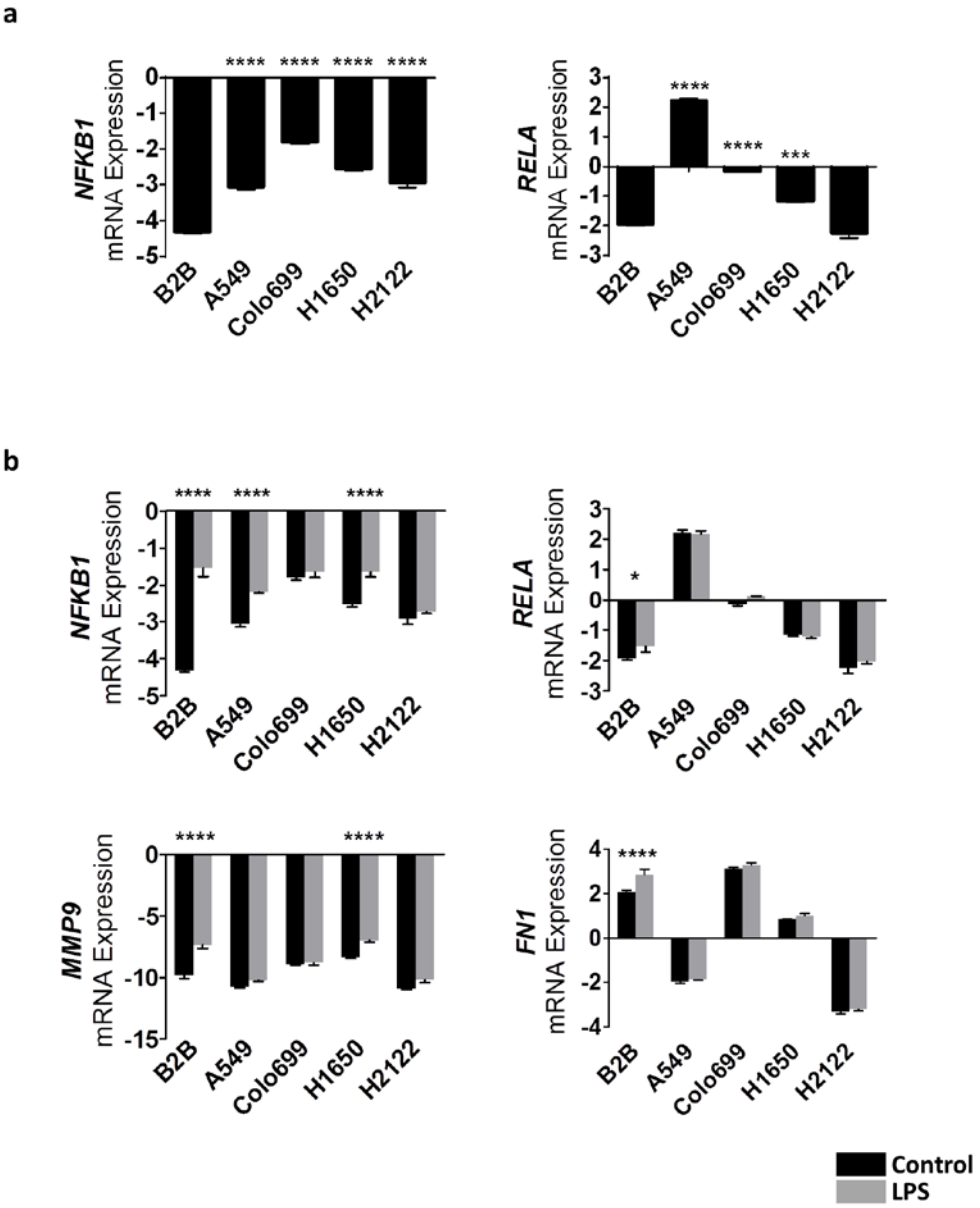

Figure 4.1 Activation of classical NF-kB pathway in different human cancer cell lines. a) Basal expression of NFKB1 and RELA in adenocarcinoma cell lines compared to BEAS-2B (B2B) cells as healthy control. b) Cells were stimulated with LPS (5µg/ml) for 2h. The level of mRNA expression of NF-kB and target genes fibronectin (FN1) and MMP9 was calculated as ΔCt of the gene of interest normalized to HPRT as housekeeping gene. Data are represented as mean ± SEM. * p ≤ 0.05, ***p≤ 0.001, ****p≤ 0.0001 (n=3) compared to untreated sample of the respective cell line.

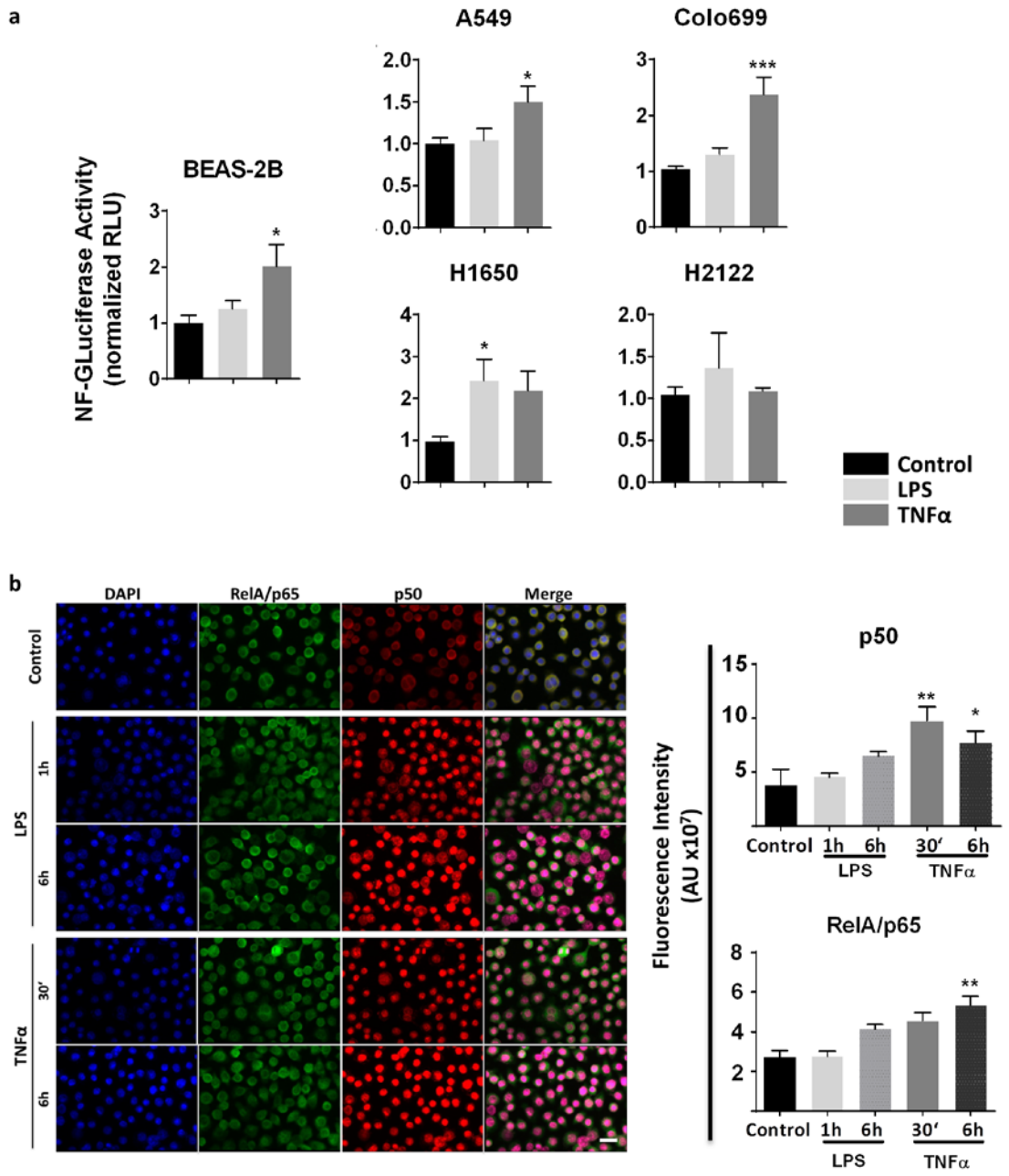

Figure 4.2 NF-kB activity and localization upon stimulation with LPS and TNFα. a) NF-GLuciferase reporter assay after treatment with LPS (5µg/ml) and TNFα (5ng/ml) for 24h. Activity is represented as relative luminescence unit (RLU) normalized to the activity of the corresponding untreated control. Data are represented as mean ± SEM. * $p \leq 0.05$, *** $p \leq 0.001$. b) Immunocytochemistry for H2122 after LPS stimulation for 1h and 6h and after TNFα treatment for 30 minutes and 6h showing nuclear translocation of p50 (red) and p65 (green) with DAPI as nuclear counterstain. Scale bar is 25µm. Right panels show quantification of fluorescence intensity of individual channels of five representative images as analysed with ImageJ software.

4.1.1 NF-ƙB is classically regulated and activated via IKK2

As NF-ƙB heterodimer consists of p50 and p65, looking for an upstream yet specific regulator would impact both entities but only in their active form. It is known that IKK2, a kinase member of the trimeric IKK-complex together with IKK1 and NEMO, regulates the heterodimer p50/p65 via phosphorylation of IƙB so that the inhibitor is degraded by the proteasome and the p50/p65 dimer is translocated to the nucleus where it drives the expression of various target genes[95]. In this respect, A549 were stably transfected with $IKK2^{CA}$, a constitutively active form of IKK2. Overexpression of $IKK2^{CA}$ increased NF-ƙB activity as seen by NF-Gluc reporter assay (Fig. 4.3a, left panel) as well as in Western blots. At protein level, $IKK2^{CA}$ showed less IƙB and less p105, both known as NF-ƙB signalling inhibitors, compared to A549 with empty vector (EV). Less IƙB is a sign of the fast degradation of IƙB due to IKK2-dependent phosphorylation. Lower levels of p105, the precursor for p50, indicates its proteosomal degradation into p50 upon NF-ƙB activation. Besides, the level of CyclinD1, a target gene of NF-ƙB signalling, was elevated (Figure 4.3b).

Overexpression of $IKK2^{CA}$ also increased both proliferation and migration of A549 cells (Figure 4.3c and 4.3d). In addition, cells were treated with different concentrations of a selective IKK2 inhibitor, sc-514, that prevents its phosphorylation and thus the downstream activation of p50/p65 complex. Treatment with the classical proteasome inhibitor MG-132 was used as control for the suppression of NF-ƙB activation pathway. In line with the results of $IKK2^{CA}$ overexpression, treating the cells with either inhibitor (sc-514 or MG-132) reduced the luciferase activity (Figure 4.3a) as well as the functional activity of tumour cells reflected in decreased proliferation (Figure 4.3c, right panel) and less migratory capacity (Figure 4.3d, right panel).

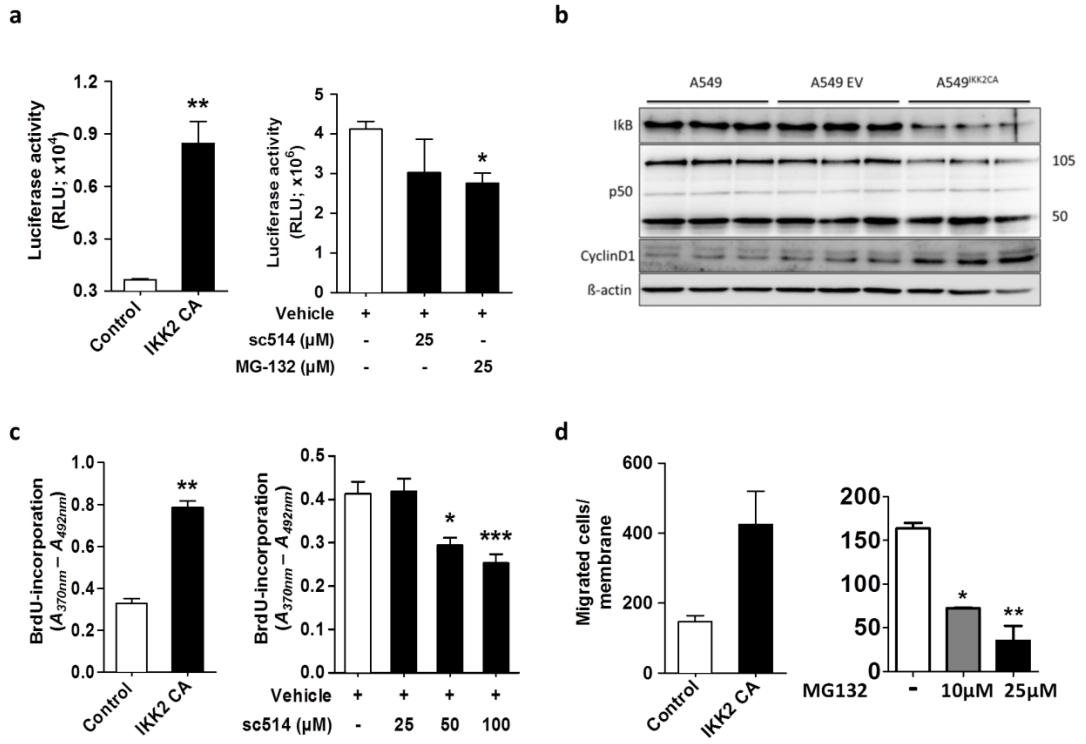

Figure 4.3 IKK2 regulation of NF-ƙB activity. A549 cells were either transfected with IKK2CA or an empty vector (EV) as control (left panels). They were also treated with sc-514, a selective IKK2 inhibitor, or with MG-132, a proteasomal inhibitor (right panels). NF-ƙB activity was assessed with a) Gaussia Luciferase reporter assay using NF-Gluc vector and is represented as relative luminescence unit (RLU) and with b) Western blot for IƙB, p105/p50 and CyclinD1 as a target gene. β-actin was used as loading control. Functional effects of IKK2 regulation was measured on c) Proliferation assessed by BrdU incorporation assay and on d) migration assay with Boyden Chamber. Data are represented as mean ± SEM. * $p \leq 0.05$, ** $p \leq 0.01$, *** $p \leq 0.001$. Data shown are representative of three individual experiments.

4.1.2 Overexpression of C-Raf activates IKK2-regulated NF-ƙB signalling pathway

The role of IKK2 in activating NF-ƙB and subsequently affecting proliferation and migration, both major steps for cell transformation, indicated the role of IKK2 in tumour progression. It was of value before proceeding to the animal model, to investigate whether IKK2 activation was also observed in known SpC C-Raf BxB model *in vitro*. C-Raf has two main domains, a regulatory domain, where there is the K-Ras interaction site, and a kinase domain (Fig.4.4a). Deletion of the regulatory domain of C-Raf creates a constitutively active form of C-Raf. This truncated form is known as C-Raf BxB[18]. A549 cells were transfected with C-Raf BxB together with a reporter luciferase under the control of NF-ƙB response elements (Fig. 4.4b). C-Raf increased the NF-ƙB activity indicating that the animal tumour model is an inflammatory model with increased basal NF-ƙB activity.

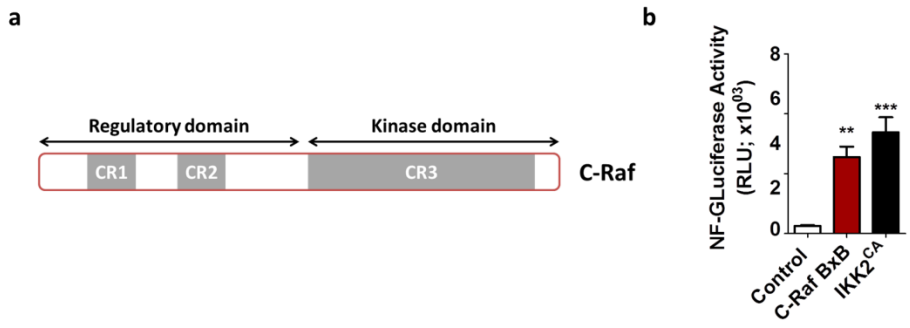

Figure 4.4 Overexpression of C-Raf BxB increases NF-kB activity. a) Schematic diagram of C-Raf domains (CR = conserved region) b) Gaussia Luciferase reporter assay using NF-Gluc vector in A549 cells transfected with C-Raf BxB and IKK2CA. Data are represented as relative luminescence unit (RLU) as mean ± SEM. ** $p \leq 0.01$, ***$p \leq 0.001$.

4.1.3 Changing IKK2 in alveolar type II cells affects tumour growth in SpC C-Raf BxB mice

SpC C-Raf BxB mice were cross bred with mice expressing a SpC rtTA/Tet-O-IKK2^{CA} (S177E, S181E), or with SpC rtTA/Tet-O-IKK2^{DN} (D145N) to generate inducible compound triple transgenic mice (SpC rtTA/Tet-O-IKK2^{CA}/SpC C-Raf BxB and SpC rtTA/Tet-O-IKK2^{DN}/SpC C-Raf BxB) . Detailed information is represented in the schematic diagram in Fig. 4.5a. After complete lung development (5 weeks old), mice were induced with Doxycycline in the food to activate the transgenes. After induction for 50-56 weeks, tumour development was assessed via magnetic resonance imaging (MRI).

As the BxB tumour model forms a dispersed pattern of lung adenomas, pixel image analysis was performed to quantify the tumour burden. Dark spaces indicate air-filled areas whereas grey areas are occupied by tissue. Downregulation of IKK2 in ATII cells (SpC/IKK2^{DN}/BxB) reduced the tumour burden compared to SpC C-Raf BxB whereas SpC/IKK2^{CA}/BxB showed higher tumour burden (Figure 4.5b). These findings were supported with histological examination which revealed that in mice with downregulated IKK2, adenomas were significantly less dispersed than in control SpC C-Raf BxB mice and in mice with activated IKK2 (Figure 4.5c).

For functional quantification of the tumour burden, lung compliance was measured. Both resistive compliance and inspiratory capacity were reduced with increasing tumour burden in mice expressing C-Raf BxB (BxB) or activated IKK2 (SpC/IKK2^{CA}/BxB) whereas tissue damping and elastance increased (Figure 4.5d). Downregulation of IKK2 in BxB mice rescued

the decreased lung compliance to a comparable level to that of control wildtype lungs. However, the differences between SpC C-Raf BxB control mice and SpC rtTA/Tet-O-IKK2^{CA} weren't significant. This can be explained by the fact that C-Raf itself drives NF-ƙB activation so further activation of the pathway didn't show any significant additional effects.

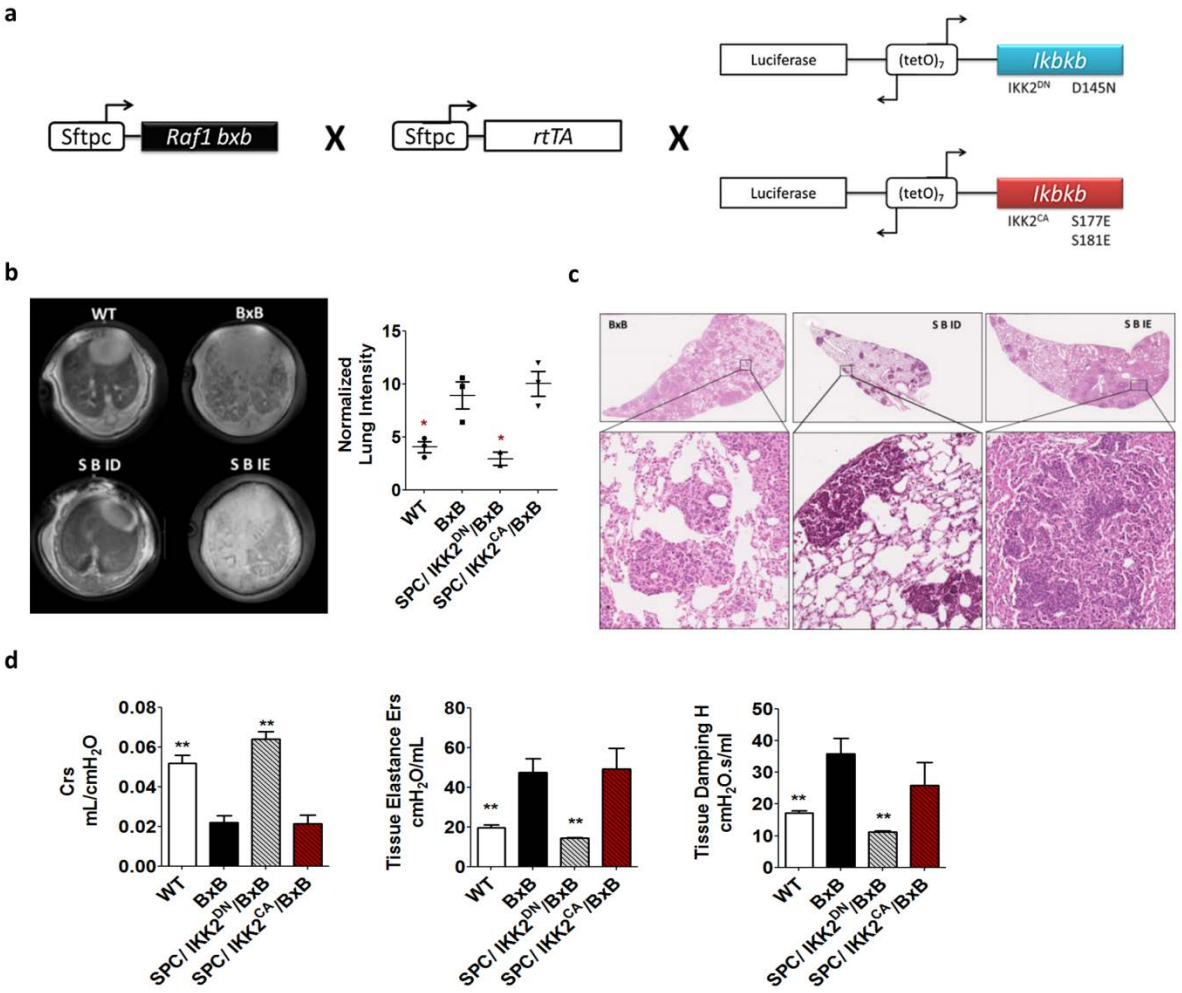

Figure 4.5 . IKK2 modulation in SpC C-Raf BxB transgenic mice. a) Schematic diagram representing the breeding scheme for the development of triple transgenic mice b) MRI representative images (left panel) and image quantification (right panel) c) Histological H&E staining of 3µm thick sections of the lung. d) Lung compliance measured as resistive compliance (Crs), Tissue elastance (Ers) and tissue damping (H) Data are represented as mean ± SEM compared to BxB. * $p \leq 0.05$, ** $p \leq 0.01$,. (n=5 for WT; n=3 for BxB; n=2 for SPC/IKK2^{CA}/BxB and for SPC/IKK2^{DN}/BxB).

To get a closer look on the activation of NF-ƙB within the cells, lung sections were fluorescently immunostained with phosphorylated p65 (Ser311) and MMP9 as a selected NF-ƙB target gene. Compound mice with activated IKK2 (IKK2^{CA}) showed higher expression of both p65 and MMP9 (Figure 4.6a). Even SpC C-Raf BxB single transgenic mice showed substantially high expression of both p65 and its target gene MMP9 indicating the intrinsic effect of C-RAF on IKK2-activated canonical pathway. Furthermore, IKK2 activation promoted

proliferation as seen with PCNA staining. C-Raf was uniformly expressed in all groups (Fig.4.6b).

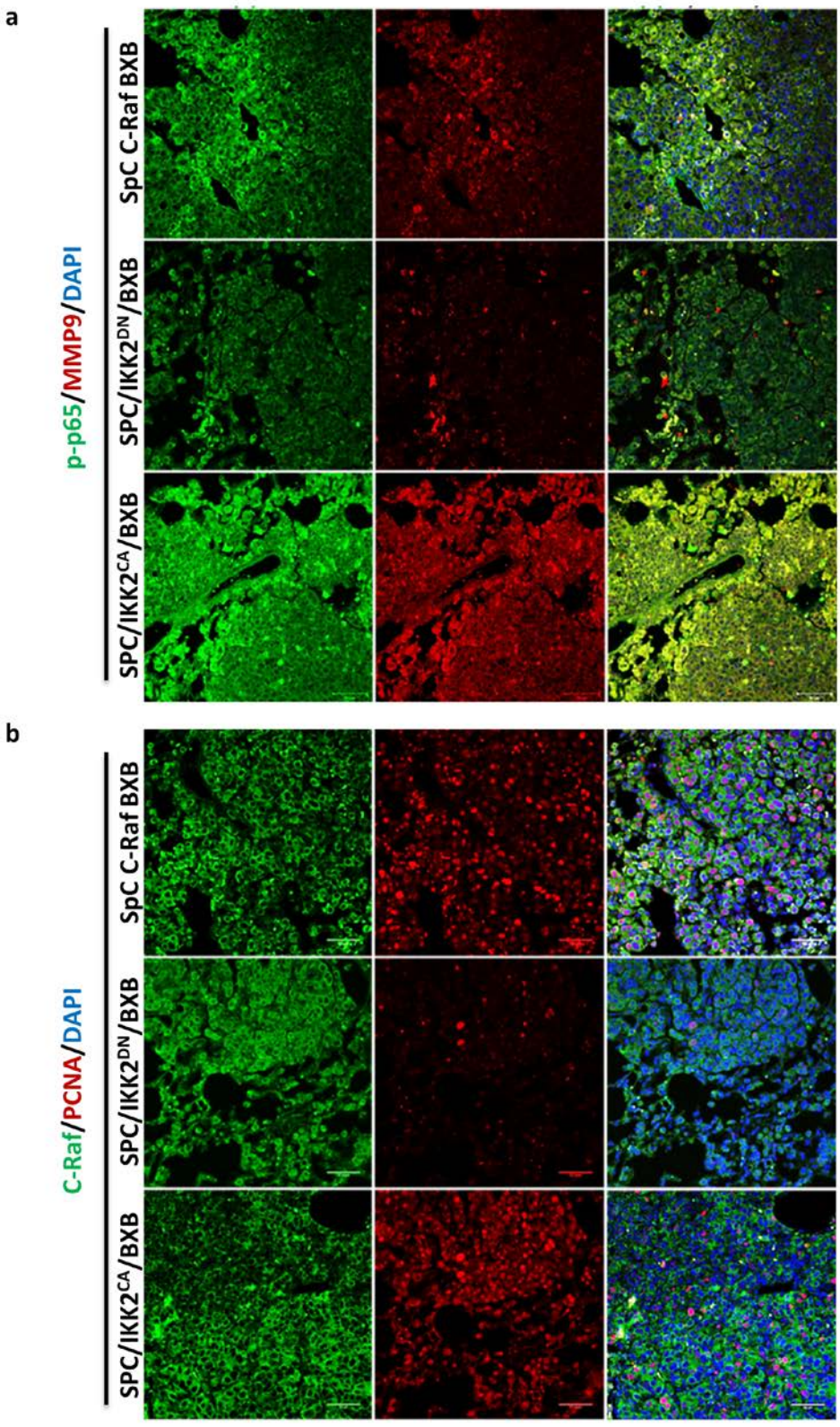

Figure 4.6 Immunofluorescence staining of the lungs of compound mice. Representative images of lung sections stained with a) phosphorylated p65 (p-p65, Ser3133) and MMP9; and b) C-Raf and PCNA using DAPI as nuclear counterstain. Scale bar represents 50µm (n=3).

4.1.1 Analysis of the tumour microenvironment in IKK2-regulated SpC C-Raf BxB mice

As the tumour microenvironment plays an important role in tumour progression, we postulated that changes in the host epithelial cells might influence the recruitment of immune cells. Upon comparison of double transgenic mice without BxB tumours, SpC/IKK2^{CA} showed increased infiltration of neutrophils and dendritic cells whereas T-cells and macrophages were not significantly changed (Fig. 4.7a). On the other hand, in presence of C-Raf BxB tumour burden, triple transgenic mice with IKK2^{CA} mainly recruited more T-cells and neutrophils. Changes in dendritic cells and macrophages showed similar tendency though a closer differentiation between the subtypes of macrophages could provide a better understanding of the effects of immune cell recruitment (Fig. 4.7b). On the contrary, IKK2 downregulation lead to less recruitment of all examined immune cells. However, these changes in the tumour microenvironment could not explain the restricted tumour growth in SpC/IKK2^{DN}/BxB suggesting that the signalling changes within the host alveolar type II cells could be the main effector for tumour restriction.

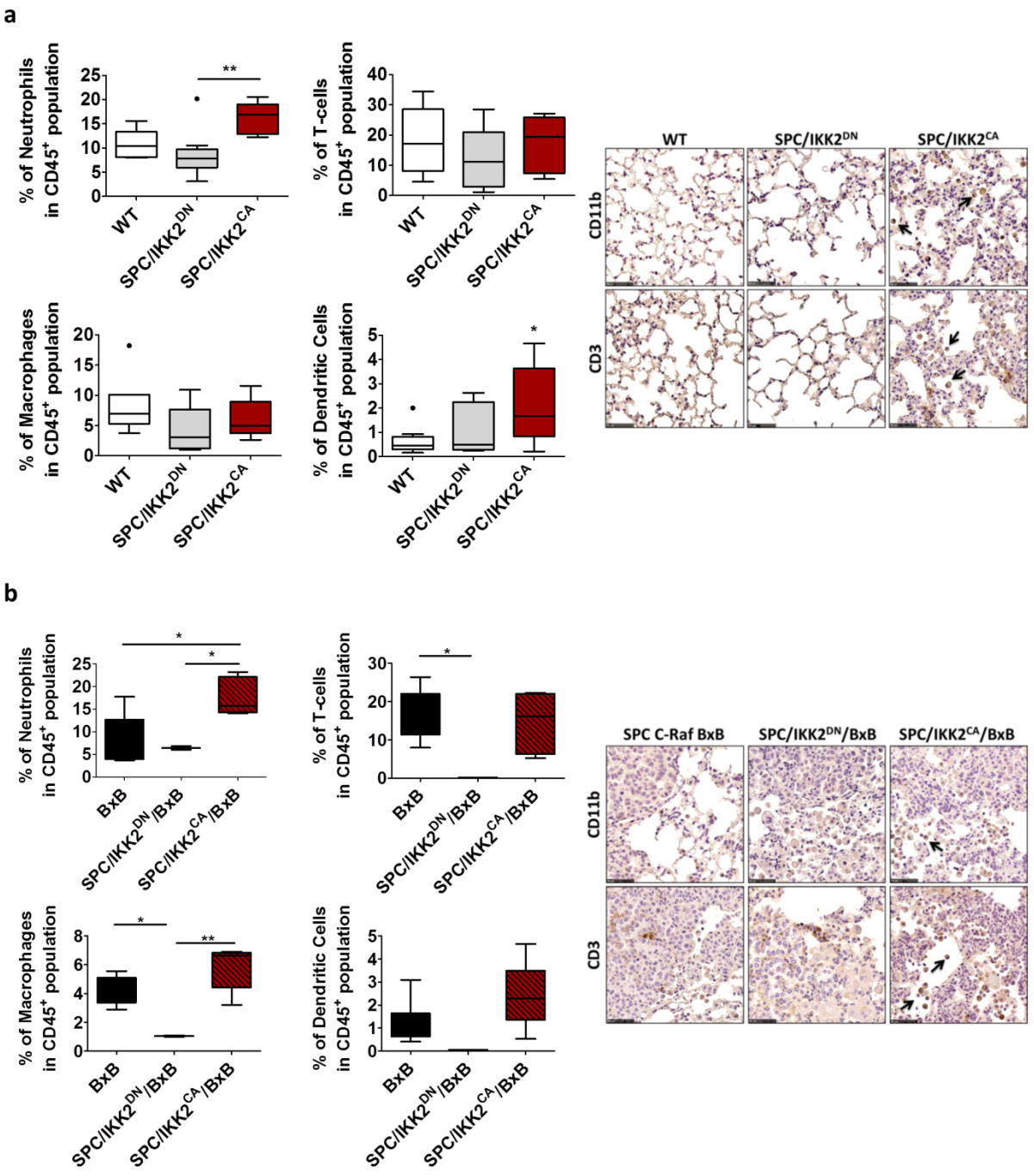

Figure 4.7 Flow cytometry of different inflammatory lung cell populations. a) quantification of neutrophils, macrophages, T-cells and dendritic cells in double compound mice compared to wildtype mice (left panel) and representative histological pictures for $CD11b^+$ cells and $CD3^+$ cells or T-cells (right panel) b) quantification of neutrophils, macrophages, T-cells and dendritic cells in triple transgenic mice compared to SPC C-Raf BxB mice (left panel) and representative histological pictures for $CD11b^+$ cells and $CD3^+$ cells or T-cells (right panel). Data are represented as mean ± SEM. * $p \leq 0.05$, ** $p \leq 0.01$. Scale bar represents 50µm (n=4).

4.1.2 IKK2 in the lung affects its role as a metastatic niche

The modulation of IKK2 in ATII cells outranged the effect in epithelial cells and extended to affect the surrounding immune environment. This is why it was of interest to investigate whether these changes would influence metastasis to the lung. A commonly used animal mouse tumour model is the xenograft subcutaneous tumour growth of Lewis Lung Carcinoma cells (LLC1) in C57Bl/6J mice, which have the same genetic background as the LLC1 cells. LLC1 cells ($3x10^6$ cells prepared in 200µl) were injected into the hind flank of double transgenic mice; SpC/IKK2^{DN} and SpC/IKK2^{CA}, along with matched wildtype controls. Monitoring the primary tumour growth showed no significant differences between the groups (Fig. 4.8a). However, mice with SpC/IKK2^{CA} genotype carried more lung nodules than controls or SpC/IKK2^{DN} (Fig.4.8b,c). This inclines that changes of IKK2 within ATII cells had other molecular effects that affected the susceptibility of the lung to become a metastatic niche for homing cancer cells.

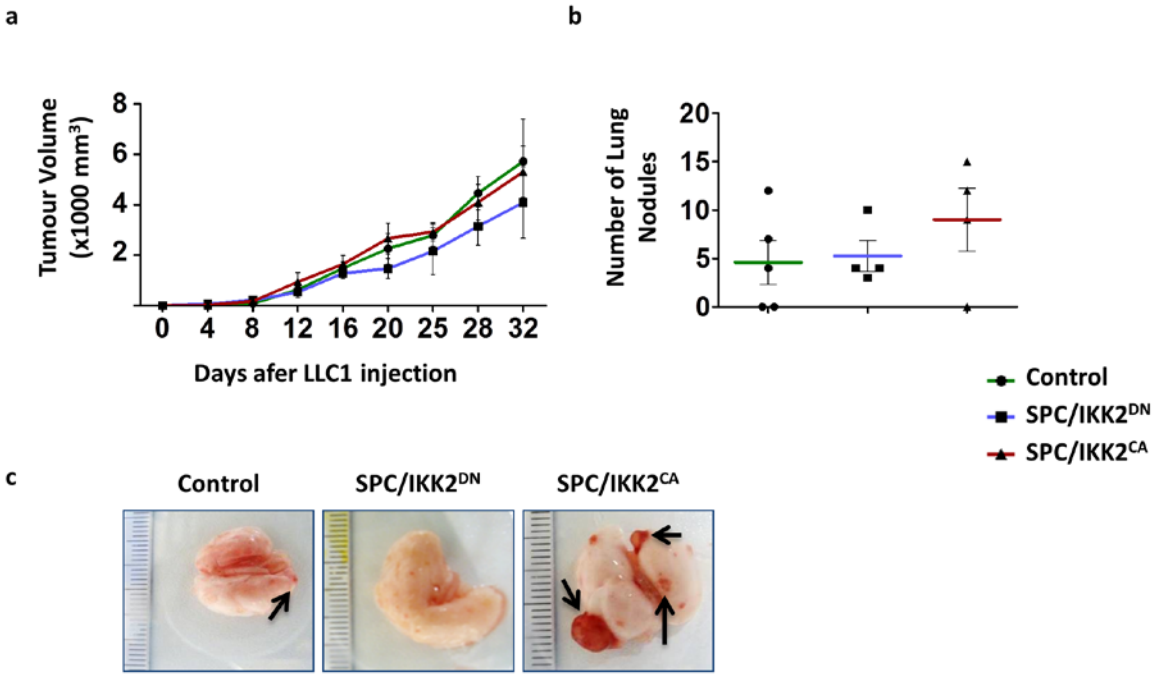

Figure 4.8 LLC1 xenograft subcutaneous model in SpC/IKK2DN and SpC/IKK2CA. a)Tumour volume of subcutaneous tumours measured every four days of the experiment. b) Number of nodules counted in the isolated lungs. Data are represented as mean ± SEM. c) Representative pictures of the isolated lung with arrows pointing at tumour nodules. (n=4 for SpC/IKK2^{DN} and SpC/IKK2^{CA} and n=5 for control group).

4.1.3 IKK2 regulates a panel of genes in alveolar type II cells

Alveolar type II cells (ATII) were isolated from the lungs of adult and long-term induced SPC-rtTA/Tet-O-IKK2^{DN} and SPC-rtTA/Tet-O-IKK2^{CA} mice and age-matched wildtype mice as control as described in the methods section. After culturing the cells for two days, they were stained for SPC to check for purity (Fig. 4.9b). The isolated cells expressed surfactant protein C (SPC), a key marker of alveolar type II cells. ATII cells isolated from SpC/IKK2^{DN} showed less nuclear p50 signal compared to control cells indicating the reduced activation of NF-kB pathway in these cells. After lysing the cells for total RNA isolation, the expression of NF-kB members was assessed. Expression of *Rela*, *Nfkb1* and *Mmp9* was downregulated in ATII cells of SpC/IKK2^{DN} mice compared to wildtype or SpC/IKK2^{CA} (Fig. 4.9c)

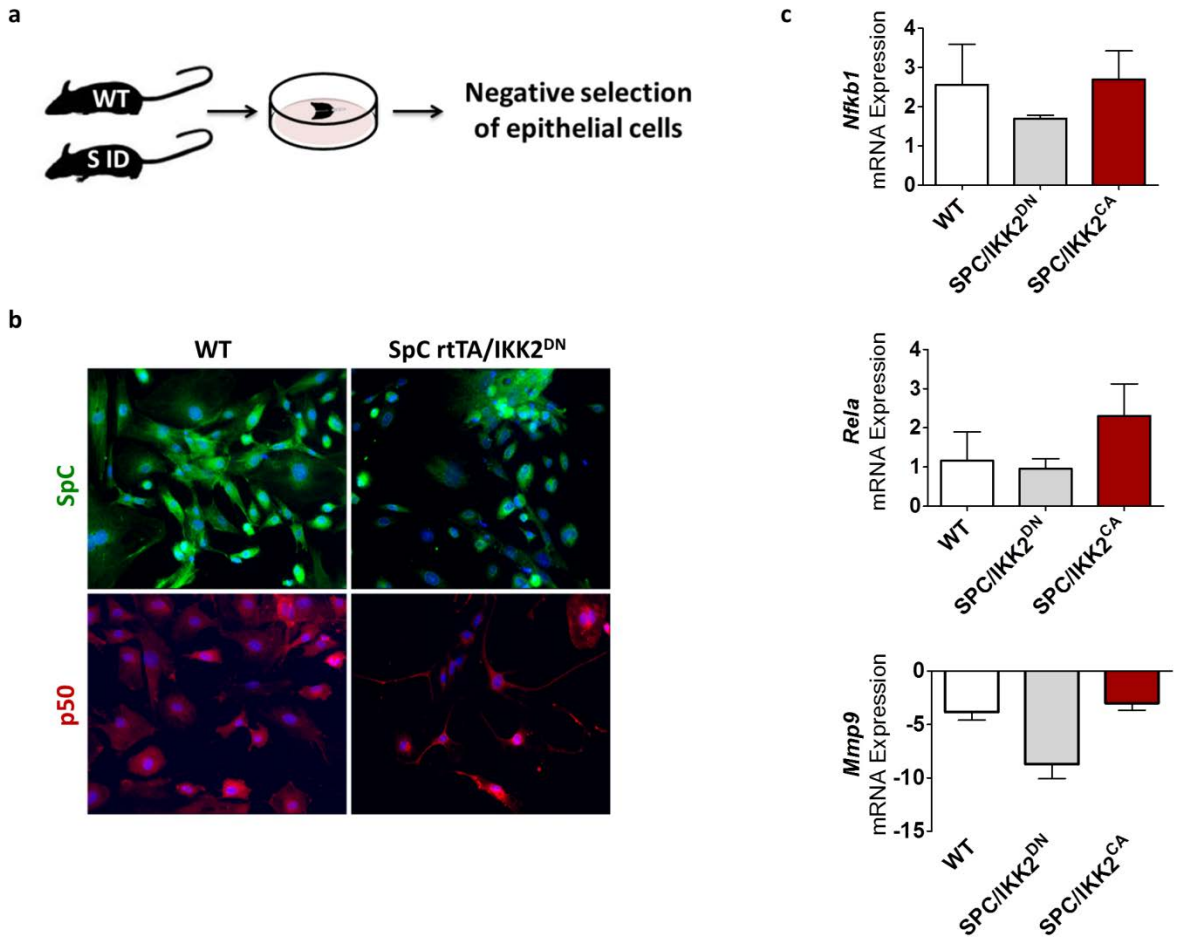

Figure 4.9 Isolation of alveolar type II cells. a) Schematic diagram for the isolation of ATII cells b) Immunocytochemistry of ATII cells with SPC and p50 antibodies c) Quantitative PCR for mRNA expression calculated as ΔCt of the gene of interest normalized to Hprt as housekeeping gene (n=4 for WT; n=2 for SPC/IKK2^{DN}; n=3 for SPC/IKK2^{CA}).

The cDNA from wildtype mice and from SPC/IKK2^{DN} was used on a RT² Profiler™ PCR Array Mouse Cancer PathwayFinder™ (Qiagen) which can determine the expression level of selected genes from various pathways involved in cancer, like growth control, apoptosis, angiogenesis, cell adhesion and metastasis. Based on the fold change compared to wildtype controls, the top ten upregulated genes and downregulated genes were selected (Table 4.1). From the list, those genes were selected that were novel, related to metastasis and were druggable.

After screening and validation of several targets, metastasis-associated protein member 2 (MTA2) was selected as a good candidate because it is known to be upregulated in many cancers and is an indicator for poor prognosis[77]. Interestingly, on examining the promoter of MTA2 for transcription factors binding sites, NF-ƙB binding sites were not found. Instead MTA2 promoter had binding sites for Oct factors which makes MTA2 a better candidate for studying. By examining the expression of MTA2 in existing mouse tumour models, Kras^{LA2} and SpC C-Raf BxB, MTA2 was found to be higher expressed in both tumour types (Fig. 4.10a). This suggests that MTA2 overexpression is an event of tumorigenesis. Interestingly, in human cancer cell lines, the expression of MTA2 was especially higher in those cell lines deriving from a metastatic site (H1437,H1299, Colo699) compared to control cell lines (BEAS-2B and isolated human fibroblasts) as well as to the cell lines A549, A427, H1975 and H23 which originate from primary sites (Fig. 4.10b).

Table 4.1 Top target genes regulated in alveolar type II cells by IKK2-downregulation compared to wildtype

Gene	Description	Fold Change	Binding sites to Transcription factors
Tert	Telomerase reverse transcriptase	0.014	CREB
Tek	Endothelial-specific receptor tyrosine kinase	0.119	CREB, Oct factors, GATA 1
Fgf1	Fibroblast growth factor 1	0.168	NF-ƙB
Mmp9	Matrix metallopeptidase 9	0.304	NF-ƙB
Pdgfa	Platelet derived growth factor, alpha	0.316	NF-ƙB
Sykb	Spleen tyrosine kinase	0.339	Oct factors
Bcl2	B-cell leukemia/lymphoma 2	0.344	NF-ƙB
Ncam1	Neural cell adhesion molecule 1	0.346	NF-ƙB
Twist1	Twist homolog 1 (Drosophila)	0.39	SP1
Mta2	Metastasis-associated gene family, member 2	0.398	Oct factors
Cdkn1a	Cyclin-dependent kinase inhibitor 1A (p21)	1.693	SP1
Mmp2	Matrix metallopeptidase 2	1.79	NF-ƙB
Pdgfb	Platelet derived growth factor, B polypeptide	1.79	NF-ƙB
Myc	Myelocytomatosis oncogene	1.866	CREB
Angpt1	Angiopoietin 1	1.972	NF-ƙB
Mdm2	Transformed mouse 3T3 cell double minute 2	2.056	Oct factors
Itga2	Integrin alpha 2	2.789	NF-ƙB, GATA 1
Hgf	Hepatocyte growth factor	2.949	TFII
Vegfc	Vascular endothelial growth factor C	4.028	NF-ƙB

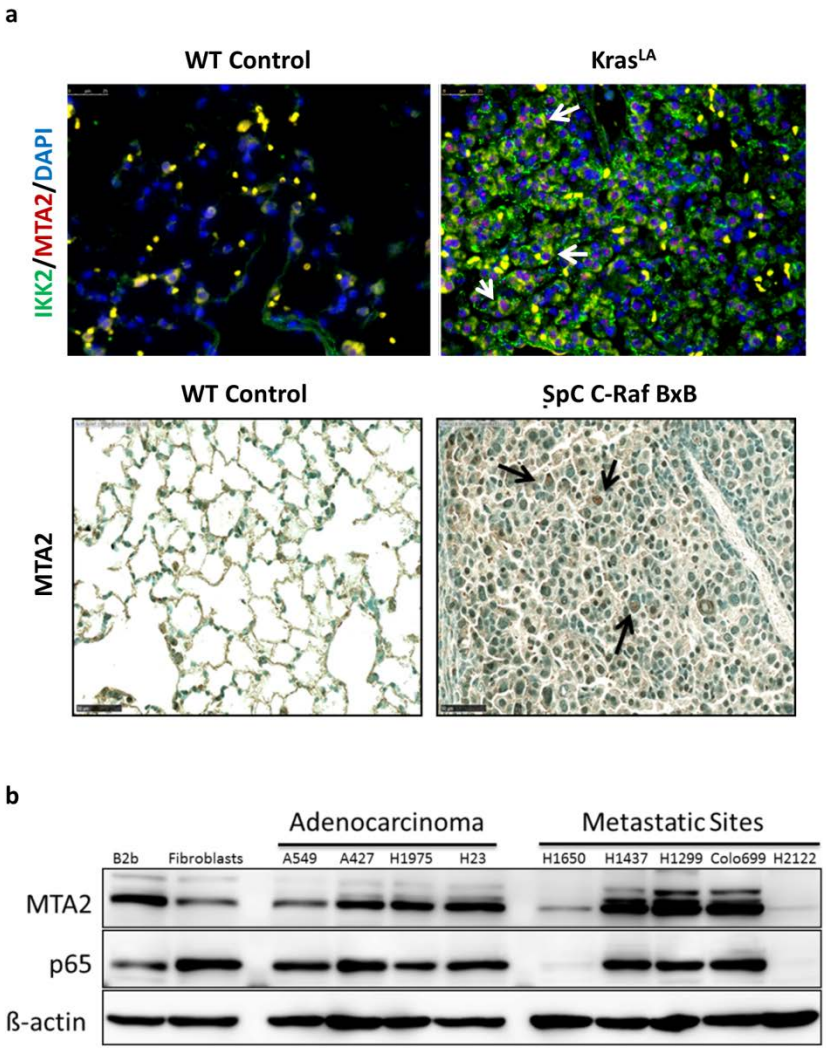

Figure 4.10 MTA2 expression in different mouse and human cancer types. a) Immunofluorescence of MTA2 and IKK2 in $KRas^{LA2}$ mouse lung compared to wildtype control with DAPI as nuclear stain (upper panel, scale bar 25µm) and immunohistochemistry of MTA2 in SpC C-Raf BxB lungs and control lungs with Methyl green as counterstain (lower panel, scale bar 10µm) b) Western blot of various human adenocarcinoma cell lines with BEAS-2B (B2B) and human fibroblasts as control. Cell lines were sorted according to their isolation sites either primary (adenocarcinoma) or metastatic sites. β-actin was used as loading control. Representative blot of three experimental replicas.

4.2 MTA2 regulates NF-ƙB activity in cancer cells

4.2.1 Is MTA2 downstream of NF-ƙB?

To verify whether NF-ƙB had transcriptional control on MTA2, A549 cells were treated with LPS as a classical stimulant of the canonical NF-ƙB pathway at two different concentrations. The expression of NF-ƙB target gene *MMP9* was increased in response to LPS, and the stimulatory effect subsided with time. Surprisingly, the levels of MTA2 declined unlike the expression of target genes, or of *NFKB1* and *RELA* (Fig. 4.11a). Even on protein level, the stimulation with TNFα failed to produce substantial changes in MTA2 levels. The minute increase in nuclear MTA2 levels after treatment was not proportional to the strong nuclear translocation of p50/p65 (Fig. 4.11b). Finally, to verify whether the irresponsiveness of MTA2 to extrinsic stimulus is specific to NF-ƙB pathway, MTA2 expression was checked in A549 overexpressing $IKK2^{CA}$. In corroboration with the data observed upon LPS stimulation, MTA2 was downregulated in these cells compared to control A549 or A549 carrying the empty vector (Fig. 4.11c).

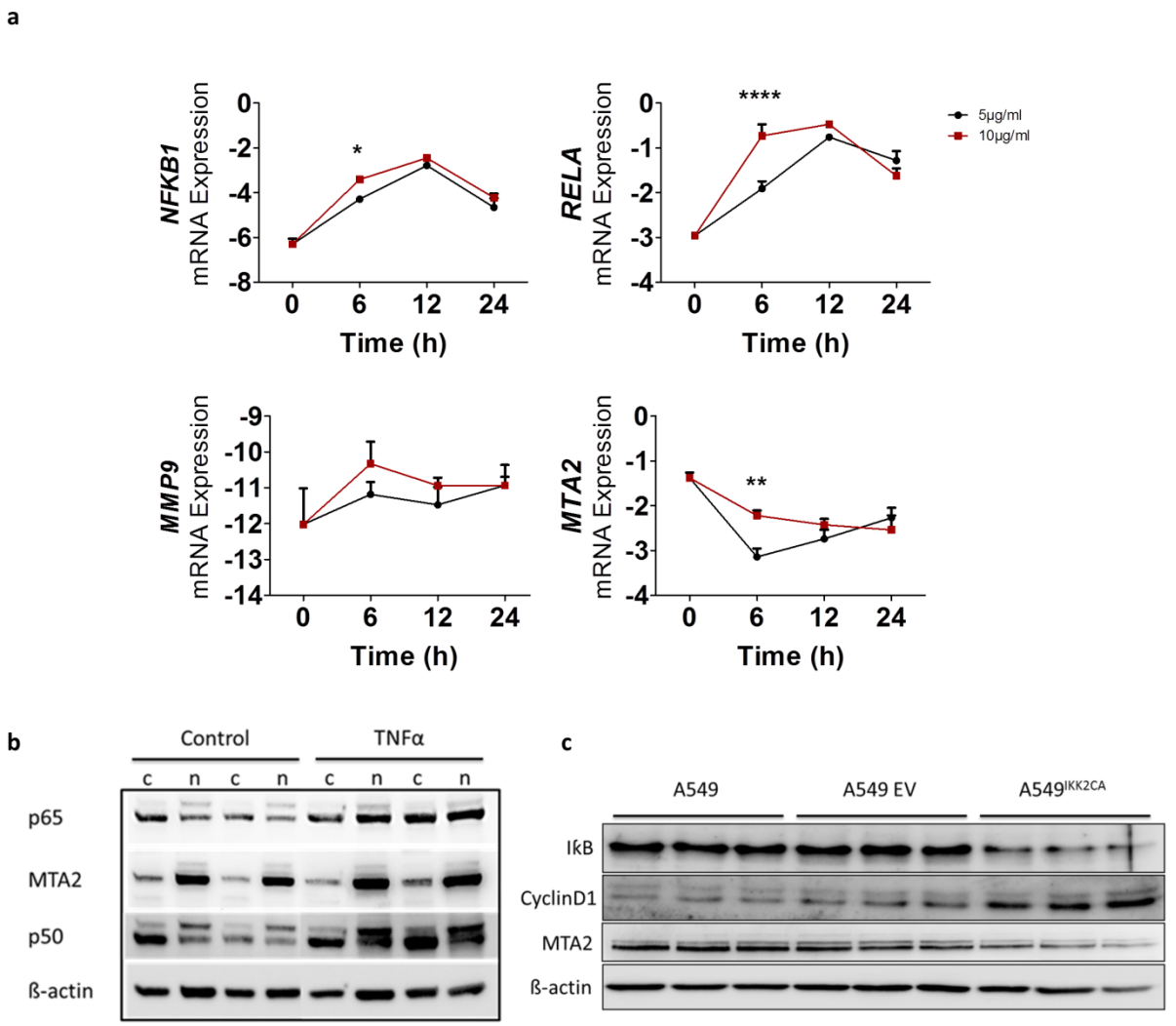

Figure 4.11 Expression of MTA2 upon activation of NF-kB pathway. a) RNA expression in A549 after stimulation with LPS at 5µg/ml and 10µg/ml for 6h, 12h and 24h calculated as ΔCt of the gene of interest normalized to *HPRT* as housekeeping gene. Data are represented as mean ± SEM. * $p \leq 0.05$, ** $p \leq 0.01$, **** $p \leq 0.001$. b) Western blot of cytoplasmic and nuclear fractions of A549 cells stimulated with TNFα (5ng/ml). c) Western blot of A549 overexpressing $IKK2^{CA}$ or the empty vector (EV) with β-actin as loading control. Representative blot of three experimental replicas.

Furthermore, LLC1 cells were checked for NF-kB activity. Similar to human cancer cell lines it showed basal NF-kB activity and thus LLC1 cells were treated with a panel of classical IKK2 inhibitors: sc-514, Bay11-7085, Parthenolide, and with the general proteasomal inhibitor MG-132. This treatment not only decreased NF-kB activity measured by a reporter assay with NF-Gluc (Fig. 4.12a) but strikingly MTA2 expression was downregulated (Fig. 4.12b).

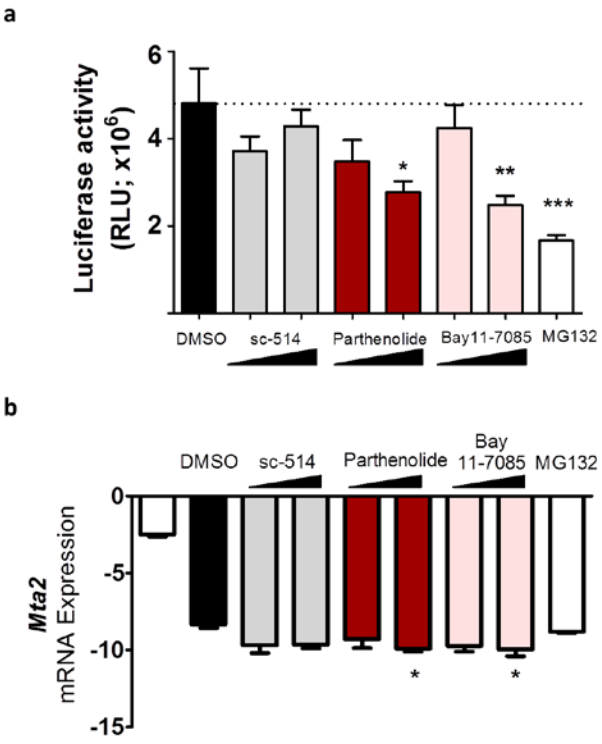

Figure 4.12 Expression of MTA2 upon downregulation of NF-ƙB pathway in LLC1 cells. LLC1 cells were treated with sc-514 (12.5µM and 25µM), Parthenolide (10µM and 20 µM), Bay11-7085 (5µM and 10µM) or MG-132 (25µM) for 24h. a) NF-ƙB activity assessed with Gaussia Luciferase reporter assay using NF-Gluc vector and data is represented as relative luminescence unit (RLU). b) mRNA expression of MTA2 calculated as ΔCt normalized to *Hprt* as housekeeping gene. Statistical analysis was performed using DMSO as control. Data are represented as mean ± SEM. * $p \leq 0.05$, ** $p \leq 0.01$, *** $p \leq 0.001$ compared to vehicle control (DMSO).

4.2.2 MTA2 downregulates NF-ƙB activity

As the response of MTA2 to stimulants and inhibitors of NF-ƙB pathway was ambiguous, it was less likely that MTA2 is downstream of NF-ƙB. To verify whether MTA2 affects NF-ƙB signalling, MTA2 was overexpressed in human A549 and RNA expression revealed a decline in the expression of *RELA* and *FN1*. However, the overexpression of MTA2 lead to the downregulation of *MTA1* inclining a possible complementary effect (Fig.4.13a). On the other hand, MTA family gene member 3 (MTA3) was not affected at all (Data not shown). A significant decline in NF-ƙB activity was also observed upon co-transfection of MTA2 and NF-Gluc, a Gaussia luciferase reporter. The decline in activity through MTA2 was stronger than that caused by IKK2 inhibitors, sc-514 and MG-132, suggesting a stronger or more downstream regulatory mechanism of MTA2 on NF-ƙB. Even the stimulatory effect of LPS was almost completely reversed in presence of MTA2 (Fig. 4.13b). In order to check whether this inhibitory effect was specific to A549 cells, other cancer cell lines (A427 and H460) as

well as HEK as control were transfected with MTA2 and in all cell lines tested, a significant reduction of NF-ƙB activity was observed (Fig. 4.13c). However, the reduction of NF-ƙB activity in cancer cell lines were stronger than in HEK cells disposing a sturdier role in cancer compared to normal cells.

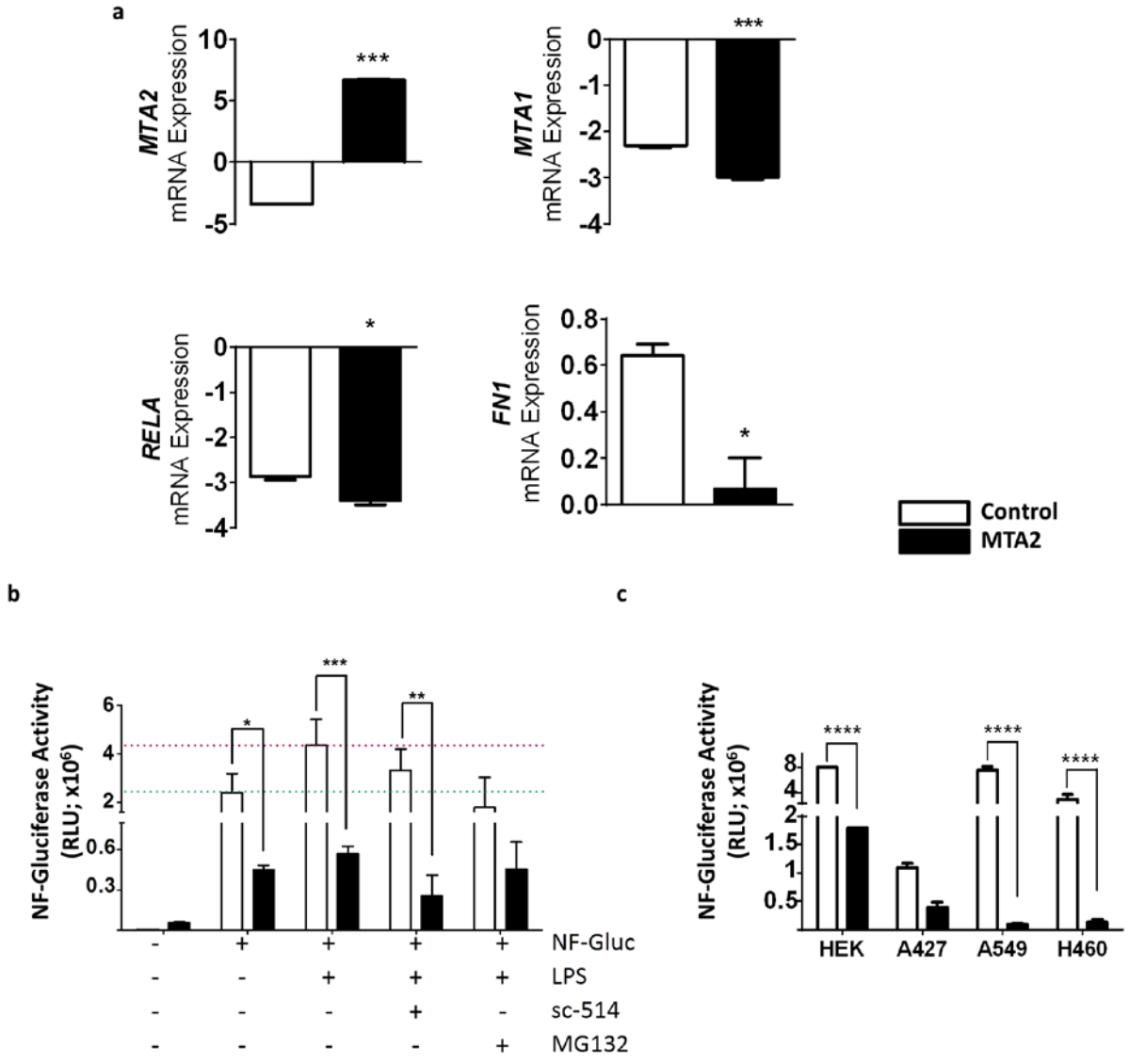

Figure 4.13 Effect of MTA2 overexpression on NF-ƙB activity. a) A549 mRNA expression of MTA2 family and target genes of NF-ƙB calculated as ΔCt and normalized to *HPRT* as housekeeping gene. Data are represented as mean ± SEM. * $p \leq 0.05$, ** $p \leq 0.01$, *** $p \leq 0.001$. NF-ƙB activity via Gaussia Luciferase reporter assay in b) A549 after treatment with LPS (5µg/ml), sc-514 (25µM) and MG-132 (25µM) and co-transfection with MTA2 for 24h and in c) various cell lines. Data is represented as relative luminescence unit (RLU).

Similar behaviour was observed in mouse LLC1 cells upon overexpression MTA2 even when examining a panel of target genes (Fig. 4.14). Effects on different target genes were summarized in Table 4.2.

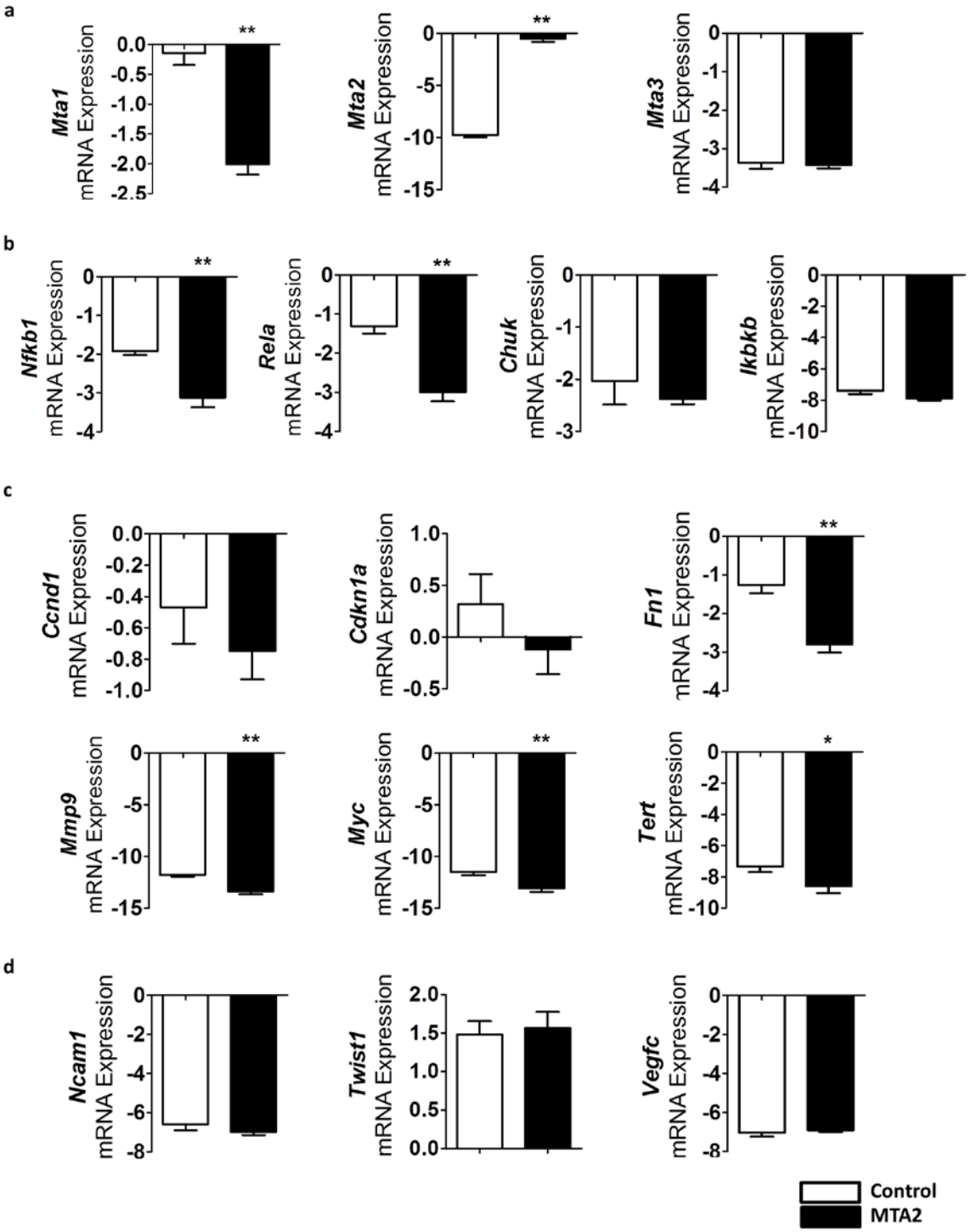

Figure 4.14 Effect of MTA2 overexpression in LLC1 cells. LLC1 cells were transfected with MTA2 for 24h before the isolation of RNA. RNA expression was assessed by quantitative PCR of a) genes of MTA family b) genes of the NF-ƙB family and the IKK regulating it c) target genes of NF-ƙB which were regulated by MTA2 d) target genes of NF-ƙB which were not regulated by MTA2. Data was calculated as ΔCt, normalized to *Hprt* as housekeeping gene and represented as mean ± SEM. * $p \leq 0.05$, ** $p \leq 0.01$. Representative data of three individual experiments.

Table 4.2 Genes regulated by overexpression of MTA2 in relation to NF-ƙB pathway.

a) Known NF-ƙB target genes, b) Non-target genes of NF-ƙB regulated by MTA2

a.

Gene	Name & Role	Regulation by MTA overexpression
Ccnd1	Cyclin D1; Cell-cycle regulation	↓
Cdkn1a	p21; cyclin-dependent kinase inhibitor 1; Cell-cycle regulation	↓
Fn1	Fibronectin; Extracellular attachment	↓↓↓
Mmp9	Matrix metalloproteinase 9; cell adhesion ; secreted collagenase involved in metastasis	↓↓↓
Myc	C-myc; Proto-oncogene	↓↓↓
Ncam1	Neural cell adhesion molecule	Not regulated
Nfkb1	Nuclear factor kappa B; inflammation	↓↓↓
Rela	V-Rel avian reticuloendotheliosis viral oncogene, homologue A	↓↓↓
Twist1	Transcription repressor	Not regulated
Vegf c	Vascular Endothelial Growth Factor; angiogenesis	Not regulated

b.

Gene	Name & Role	Regulation by MTA overexpression
Ki67	Antigen identified by monoclonal antibody Ki-67 (All phases except G_o); proliferation	↑↑↑
Pcna	Proliferating cell nuclear antigen (Phase S) ; proliferation	↑↑↑
Cdkn1b	p27; Cell cycle-dependent kinase inhibitor; proliferation	Not regulated
Raf1	C-Raf; Proto-oncogene serine/threonine-protein kinase (Mitogenic cascade); proliferation	Not regulated
Cdh1	E-Cadherin; epithelial marker; Epithelial-mesenchymal transition	Not regulated
Tgfb	Transforming growth factor beta 1, Epithelial-mesenchymal transition	↓↓↓
Mmp2	Matrix metalloproteinase 2; cell adhesion & angiogenesis	Not regulated
Vegfa	Vascular endothelial growth factor A; angiogenesis	↓↓↓

4.2.3 MTA2 and members of the NuRD complex interact with p50/p65 complex

MTA2 is known to be a part of the nucleosome and histone deacetylase remodelling (NuRD) complex[68]. This complex was shown to interact with different transcription factors to repress their transcriptional activity. To check whether NF-ƙB members and MTA2 are interacting within the cancer cells, cytoplasmic and nuclear proteins were isolated from A549 cells. The protein fractions were pulled down with p65 and MTA2. Western blots revealed the binding of p65 to MTA2 and HDAC1, another component of the NuRD complex. This binding was missing in the nuclear fraction when cells were treated with sc-514, an inhibitor known to prevent the nuclear translocation of p50/p65 (Fig.4.15a upper panel). Similarly when cells were stimulated with LPS and TNFα, pulldown with MTA2 co-precipitated p65 indicating a possible interaction between of the two proteins (Figure 4.15a lower panel).

In order to show whether this interaction is direct, proximity ligation assay (PLA) was performed using antibodies against MTA2 and phosphorylated RelA/p65 (Ser311). This assay can detect proteins which are in close proximity to each other in a range of 40nm. In A549 overexpressing $IKK2^{CA}$ there was significant nuclear signal of the proximity of both proteins. This signal was specific as overexpression of MTA2 clearly increased it whereas knocking down MTA2 via shRNA barely showed any interaction (Fig.4.15b). Collectively, these data suggest an interaction of both NF-ƙB and NuRD complexes.

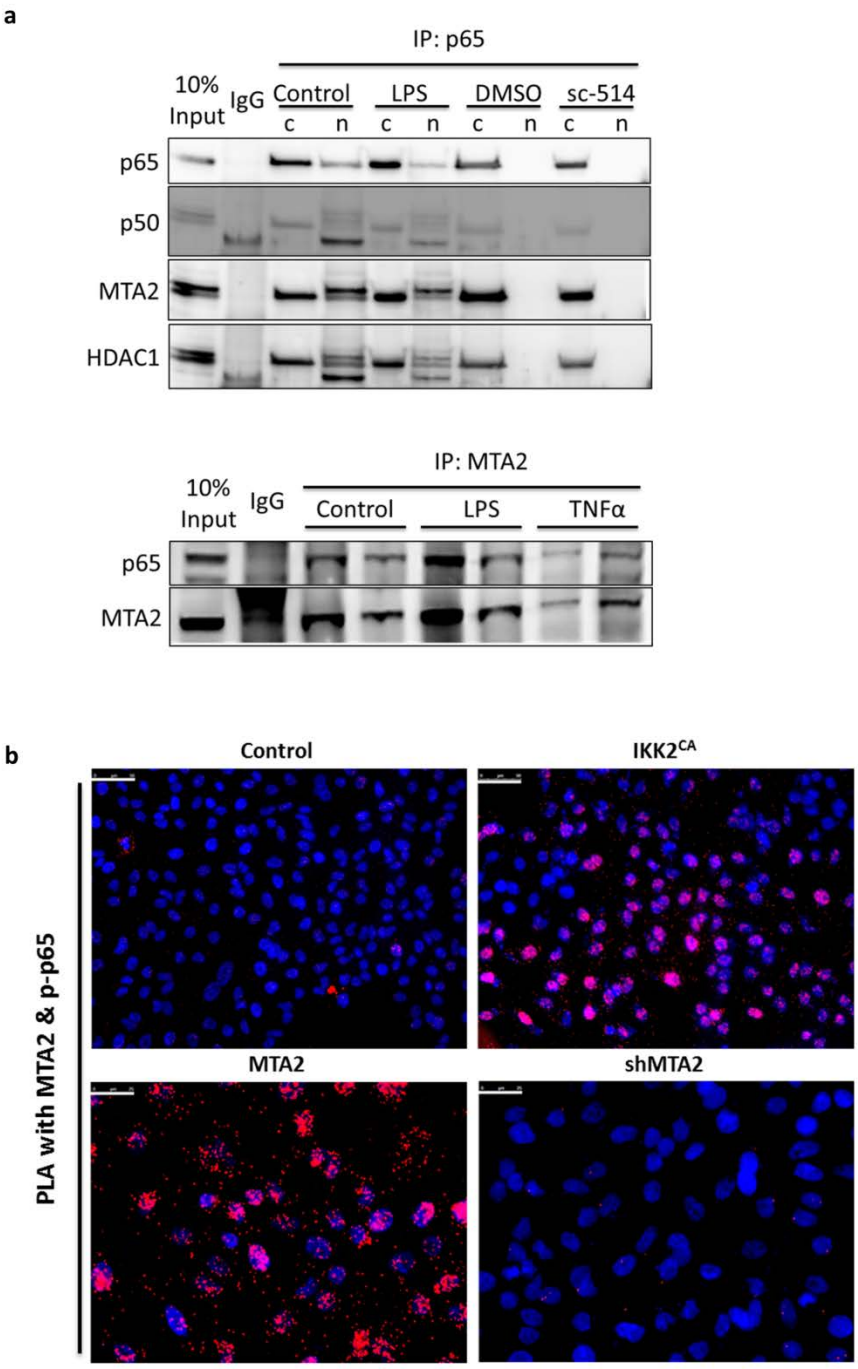

Figure 4.15 Interaction of RelA/p65 and MTA2 in A549 cells. a) Co-immunoprecipitation of A549 using pulldown with p65 after treatment with LPS and 25µM sc-514 (upper panel) and b) pulldown with MTA2 after stimulation with LPS and TNFα. b) Proximity ligation assay (PLA) using antibodies against MTA2 and phosphorylated RelA/p65 (Ser311) of control cells and A549 overexpressing $IKK2^{CA}$ (upper panel; scale bar represents 50µm at a magnification of 20x) and of cells overexpressing MTA2 or have knockdown of MTA2 (lower panel; scale bar represents 25µm at a magnification of 40x).

For a better understanding on the effects of such interaction on the activities of NF-ƙB complex as well as on the NuRD complex, H1650 cells were treated with LPS (10µg/ml) or TNFα (5ng/ml) for 6h after which the nuclear lysate of cells was prepared. Using a sucrose gradient, the nuclear lysate was fractionated via ultracentrifugation to obtain various nuclear complexes. Different components of both complexes were detected in selected fractions as shown in Fig 4.16a-c.

Both members of the NF-ƙB heterodimer were detected in fractions 7-15 where p65 showed strongest peak in fraction 13 in control, LPS and TNFα conditions. On the other hand, p50 was higher in control samples rather than in LPS or TNFα stimulation, assumingly due to the fact that p50 homodimer is known to act as repressor. Upon stimulation the amount of p50 was relatively reduced being solely contributing in the active heterodimer. Looking on the members of the NuRD complex, they were detected in fractions 5-17. MTA2 peaked in fraction 7 in all conditions but was more expressed in the control sample. HDAC1 rather peaked in fraction 9 but interestingly there was another band detected only in the stimulated conditions. HDAC2 was relatively constant in all fractions 5-17 with a slight peak in fraction 7. Furthermore, CHD4 correlated with MTA2 as it was higher in the control samples compared to stimulated conditions. The protein p300 was also detected in the same fractions albeit didn't correlate with HDAC1 acetylation.

To correlate the presence of the individual members with the activity of each complex, NF-ƙB and pan-HDAC activity assays were performed. NF-ƙB activity was measured based on p65 binding to NF-ƙB binding domain. In LPS and TNFα stimulated fractions, more activity was observed in input as well as in fractions 7-15 peaking at fraction 13 (Fig. 4.16d). Interestingly, HDAC activity was decreased upon stimulation in the input. In the first fraction, there was increased HDAC activity that seemed to be independent of NF-ƙB heterodimer. Fraction 9 showed significant decrease in HDAC activity upon stimulation, whereas fraction 7 showed increased HDAC activity upon LPS stimulation (Fig. 4.16e).

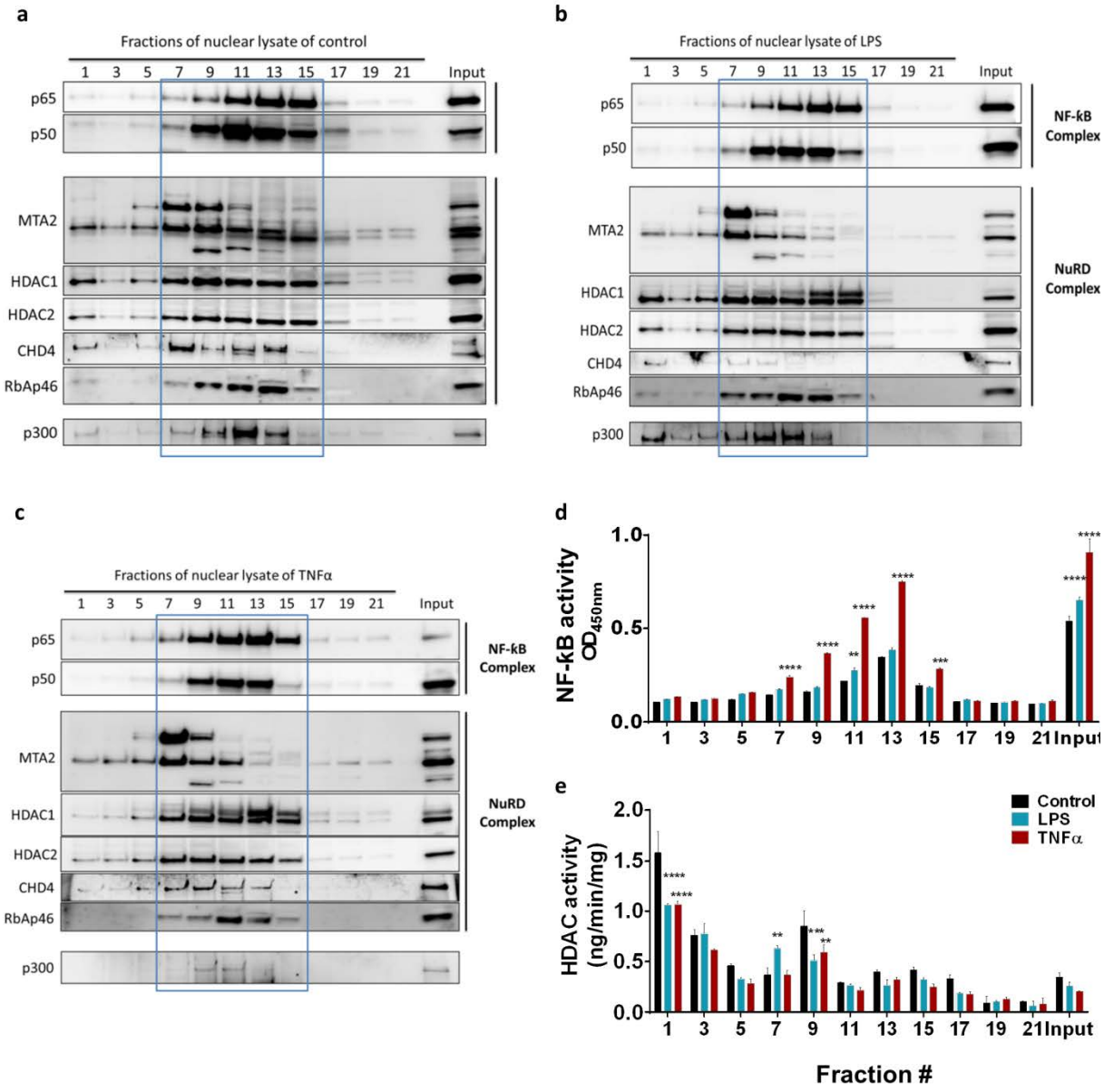

Figure 4.16 Fractionation of nuclear lysates after stimulation with LPS or TNFα. H1650 cells were treated with LPS (10µg/ml) or TNFα (5ng/ml) for 6h. Nuclear lysates were isolated and fractionated using a sucrose gradient. Odd fractions were analysed on Western blot (a-c), for NF-kB activity (d) and for HDAC activity assay (e). Data represented as mean ± SEM. ** p ≤ 0.01, *** p ≤ 0.001, ****p≤ 0.0001 compared to control sample of individual fractions.

4.2.4 MTA2 and CHD4 act as repressor of p50/p65 dimer

Taken together these data showed that the NuRD complex and p50/p65 interact in the nucleus and that this interaction affected the activation status of NF-kB. To verify the specificity of this interaction, MTA2 and CHD4 were overexpressed in A549 cells together with NF-Gluc to measure NF-kB activity. Both MTA2 and CHD4 overexpression decreased NF-

ĸB activity whereas knockdown of these genes via shRNA increased the NF-ĸB activity (Figure 4.17).

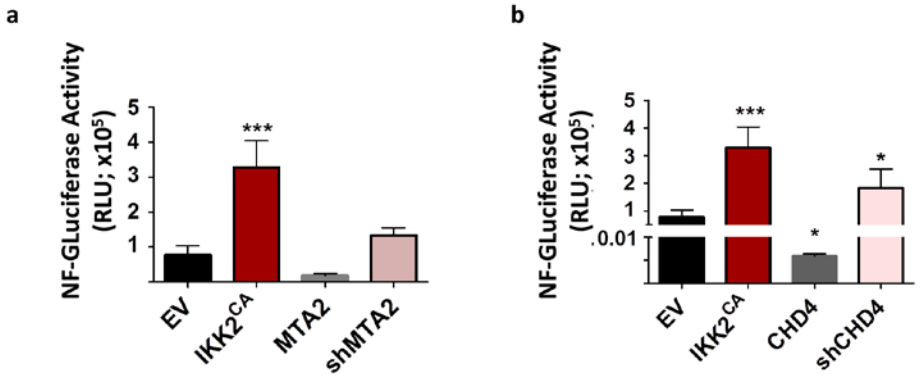

Figure 4.17 NF-ĸB activity repression via MTA2 and CHD4. Gaussia Luciferase reporter assay in A549 after overexpression and knockdown of MTA2 (a) and CHD4 (b) compared to overexpression of $IKK2^{CA}$. Data is represented as relative luminescence unit (RLU) normalized to EV. Data represented as mean ± SEM. * $p \leq 0.05$, *** $p \leq 0.001$ compared to empty vector (EV) as control.

The NuRD complex is reported to interact with the promoter region of various genes, e.g. E-Cadherin, leading to its deactylation and thus subsequent deactivation[96]. In order to assess whether the NuRD complex is recruited to the promoter of NF-ĸB or other target genes, chromatin immunoprecipitation was performed. A549 cells were stimulated with LPS to estimate the preferential binding of MTA2. Two known target genes of NF-ĸB were selected: *NFKB1* itself and *NFKBIA* known as IĸB1a. The binding sites of the used primers are illustrated in Fig. 4.18a. Both promoters showed enrichment for RelA/p65 upon stimulation with LPS (Fig. 4.18b). However, the binding of MTA2 was only observed with *NFKB1* upstream promoter and to a very slight extent on *NFKBIA* promoter. Interestingly, the binding of MTA2 was stronger in control sample compared to LPS-stimulated cells.

In order to confirm the obtained results, A549 cells were treated with TNFα. Another member of NuRD complex was included, namely retinoblastoma binding protein 7, known as RbAp46, together with p50 for the pulldown. There was a slight enrichment of MTA2 and RbAp46 in control samples over treated ones. The binding to different promoter regions differed between LPS and TNFα inclining that every stimulant has its unique binding mechanism and kinetics. LPS stimulation showed stronger enrichment for the *NFKB1* proximal primer for RelA/p65 whereas TNFα stimulation recruited more RelA/p65 to the upstream region of *NFkB1* promoter (Fig. 4.19a). Surprisingly, when the experiment was

repeated in HEK cells the enrichment of MTA2 and RbAp46 was much stronger in control state compared to stimulated condition (Fig. 4.19b).

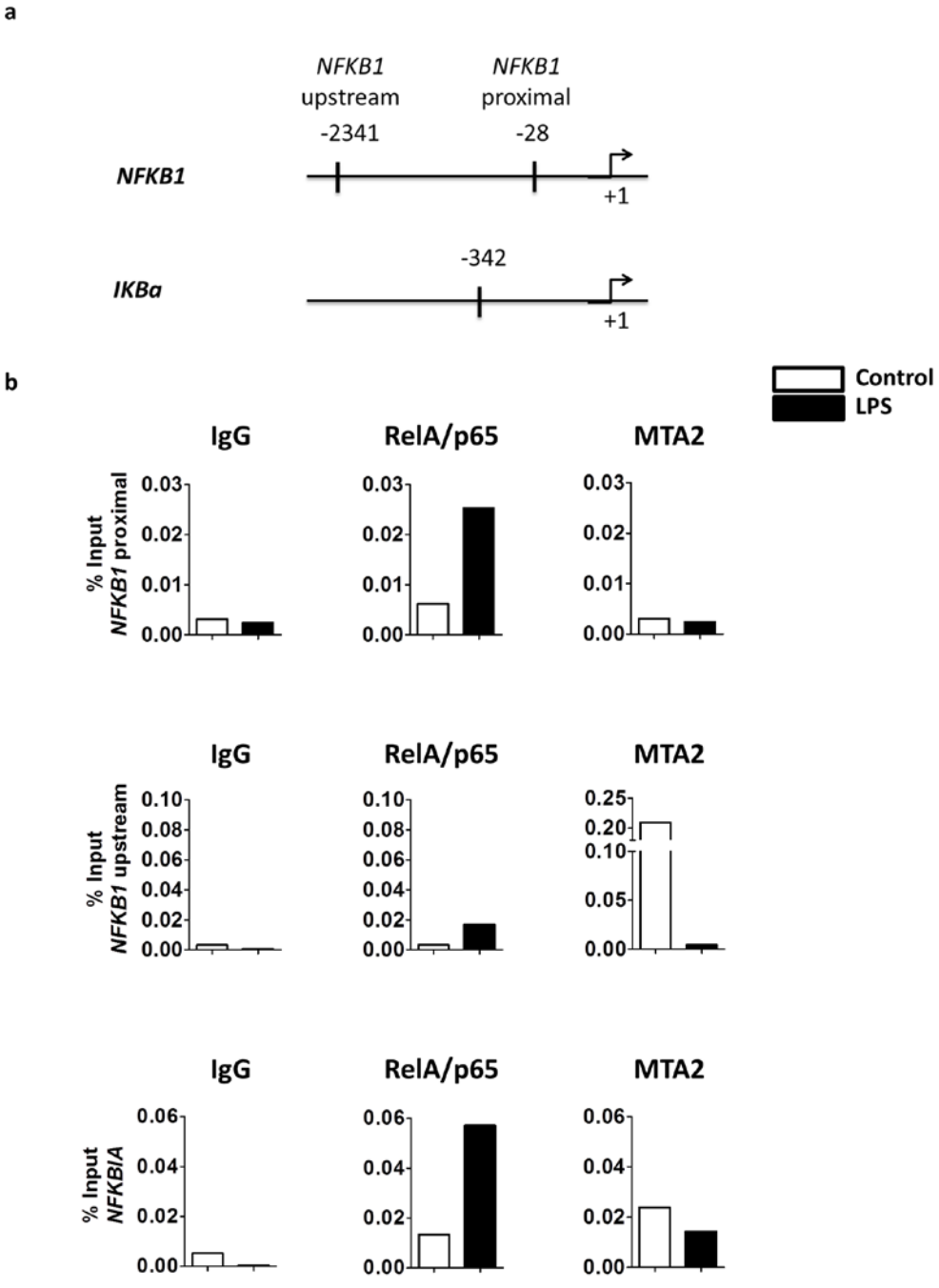

Figure 4.18 Chromatin Immunoprecipitation in A549 cells treated with LPS. a) Schematic representation of the ChIP primers binding sites. ChIP pulldown was done using antibodies against RelA/p65 and MTA2 and a corresponding rabbit IgG as control. RT-qPCR was performed using primers in the promoter region of *NFKB1* and *NFKBIA*. Data was normalized to the respective input and represented as percentage input.

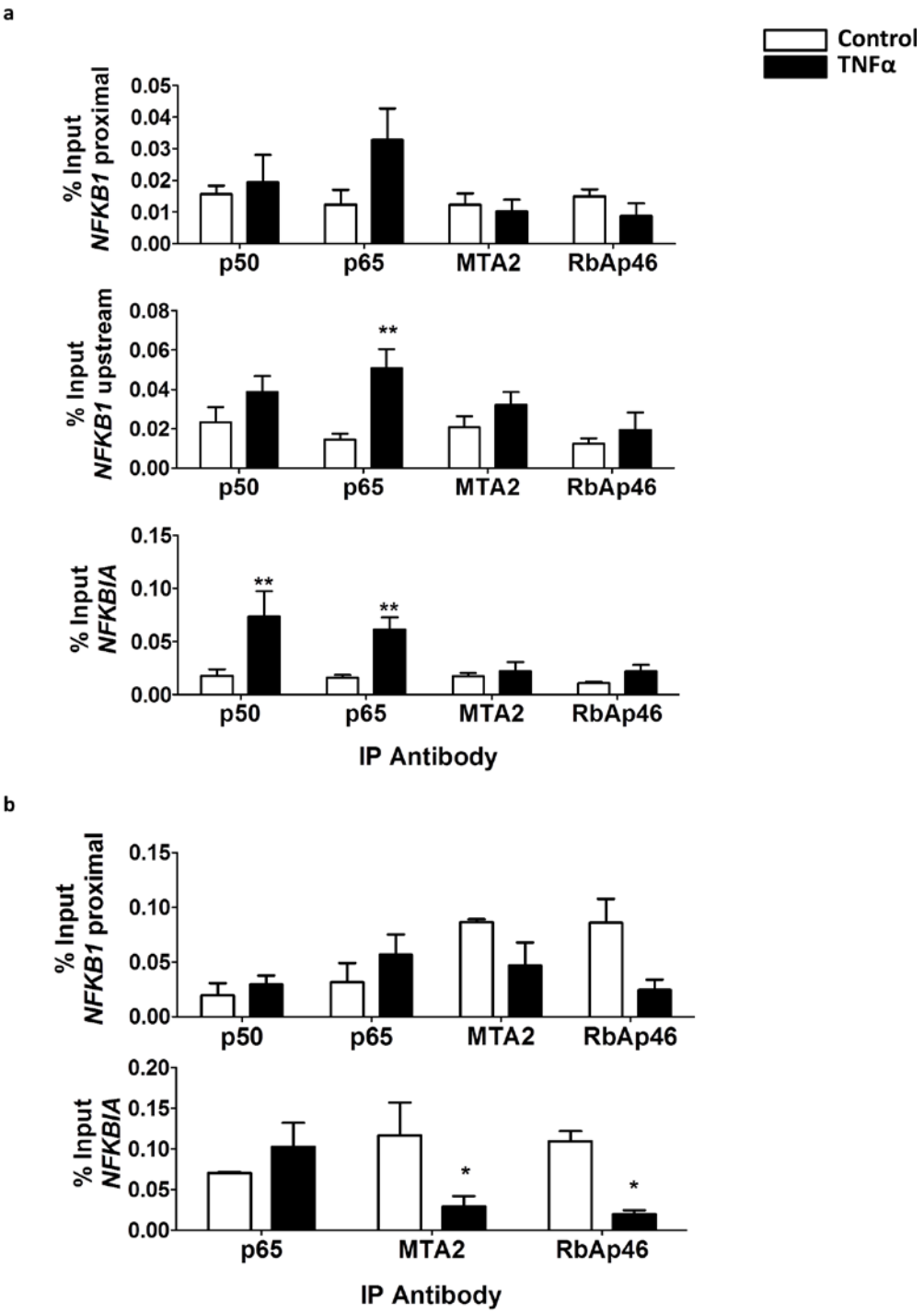

Figure 4.19 Chromatin Immunoprecipitation after TNFα stimulation. ChIP pulldown was performed in a) A549 cells b) HEK cells using antibodies against p50, RelA/p65, MTA2 and RbAp46 and a corresponding IgG as control. RT-qPCR was performed using primers in the promoter region of *NFKB1* and *NFKBIA*. Data represented as mean ± SEM. * $p \leq 0.05$, ** $p \leq 0.01$, *** $p \leq 0.001$ Data was normalized to the respective input and represented as percentage input (n=3).

4.3 Effect of IKK2^{CA} overexpression and knockdown of MTA2 on tumour growth

4.3.1 Generation of stable LLC1 cells with shMTA2 and IKK2^{CA} *& their characterization*

After showing the possible regulation of NF-ƙB by MTA2 and the NuRD complex, it was of interest to show how knocking down MTA2 would affect tumour growth. For this purpose, LLC1 cells were transfected with pCDH-GFP empty vector, pCDH-GFP-IKK2^{CA} and shMTA2. Transfected cells were characterized for their NF-ƙB activity by transiently transfecting them with NF-GLuc. Both IKK2^{CA} overexpression and the knockdown of MTA2 showed increased activity compared to their respective controls (Fig. 4.20a). Furthermore, the cells were assessed for their migratory capacity via the Boyden chamber assay, where MTA2 knockdown significantly increased the number of migrated cells (Fig. 4.20b). Finally, in order to evaluate the ability of these cells to grow independent of anchorage, soft agar assay was performed. Cells with shMTA2 formed big colonies, even bigger than those formed by LLC1-IKK2^{CA} cells (Fig. 4.20c).

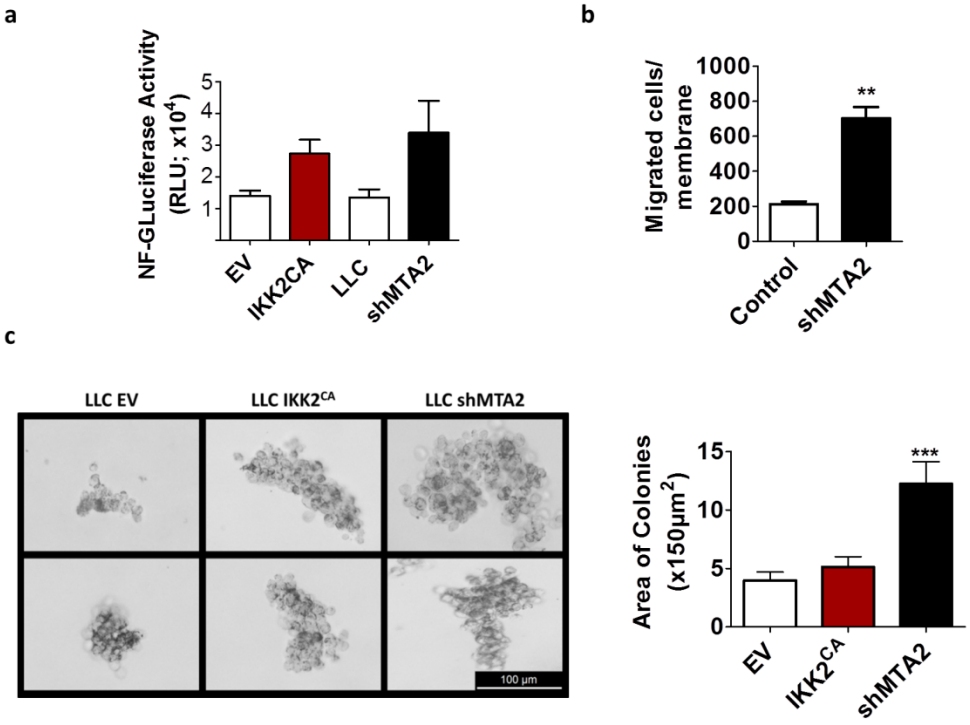

Figure 4.20 Characterization of LLC1 cells transfected with IKK2^{CA} and shMTA2. a) Gaussia Luciferase reporter assay. Data is represented as relative luminescence unit (RLU) as mean ± SEM compared to empty vector (EV) as control and to LLC1 control, respectively. b) Boyden Chamber migration assay of control LLC1 cells and LLC1-shMTA2. c) Soft agar assay showing representative colonies at Day 14 (left panel, scale bar represents 100µm). Quantification of the size of colonies represented as average area (right panel). ** $p \leq 0.01$, *** $p \leq 0.001$ (n=4).

4.3.2 Subcutaneous tumour xenograft mouse model with LLC1 cells

Mice were injected subcutaneously with $3x10^6$ cells in 200µl with different LLC1 cells; LLC1-EV, LLC1-IKK2^{CA} and LLC1-shMTA2. Measuring the tumour size revealed an increase of tumour upon silencing MTA2 even to a greater extent compared to LLC1 cells with IKK2 activation. The tumour weight was also significantly increased in the group with LLC1-shMTA2 (Fig. 4.21).

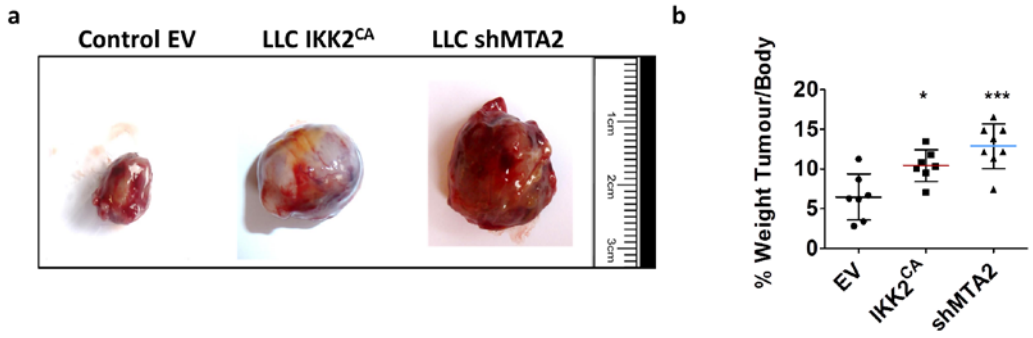

Figure 4.21 Tumour growth of subcutaneous xenograft model of LLC1-EV, LLC1-IKK2^{CA} and LLC1-shMTA2.

a) Representative pictures of the subcutaneous tumour at endpoint of the experiment. b) Diagram showing the percentage of tumour weight normalized to whole body weight. Data is represented as mean ± SEM. * $p \leq 0.05$, *** $p \leq 0.001$ compared to empty vector (EV) as control (n=6-8/group).

The subcutaneous tumours were dissected and the RNA isolated. Surprisingly, knocking down MTA2 increased the expression of *Ikbkb* (IKK2) though it is not a known target gene of p50/p65 suggesting that MTA2 might play a role in the overall NF-kB activation. Furthermore, despite of the moderate increase of IKK2 expression in LLC1-IKK2^{CA} and LLC1-shMTA2, the effects observed in the downstream target genes were stronger though the levels of MTA2 were upregulated (Fig. 4.22a). On the other hand, based on the mRNA expression, NF-kB members, p50 and p65, were upregulated upon overexpression of the activated form of IKK2 and to a greater extent in cells with knocked down MTA2. *Nfkbia* known as IkB1α which is known to regulate p50/p65 and is also a target gene was significantly upregulated in both LLC1-IKK2^{CA} and LLC1-shMTA2 (Fig. 4.22b). A similar pattern was observed with several target genes of NF-kB including *Tnf, Nfkbia, Mmp9, Ccnd1, Cdkn1a and Cdkn1b* (Fig. 4.21c). This observation goes in concordance with the *in vitro*

studies showing a repressing effect of MTA2 on the activity of NF-kB and the expression of its target genes.

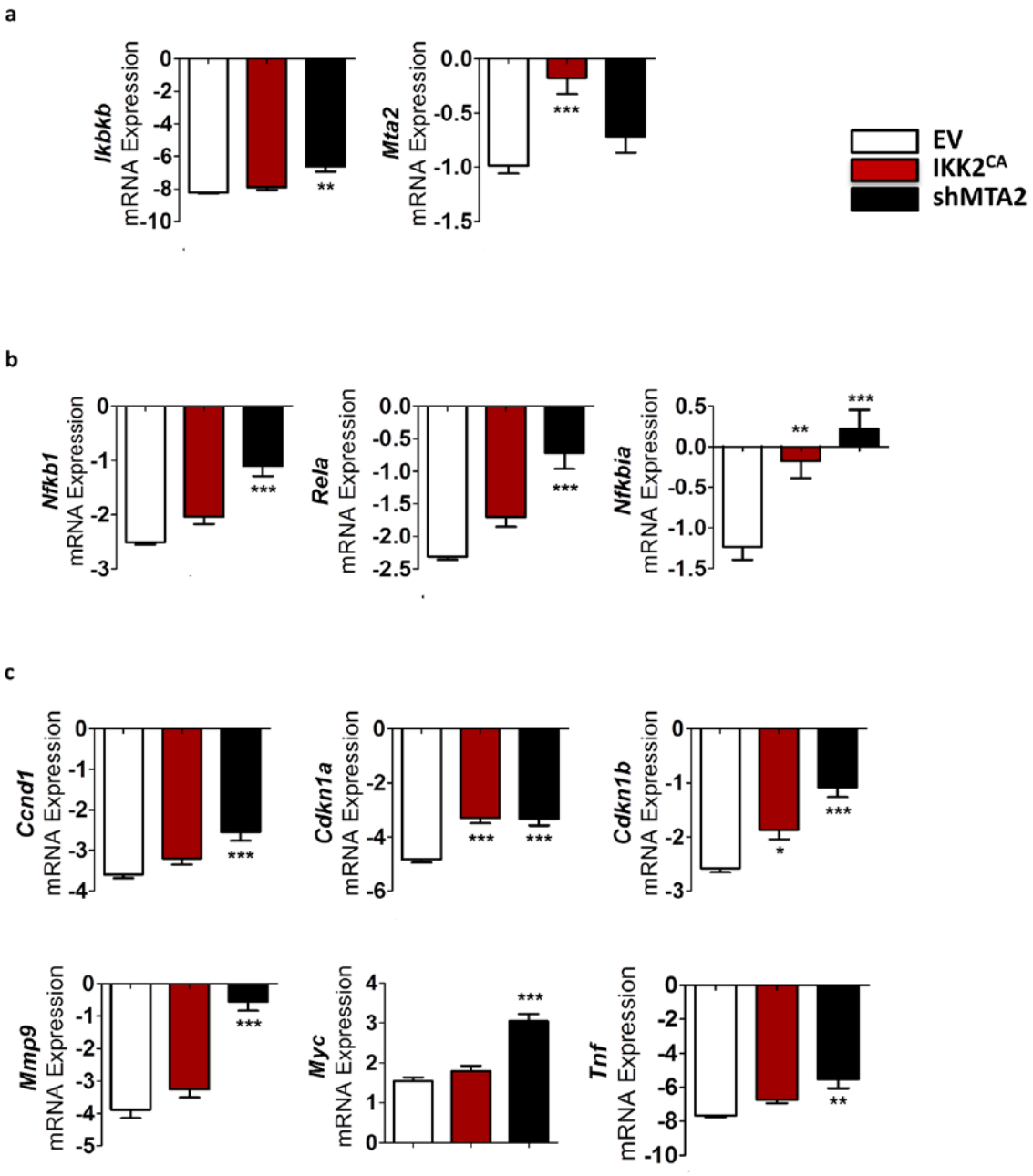

Figure 4.22 Expression profile from mRNA of subcutaneous tumours. mRNA expression was assessed by quantitative PCR of a) *Ikbkb* and *Mta2* b) genes of the NF-kB family c) target genes of NF-kB which were regulated by MTA2. Data was calculated as ΔCt, normalized to *Hprt* as housekeeping gene and represented as mean ± SEM. * p ≤ 0.05, ** p ≤ 0.01, ***p≤0.001. (n=6-8/group)

For a closer look on the cells within the tumour and their respective expression of RelA/p65 and MTA2, isolated tumours were fixed and sectioned for staining. Immunofluorescence staining clearly showed an activation of NF-kB pathway seen as nuclear translocation of RelA/p65 in cells with $IKK2^{CA}$ and shMTA2 compared to control cells (Figure 4.23, middle panel). Interestingly, the expression of MTA2 in $IKK2^{CA}$ cells appeared higher in contrast to what was observed *in vitro*, where overexpression of $IKK2^{CA}$ showed less MTA2 on protein level (Fig.4.11c). Besides, there was still residual expression of MTA2 in cells with shMTA2 (Fig. 4.23, upper panel) that was also observed in the mRNA expression. At this point it is worth mentioning that the silencing of MTA2 was not complete in LLC1 cells. Both observations indicate that the *in vivo* system, where there are other cell types contributing to the tumour microenvironment, might have influence on the tumour behaviour.

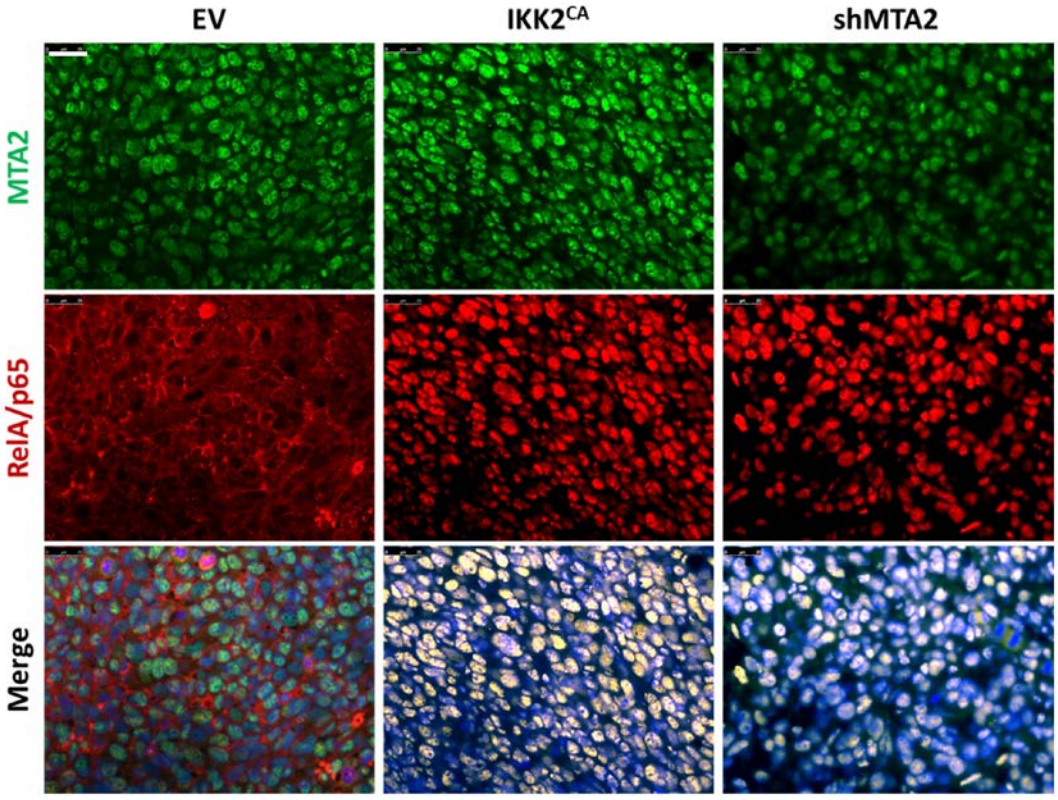

Figure 4.23 Immunofluorescence of subcutaneous tumour sections. Representative images showing MTA2 (green) and nuclear translocation of RelA/p65 (red) with DAPI as nuclear counterstain. Scale bar represents 25µm.

Hence, part of the tumours were digested and analysed by flow cytometry for the immune cell repertoire using a panel of immune cell markers depicted in Fig. 4.24a. Flow cytometric analysis revealed that B lymphocytes (Fig. 4.24b, upper panel) which are known to be pro-tumorigenic were significantly higher in LLC1-shMTA2 cells. This can explain the bigger tumour size produced by this cell type. Moreover, T cells, T regulatory cells, $CD4^+$ cells and $CD8^+$ T-lymphocytes were reduced in bigger tumours of both $IKK2^{CA}$ and shMTA2. Strikingly, the subcutaneous tumour of LLC1-shMTA2 and LLC1-$IKK2^{CA}$ harbored more MHC-II^- TAMs and less MHC-II^+ TAMs compared to control cells. Taken together, the flow cytometric analysis suggested a more tumour-favourable immune microenvironment in the tumours originating from LLC1 with knockdown of MTA2 or activation of IKK2. These data support the pro-tumorigenic effects of NF-ƙB pathway and highlight the potential role of MTA2 in regulating these effects.

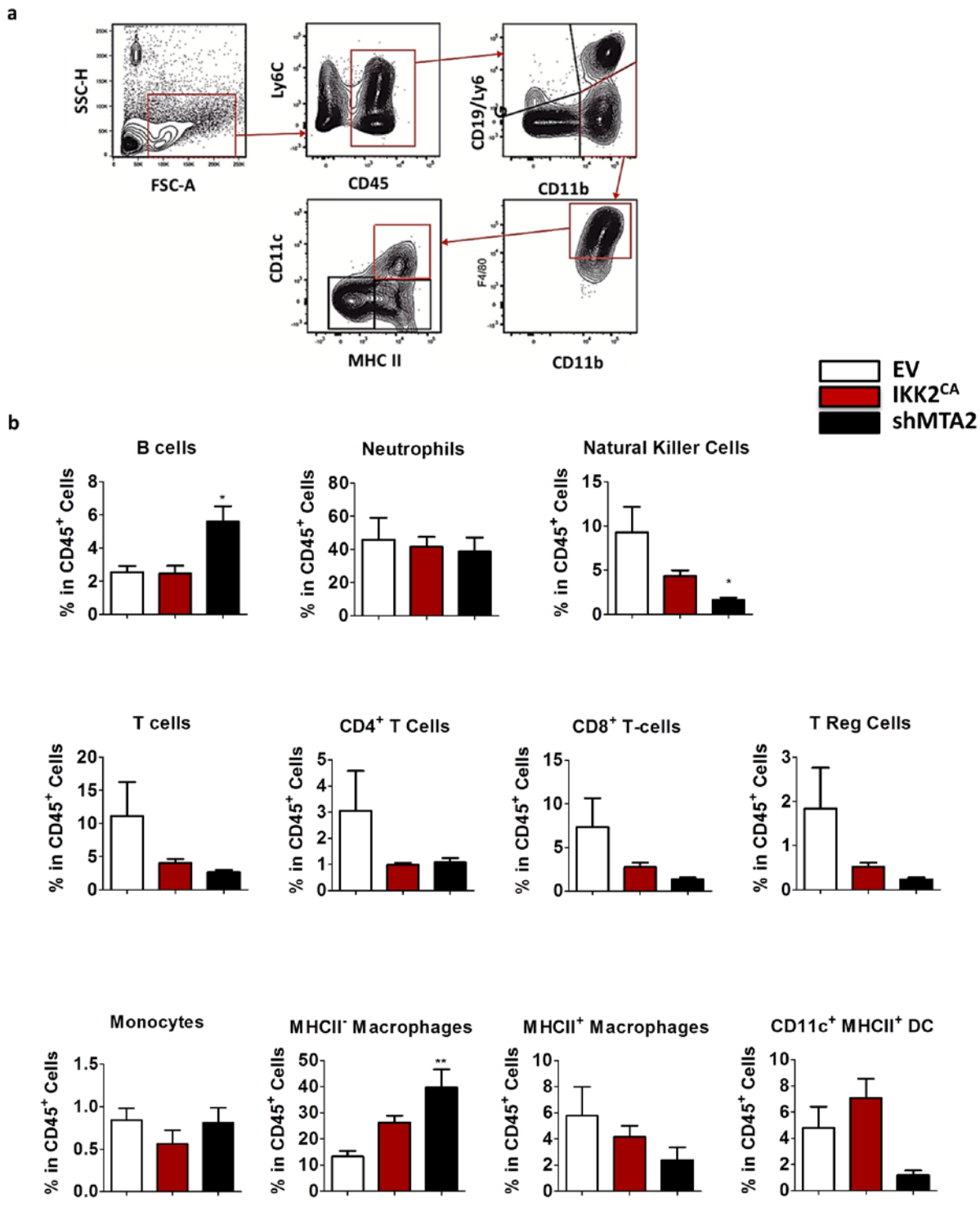

Figure 4.24 Flow cytometry of immune cells repertoire in LLC1 subcutaneous tumours. a) Schematic diagram of the gating strategy using the different immune cell markers b) Quantification plots of different immune cells calculated as percentage of total CD45$^+$ cells. Data represented as mean ± SEM. * $p \leq 0.05$, ** $p \leq 0.01$, ***$p \leq 0.001$. (n=4/group).

5 Discussion

Inflammation and cancer were linked more than a century ago when Rudolf Virchow identified leukocytes infiltration in neoplastic tissues[97]. Many years of research followed until the discovery of NF-ƙB three decades ago which paved the way to more insight into the contribution of inflammatory signalling to cancer development. NF-ƙB is not only involved in innate and adaptive immune responses but it governs the expression of wide set of diverse genes regulating cell growth and adhesion, cell cycle regulation, apoptosis, angiogenesis – all established hallmarks of neoplastic transformation[47, 52]. Many tumours, especially solid tumours, exhibit constitutive activation of NF-ƙB canonical signalling pathway. This fact encouraged several researchers to develop NF-ƙB inhibitors and IKK2 inhibitors as adjunct therapy to existing cancer treatment modalities, however, with modest success. More studies are required for a better understanding of NF-ƙB activation in cancer and the underlying regulatory mechanisms.

5.1 Aberrant NF-ƙB activity in lung cancer

5.1.1 Basal expression of NF-ƙB in different cancer cell lines

Basal NF-ƙB activity was detected in several lung adenocarcinoma cell lines (A549, A427, Colo699, H1650, and H2122) as well as non-tumour cell line (BEAS-2B). *NFKB1*, *RELA* and *MMP9* expression levels were lowest in BEAS-2B control cells compared to tumour cell lines though almost all cell lines showed increased expression levels of these genes upon LPS stimulation. This goes in concordance with several other studies which show a correlation between elevated NF-ƙB activation and cancer progression[98].

Both LPS and TNFα induced NF-ƙB nuclear translocation and subsequent activation varied between cell lines. The differences in the strength of the response probably refer to different activation kinetics, stimuli used and target genes examined. Another important parameter playing a role in NF-ƙB activation is the binding of IƙB proteins to NF-ƙB and the formation of IƙB/NF-ƙB complexes. Such association not just masks the nuclear localization signal (NLS) of NF-ƙB but also allows its export from the nucleus. These shuttling processes together with binding and dissociation contribute to the basal activity within the cells and affect their response to stimuli[26]. Even in H2122 cells, where the expression of NF-ƙB target genes was marginally affected on RNA level, a clear nuclear translocation was observed

within the cells (Fig.4.1 and Fig 4.2). This indicates that there are different levels of NF-ƙB activation and that the transcriptional activation varies between target genes examined (*NFKB1*, *RELA*, *MMP9* and *FN1*). Tobar *et al.* demonstrated that TGF-β1-mediated cell invasion and migration regulates MMP9 expression through the activation of NF-ƙB via Rac1-ROS mechanism. Inhibition of NF-ƙB and reactive oxygen species (ROS) hampers TGF-ß1-mediated EMT[99]. Whole genome data analysis attempted to identify cancer subtypes by their genetic signature. In this respect Guan *et al.* identified NFKB and FN1 as markers for ovarian cancer[100].

However, it is necessary to differentiate between the different members of NF-ƙB and the distinct complexes they form. Whereas p50/p65 heterodimer was linked to activation, the p50 homodimer plays an opposite role. The presence of p50 in the nucleus was identified in LPS intolerance and is associated with inactivation if present as p50-homodimer. As p50 is devoid of the transactivating domain (TAD), its presence in the nucleus rather blocks access of the active heterodimer to NF-ƙB binding sites[83].

5.1.2 Activity of NF-ƙB in SpC C-Raf BxB mouse model

In the used transgenic mouse model, C-Raf BxB is expressed constitutively under the control of SpC promoter. Similar to several cancer models, like K-Ras and B-Raf models, SpC C-Raf BxB has an activation mutation in the mitogenic cascade[101, 102]. Such genetic abnormalities in epithelial cells (e.g. K-Ras mutation identified in 25-40% of lung cancer samples and in several other tumour types) encourage activation of NF-ƙB[103]. *In vitro* in A549 cells, C-Raf BxB exhibited high NF-ƙB activity similar to the activation induced by IKK2 (Fig.4.4b). This was observed in several other models; in a mouse model of precancerous pancreatic lesions Daniluk *et al.* showed that oncogenic Ras initiate a positive feedback loop of NF-ƙB activation that further pathologically activates Ras. Inhibition of Cox-2 interrupted this loop and attenuated the inflammatory and oncogenic stimuli[104]. Previous studies showed that C-Raf doesn't directly activate IKK complex but its activation is rather conveyed indirectly by another membrane shuttle kinase known as MEKK1[21].

Diverse mutations, genetic deletions and amplifications, as well as chromosomal translocations observed in different lymphoid cancers, like Hodgkin lymphoma and B cell lymphoma, were supported by constitutive activation of NF-ƙB[103]. Most of the reported aberrant NF-ƙB activity in cancer was related to IKK2 canonical signalling.

5.2 Role of IKK2 in lung cancer progression

IKK2 is a kinase member of the trimeric IKK-complex involved in the activation of NF-ƙB in the canonical signalling pathway[32]. This upstream kinase is stimulated by several cytokine and growth-inducing signals to phosphorylate IƙB, sequestering p50/p65 to the cytoplasm in unstimulated state, so that NF-ƙB complex becomes free to shuttle to the nucleus.

5.2.1 NF-ƙB activation depends on IKK2 pathway

The functional effects of NF-ƙB activation were reflected in increased proliferation and migration. Specific IKK2 inhibitors like sc-514, parthenolide or Bay11-7085 as well as MG-132 showed reduction in both the proliferative and migratory capacity of cells indicating the pivotal role of IKK2 activation in cancer cells. Several IKK2 inhibitors were thus studied in different cancers; a pharmaceutical IKK2 inhibitor AS602868 was shown to inhibit growth of multiple myeloma cells *in vitro*[105]. A recent study by Deng *et. al* showed the beneficial cytotoxic effect of the novel IKK2 inhibitor LY2409881 in a preclinical model of lymphoma. They suggest the use of LY2409881 together with HDAC inhibitor romidepsin for the treatment of B- and T-cell lymphoma[106].

5.2.2 IKK2 modulation in SpC C-Raf BxB tumour model

In corroboration with data obtained *in vitro*, the SpC C-Raf BxB animal model confirmed the impact of IKK2 on tumour growth. Mice with SpCrtTA/IKK2^{DN}/SpC C-Raf BxB genotype showed less tumour dispersion than SpC C-Raf BxB mice and their IKK2^{CA}-counterparts. The reduction in tumour was also reflected in improved lung compliance similar to that observed in matched wildtype controls. However, the differences between SpC C-Raf BxB mice and SpC rtTA/Tet-O-IKK2^{CA} were not significant. This can be explained by the fact that C-Raf itself drives NF-ƙB activation so further activation of the pathway did not show any significant additional effects. Looking closer at the compliance data in mice with IKK2^{DN}, it was noticed that tissue elastance (Ers) and tissue damping (H) were even less than in wildtype controls. This can be due to the loss of alveolar structure observed in SpCrtTA/IKK2^{DN}/SpC C-Raf BxB lungs producing an emphysema-like effect. A study by Xia *et al*. reported that IKK2 depletion in mouse lungs lead to reduced tumour proliferation mediated by a reduction in the Timp-1 expression. Timp-1, a known target gene of NF-ƙB, is required for Erk signalling activation and consequent cell proliferation[107].

The activation of NF-ƙB was also assessed immunohistochemically using an antibody against phosphorylated RelA/p65 at Ser311. The expression of p-p65 (Ser311) was reduced upon downregulation of IKK2 in BxB lungs, whereas in SpC/IKK2^{CA}/BxB p-p65 was very strong compared to SpC C-Raf BxB. Phosphorylation at Ser311 is known to occur in response to TNFα stimulation where it facilitates the recruitment of the co-activator CBP and enforces the interaction between RelA/p65 and CBP. The responsible kinase is the atypical protein kinase PKCζ[38]. Other phosphorylation sites on RelA/p65 are targeted by several kinases including IKK2. A better analysis of phosphorylation and other post-translational modification of different members of NF-ƙB will give more insight into the dynamics of their transcriptional activation.

The vast variety of post-translational modifications can be one reason why IKK2 alone wasn't sufficient to tightly regulate NF-ƙB activation. Many studies showed the tumour inhibitory effect of IKK2 inhibition in several cancer types, however, IKK2 inhibitors showed modest clinical efficacy[108]. Clinical studies suggest the necessity to differentiate between anti-apoptotic and pro-apoptotic roles of NF-ƙB by defining the biological context before therapy, or suggest the treatment by NF-ƙB inhibitors only for short duration either alone or in conjunction with other therapeutics[95, 109]. IKK2 not only regulates NF-ƙB but also has NF-ƙB-independent effects leading to several off-target effects. Chariot reported that IKK subunits can phosphorylate essential targets like FOXO3a and p53 through NF-ƙB-independent pathways[110]. A more extensive understanding is still required to dissect the role IKK-complex in tumour development.

5.3 MTA2 expression in tumours

In order to analyse the molecular impact of altering IKK2 in mouse lungs, alveolar type II cells were isolated from SpC-rtTA/Tet-O-IKK2^{DN} and wildtype lungs to compare the expression of major genes known to play a role in carcinogenesis. MTA2 was identified as one of the highly affected genes (Table 4.1). Its expression was high in lung tumours of both Kras^{LA2} and SpC C-Raf BxB lung tumours. It is noteworthy that in animal mouse models, mutations of both *Kras* and *Tp53* in the lung lead to the formation of aggressive metastatic lesions though *Kras* mutations alone merely formed adenocarcinomas[111]. SpC C-Raf BxB leads to the formation of benign adenomas. This suggests that MTA2 overexpression is an early event of tumorigenesis.

When comparing expression of MTA2 in different lung adenocarcinoma cells lines, immunoblots showed that cell lines originating from a metastatic site (e.g. H1437, H1299 and Colo699) expressed more MTA2. An additional band of higher molecular weight was observed in these cell lines but was almost absent in cells isolated from primary sites (e.g. A549, A427, H1975 and H23). This band could represent the acetylated form of MTA2 which is reported to be the activated form of the protein. Histone acetyltransferase p300 acetylates MTA2 at K152 which promoted growth and migration of colorectal cancer cells[112]. Hitherto, several studies correlated the overexpression of MTA2 with poor prognosis in different cancer types, like lung cancer[113], colorectal cancer[114] and oestrogen receptor-negative breast cancer[115].

5.4 MTA2: a regulator of NF-ƙB activity

MTA2 builds a complex together with HDAC1/2, CHD4 and structural components, such as RbAp46, to form the NuRD complex. Most studies correlate NuRD complex association with transcriptional repression though lately there is increasing evidence on the activating potential of NuRD binding to promoters[116-118]. In human as well as mouse cells, MTA2 overexpression reduced NF-ƙB activity as seen by reporter assay and on RNA expression levels of selected NF-ƙB target genes.

5.4.1 MTA2/NuRD interacts with NF-ƙB

Both p50/p65 members and HDAC1 and MTA2 were bound together as seen by immunoprecipitation with both p65 and MTA2. Seemingly this interaction is direct as PLA could detect both MTA2 and p-p65 within a distance of 40nm. The interaction was almost exclusively in the nucleus in A549 cells overexpressing $IKK2^{CA}$ whereas overexpression of MTA2 showed nuclear as well as cytoplasmic interaction. In literature, there is scrutiny concerning the subcellular localization of MTA2. While most reports showed nuclear localization[119, 120], Lui *et al*. revealed immunohistological proof of both nuclear and cytoplasmic distribution [77]. On the other hand, MTA1 was shown to localize both in the nucleus and in the cytoplasm, where it regulates -among other functions- the cytoskeletal structure[79]. Whether MTA2 plays a similar role and localizes to microtubules still has to be studied.

Further correlation of nuclear fractions with the respective NF-ƙB and HDAC activity assays demonstrated that there is an inverse relation. Where treatment with LPS or TNFα increased NF-ƙB activity, HDAC activity declined with treatment as seen in input samples. In addition, fractions with high NF-ƙB activity (F9-13) showed lower HDAC activity (Fig 4.16). Surprisingly, fraction 7 showed increased HDAC activity upon LPS stimulation. This could be related to the role of p50 as repressor. The p50-homodimer acts as repressor for NF-ƙB pathway because, unlike p65 and RelB, p50 lacks the transactivation domain so it binds to the promoter blocking activation via p50/p65[83, 121]. Previously it was reported that p50/HDAC1 interaction plays a role in LPS tolerance and the attenuation of its stimulatory effect[83]. It is worth mentioning that the kit used for the assay detects all HDACs except for sirtuins. Further experiments should be performed to exclusively determine the activation status of HDAC1/2.

Immunoblots of the various fractions showed a double band of HDAC1 in samples treated with either LPS or TNFα. This band, observed mainly in fractions 13 and 15, could refer to the acetylated form of HDAC1 which is reported to be inactive[70]. In case of MTA2, a band was detected with higher molecular weight, which could refer to posttranslational modification of MTA2. It was reported that p300 is responsible for the acetylation of MTA2, a modification correlating with increased NuRD complex activity[112].

5.4.2 MTA2 binds to promoters of NF-ƙB target genes

MTA2/NuRD complex as well as p50/p65 binding was identified in the promoter region of *NFKB1* and *NFKBIA* genes, both target genes of NF-ƙB, as seen by ChIP in both A549 and HEK cells. For *NFKB1* gene, two promoter regions were examined, *NFKB1* proximal at -28 and *NFKB1* upstream at -2341. Interestingly, MTA2 was enriched at the upstream region whereas RelA/p65 bound to both regions yet stronger to the proximal region in both A549 and HEK cells. However, the response to stimuli was different in A549 paralleled to HEK cells. Stimulation with LPS and TNFα showed higher enrichment of RelA/p65 and p50 in A549 at all tested sites compared to control cells. On the contrary, stimulation with LPS showed lower enrichment of MTA2 on *NFKB1* upstream and *NFKBIA* promoter region compared to control suggesting a repressing effect of MTA2 in unstimulated state. This effect was not as evident upon stimulation with TNFα in A549 cells. In contrast, TNFα stimulation in HEK cells revealed a lower enrichment of both MTA2 and RbAp46 at *NFKB1* proximal and *NFKBIA* promoter region compared to control condition. This could be explained by the fact that cancer cells like A549 already have higher basal NF-ƙB activity which means that even in unstimulated state there is already promoter activity. In order to confirm this assumption more experiments should be performed to compare different normal cells with various cancer cell lines. Furthermore, it is of interest to determine the kinetics of such interaction together with the examination of more NF-ƙB target genes.

Several studies have described the repressive effects of NuRD complex in different cancer types. An interesting study by Fu *et al.* showed that TWIST, an oncogene playing an essential role in epithelial mesenchymal transition, binds and interacts with NuRD complex and recruits it to the promoter of E-cadherin. This recruitment results in the repression of E-Cadherin expression and facilitates the switch to a metastatic mesenchymal phenotype[96]. Another study in colorectal cancer cells provided proof that the NuRD complex binds to promoters of several tumour suppressor genes together with DNA methyltransferases to maintain their silencing [122]. Such evidence emphasizes the role of NuRD in tumorigenesis.

5.5 Knockdown of MTA2 supported tumour growth

Next, it was of interest to examine the effect of MTA2 silencing on tumour growth *in vivo*. Mice were injected subcutaneously with LLC1-shMTA2, LLC1-IKK2^{CA} and LLC1-EV. Tumours of LLC1-shMTA2 were the biggest in size followed by those formed by LLC1-IKK2^{CA}. Furthermore, a set of examined NF-ƙB target genes (*Tnf, Nfkbia, Mmp9, Ccnd1, Cdkn1a and Cdkn1b)* was upregulated on transcriptional level in the tumours of LLC1-IKK2^{CA} and even more in LLC1-shMTA2. This observation goes in concordance with the *in vitro* studies showing a repressing effect of MTA2 on the activity of NF-ƙB and the expression of its target genes. A possible explanation would be that knocking down MTA via shRNA released the repressive effect on NF-ƙB and thus promoted tumour growth. MTA2 knock down also upregulated IKK2 expression though it isn't a target gene of NF-ƙB suggesting that MTA2 might play a role in the overall NF-ƙB activation.

Though there are not many publications showing the effect of silencing of MTA2 on tumour growth, Lu *et al*. showed that shMTA2 reduced both primary and metastatic tumour growth in a human breast cancer model with MDA-MB231 cells[123]. This opposing effect to that observed in our lung tumour model inclines that different cellular scenarios might exist and that more experiments are required to fully unravel the underlying mechanisms of MTA2 regulation of tumorigenic processes. Other studies showed that MTA2 promoted cancer progression via the repression of tumour suppression genes like p53[75] or through the repression of E-cadherin expression mediated by TWIST oncogene and thus driving the cell towards a mesenchymal fate[96].

5.6 Impact of genetic changes in epithelial host cells on the immune cell repertoire

The genetic changes in host epithelial cells affect the cross-talk between host cells and their surrounding milieu. Especially in tumours, the role of the microenvironment was recently started to gain more attention in different cancer types[124].

5.6.1 In SpC C-Raf BxB mouse model

The immune cell repertoire in SpC C-Raf BxB was studied in reference to IKK2 modulation. IKK2 downregulation within SpC C-Raf BxB lungs reduced the infiltration of neutrophils, T cells, macrophages and dendritic cells compared to lungs with IKK activation.

This goes in concordance with the publication of Perez-Nazario *et.al.* who showed that host epithelial IKK2-dependent responses are important regulators of pulmonary adaptive immune responses[44]. Macrophages are the main phagocytic cells that would attack tumour cells. However, these changes in the tumour microenvironment could not explain the restricted tumour growth in SpC/IKK2^{DN}/BxB suggesting that both the signalling changes within the host alveolar type II cells as well as the tumour microenvironment intricately control tumour development.

5.6.2 In xenograft model

Flow cytometric analysis revealed the impact of the immune tumour microenvironment on tumour growth (Fig.4.24). Pro-tumorigenic B lymphocytes were abundantly present in LLC1-shMTA2 cells. Other immune cells which are known to be anti-tumorigenic, like cytotoxic natural killer cells and CD8$^+$ T-lymphocytes, were both less represented in tumours from both IKK2^{CA} and shMTA2. Interestingly, CD4$^+$ cells which are responsible for the balance between the two T-helper cell populations, T_H1 and T_H2, were also less in the bigger tumours suggesting that the balance was probably shifted towards the pro-tumorigenic T_H2. A similar tendency was observed with T regulatory cells which though supposed to act as pro-tumorigenic but their presence is often correlated with better patient survival[125].

Most interestingly was the analysis of macrophages and their subtypes. MHC-II$^+$ tumour-associated macrophages (TAMs) are considered as M1-like macrophages which are anti-tumorigenic, whereas MHC-II$^-$ TAMs are generally accepted to be pro-tumorigenic M2-like macrophages[126]. In the subcutaneous tumour of LLC1-shMTA2 and LLC1-IKK2^{CA} there were more MHC-II$^-$ TAMs and less MHC-II$^+$ TAMs compared to control cells.

Nevertheless, it is still debatable that MTA2 is often overexpressed in tumours and is thus correlated with poor prognosis in several cancer types. There is a possibility that there is a negative feedback loop that recruits more MTA2 together with the NuRD complex to suppress the activity of NF-ƙB. As most cancers retain a sustained activation of NF-ƙB, more MTA2 is needed to tightly control excessive activation and is thus recruited to NF-ƙB promoter binding sites leading to expressional repression.

5.7 NF-ƙB in epigenetic regulation

Owing to its seminal role many biological processes, NF-ƙB is regulated at different levels, e.g. by binding to IƙB to stay in the cytoplasm, by post-translational modifications like phosphorylation and acetylation and also by epigenetic modifications. Zhong *et al*. demonstrated that p50 homodimers bind to HDAC1 in resting unstimulated conditions. Once appropriately stimulated, phosphorylated p65 translocates to the nucleus, associates with CBP and displaces p50-HDAC1 complex from the promoter region leading to expression of target genes[127].

Methylation and demethylation processes also play a role in transcriptional activation. Pacaud *et al.* could show that DNA (cytosine-5)-methyltransferase 3-like protein (DNMT3L) forms a complex with DNMT3B and NFkB-p65 at the TRAF1 promoter in the T98G glioma cell line. Higher expression of TRAF1 was observed in cells treated with siRNA against DNMT3L and p65 was recruited to the promoter indicating the role of p65/DNMT3L complex in the control of DNA methylation at TRAF1 promoter[128].

These studies provide evidence of the tight epigenetic control by and on the NF-ƙB complexes. MTA2/NuRD interaction with NF-ƙB can define new regulatory mechanism.

5.8 Conclusion

In this work, the role of NF-ƙB activation via IKK2 in lung cancer was studied *in vitro* and in different preclinical models of lung cancer. Downregulation of IKK2 and subsequent interruption of NF-ƙB activation showed tumour inhibitory effects both directly in host cells as well as indirectly through manipulation of the tumour microenvironment. Interfering with upstream regulators of NF-ƙB usually resulted in many off-target effects making this approach disadvantageous for cancer therapy. Instead, this study attempted a deeper insight into the differential regulation of NF-ƙB signalling via MTA2/NuRD complex. Reporter activity assays, localization studies as well as the expression profile of NF-ƙB target genes confirmed the interaction of MTA2/NuRD complex with p50/p65 leading to the repression of NF-ƙB signalling.

Nevertheless, it is still intriguing how MTA2 is often overexpressed in tumours and is thus correlated with poor prognosis in several cancer types and it represses NF-ƙB which is also aberrantly activated in most cancers. *In vivo* there are several factors contributing to the overall process of tumorigenesis. Our model posits that MTA2 might have a biphasic role in cancer. Increased growth and inflammatory stimuli activate NF-ƙB signalling pathway and thus switching on both positive and negative feedback loops. Excessive activation of NF-ƙB in cancer cells is accomplished via the formation of new cytokines and cell growth signals. At the same time tight regulatory mechanisms are mediated as well through the expression of negative regulators, e.g. IƙB proteins, and through recruitment of MTA2/NuRD complex to NF-ƙB target genes poising their expression. With persistent activation of NF-ƙB in cancer cells, more MTA2 is produced and recruited to respective promoters attempting to constrain excessive activation (Fig. 5.1). This overall balance determines the final fate of the cells; in normal cellular context the activating signal is attenuated, whereas in cancer cells a continuous activation overcomes the tight control mechanisms.

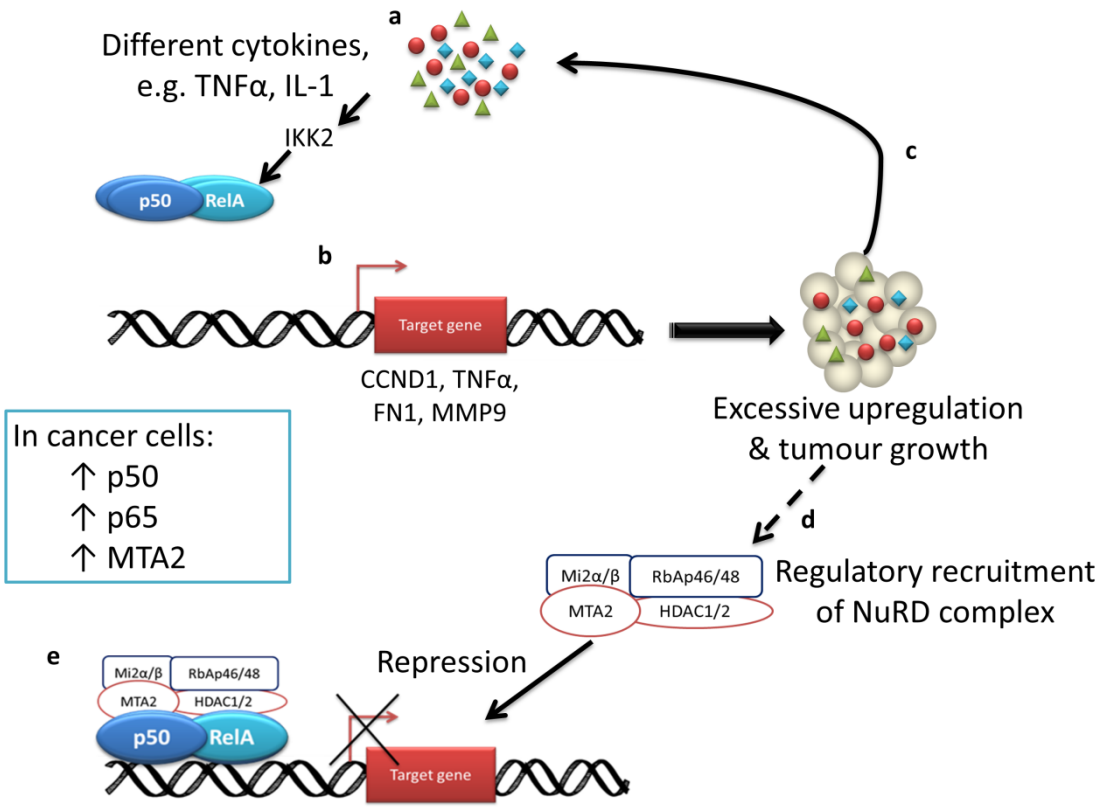

Figure 5.1 Recruitment of MTA2 to NF-kB target genes. a) Cytokines and cellular stimuli activate IKK2 to drive nuclear translocation of p50/p65, b) active transcription of various NF-kB target genes that support tumour growth, c) tumour niche produces more cytokines that further activate NF-kB signalling, d) excessive upregulation of NF-kB recruits MTA2/NuRD complex to promoter region of NF-kB target genes, e) MTA2/NuRD binds to p50/p65 preventing its transcriptional activity.

In conclusion, NF-kB signalling pathway plays a crucial role in tumour development but it is also seminal for maintaining homeostasis. Direct interference with this pathway was to date not satisfactory on therapeutic level. Thus, studying the role of its intricate regulation via MTA2/NuRD complex might provide useful insight into new therapeutic modalities targeting the binding of MTA2 and p50/p65 to each other. Yet, more research is required to delineate the dynamics of this interaction and its specificity within different cellular scenarios.

6 Future Perspectives

Lung cancer is a major challenge stressing a relatively large set of the world population. It is a multifactorial disease controlling several vital processes and the hitherto existing treatment regimens are faced with limited success. Thus there is a compelling need to develop novel but more specific therapies which require a deeper insight into the molecular background within the cancer cells.

Increasing evidence emphasize the role of NF-ƙB in tumorigenesis. Our work clearly showed that IKK2 can regulate tumour growth and metastasis and that MTA2/NuRD complex regulates NF-ƙB. The identified interaction between p50/p65 and MTA2/NuRD complex can be extended to map for their specific interaction domains. This can be attempted by generation of domain deletion variants and analysing their capability of interaction. Such data would be beneficial in targeting the interaction by synthesis of domain specific peptides that would compete with the fully functional proteins and thus hamper the repressing activity of MTA2.

Moreover, both MTA2/NuRD and NF-ƙB family members are capable of forming different complexes suggesting the possible formation of a horde of coexisting complexes with differential activity. Identification of these complexes via mass spectrometry would help in the understanding of the disparity of responses observed in cancer versus normal cells. It would be of benefit to investigate the interaction and its kinetics in other solid tumours such as breast cancer and hepatocellular carcinoma.

Using the existing high throughput platforms, like ChIP-Seq and RNA Seq, it would be possible to identify specific target genes and their respective specific MTA2-binding motifs. This would aid in understanding the paradoxical effects of MTA2/NuRD complex reported in several cancer types.

Understanding these underlying mechanisms combining a crucial inflammatory regulator, NF-ƙB, with the NuRD complex as an essential chromatin remodelling complex, holds great promises for the developing of novel intervention tools in cancer management.

7 Summary

Inflammation and cancer have been linked more than a century ago when Rudolf Virchow identified leukocytes infiltration in neoplastic tissues. Many years of research followed until the discovery of NF-ƙB, which paved the way to more insight into the contribution of inflammatory signalling to cancer development. NF-ƙB is not only involved in many innate and adaptive immune responses but also governs the expression of wide set of diverse genes regulating cell growth and adhesion, cell cycle regulation, apoptosis, angiogenesis – all established hallmarks of neoplastic transformation. Many tumours, especially solid tumours, exhibit constitutive activation of NF-ƙB canonical signalling pathway. This fact encouraged several researchers to develop NF-ƙB inhibitors and IKK2 inhibitors as adjunct therapy to existing cancer treatment modalities, however, with modest success. More studies are required for a better understanding of NF-ƙB activation in cancer and the underlying regulatory mechanisms.

In this work, NF-ƙB canonical signalling was studied in lung adenocarcinoma cell lines and animal model. Chemical stimulation of various adenocarcinoma cells lines (A549, A427, Colo699, H1650, and H2122) as well as non-tumour cell lines (BEAS-2B and HEK) with LPS and TNFα induced NF-ƙB nuclear translocation and subsequent activation. The functional effects of NF-ƙB activation were reflected in increased proliferation and migration. Specific IKK2 inhibitors like sc-514, parthenolide or Bay11-7085 as well as proteosomal inhibitor like MG-132 showed opposed effects indicating that the pivotal role of IKK2 activation in cancer cells. In corroboration, genetic mouse model where IKK2 was specifically constitutively activated or downregulated in SPC-expressing epithelial alveolar type II cells (SpCrtTA/Tet-O-IKK2^{CA}/SpC Ca-Raf BxB and SpCrtTA/Tet-O-IKK2^{DN}/SpC Ca-Raf BxB, respectively) led to significant alterations in tumour development. Downregulation of IKK2 decreased the tumour dispersion in the lung and improved lung function. Furthermore, IKK2 changes in host epithelial cells also affected the immune cell repertoire significantly in the tumour microenvironment.

Importantly, mouse epithelial alveolar type II cells expressing IKK2^{DN} compared to wildtype cells regulated several genes that didn't possess any known NF-ƙB consensus sequences in their promoters. Among these genes was metastasis-associated protein family member 2, known as MTA2. Further examination of MTA2 expression on protein level in

different cells lines suggested that cell lines originating from metastatic sites showed higher expression of MTA2 than those isolated from primary sites. Surprisingly, MTA2 was not upregulated in response to NF-ĸB stimulation, but regulated in response to IKK2 downregulation ($IKK2^{DN}$ or IKK2 inhibitor treatment).

MTA2 is reported as a member of the NuRD complex (consisting of MBD1/2, HDAC1/2, CHD3/4, GATA2Da/b, and RbAp46/448) that regulates gene expression at a transcriptional level. Indeed, MTA2 overexpression decreased NF-ĸB activity and the expression of a wide set of NF-ĸB target genes. Interestingly, our results indicated the presence of MTA2 together with other members of the NuRD complex and NF-ĸB heterodimer p50/p65 as assessed by fractionation, immunoprecipitation and proximity ligation assay studies. Finally, ChIP assay could identify MTA2 and RbAp46 in the promoter region of *NFKB1* and *NFKBIA*, a target gene of NF-ĸB. These data taken together support the hypothesis that MTA2 as part of NuRD complex binds to NF-ĸB and its target genes to regulate their expression.

Finally, MTA2 was knocked down in LLC1 cells via shRNA and injected into C57Bl/6J mice subcutaneously. Tumours with shMTA2 were bigger in size compared to tumours from LLC1 control or even to LLC1-$IKK2^{CA}$. Even their immune repertoire shifted towards a tumour-favouring signature with more M2-like macrophages and less cytotoxic T-lymphocytes.

In summary, this work suggests MTA2 as regulator of NF-ĸB signalling pathway in lung cancer. Increased NF-ĸB activity leads to the expression of several cytokines that continue activating the pathway. A poised mechanism to tightly regulate NF-ĸB recruits MTA2/NuRD complex to cardinal NF-ĸB target genes repressing their transcription. The proposed mechanism still needs more research to elucidate the exact kinetics of this feedback loop regulation.

8 Zusammenfassung

Seit dem letzten Jahrhundert, als Ruldof Virchow Leukozyten in Tumoren entdeckt hat, werden Tumorbildung und Entzündungsprozessen zusammengeknüpft. Viele Jahre der Forschung folgten bis zur der Entdeckung von NF-ĸB. Nuklear Faktor kappa B (NF-ĸB) ist ein wichtiger Transkriptionsfaktor für das Immunsystem und die Regulation von Entzündungsprozessen. Es gibt bereits mehrere Publikationen, die die Dysregulation von NF-ĸB in unterschiedlichen Krebsarten zeigen. Dennoch fehlt der Mechanismus dieser Regulation, der vor allem durch die aktivierende Kinase IKK2 (Inhibitor kappa B kinase beta) vorgeht.

In der vorliegenden Arbeit wurde der klassische Signalweg von NF-ĸB in Lungenkrebs-Zelllinien und anhand von Tiermodellen untersucht. Chemische Stimulation der Tumor-Zelllinien (A549, A427, Colo699, H1650, und H2122) als auch der Kontrollzelllinien (BEAS-2B and HEK) durch LPS und TNFα führte zur Translokation von p50/p65 zum Zellkern. Die darauf folgende Aktivierung der Transkription verschiedener Gene spiegelte sich in zunehmender Proliferation und Migration der Zellen. Spezifische IKK2 Inhibitoren wie sc-514, parthenolide, Bay11-7085 und MG-132 haben diesen Prozess gehemmt. Diese Ergebnisse wurden in einem Tiermodell bestätigt, wo modifiziertes IKK2 unter dem SPC –Promotor zusammen mit C-Raf BxB in alveolaren Epithelzellen exprimiert wurde (SpC rtTA/Tet-O-IKK2^{CA}/SpC C-Raf BxB and SpC rtTA/Tet-O-IKK2^{DN}/SpC C-Raf BxB). Die Runterregulation von IKK2 beschränkte die Tumorbildung, wie durch MRT und histologische Untersuchung zu erkennen war, und verbesserte damit die Lungenfunktion. Darüber hinaus haben die Veränderungen in IKK2-Aktivierung die Immunzellpopulation der Tumorumgebung beeinflusst.

Maus Epithelzellen (ATII) wurden aus Wildtyp-Tieren und SpC rtTA/Tet-O-IKK2^{DN}-Tieren isoliert. Durch den Vergleich der unterschiedlich exprimierten Gene wurde eine Gruppe von Genen identifiziert, die von IKK2^{DN} beeinflusst wurden, obwohl sie keine NF-ĸB Konsensus-Sequenz erweisen. MTA2, metastasis-associated protein family member 2, gehörte zu dieser Gruppe.

Andere Studien haben gezeigt, dass MTA2 in Nichtkleinzelligem Lungenkrebs hochreguliert wird und mit den Krebsstadien korreliert. Die Protein-Expression von MTA2 war in den Lungenkrebs-Zelllinien, die aus Metastasen stammen, höher exprimiert als in den

Zelllinien, deren Herkunft Primärtumore ist. MTA2 gehört zu dem NuRD (Nucleosome Remodelling Deacetylase)-Komplex. Dieser Komplex besteht aus mehreren Proteinen, u.a. die MTA (Metastasen-assoziierten Proteinen)-Familie (MTA1, MTA2 oder MTA3). In der vorliegenden Studie wurde gezeigt, dass MTA2 Überexpression eine repressive Wirkung auf einige NF-ƙB-Zielgene ausübt. Außerdem wurde eine Interaktion zwischen p50/p65 und MTA2/NuRD durch Immunoprecipitation, PLA (proximity ligation assay) und die Fraktionierung nuklearer Komplexe bestätigt. ChIP-Experimente wiesen MTA2 und RbAp46 in den Promotorregionen von *NFKB1* und *NFKBIA* (bekannte NF-ƙB-Zielgene) nach. Dies unterstützt unsere Hypothese, dass MTA2/NuRD-Komplex NF-ƙB-Zielgene reguliert.

Zum Schluss wurden LLC1 Zellen, die shMTA2 und $IKK2^{CA}$ exprimieren, in subkutanem Tumormodell injiziert. Tumore mit blockierten MTA2 (shMTA2) waren mächtiger und zeigten eine tumorfördernde Immunzellumgebung.

Zusammenfassend schlägt die vorliegende Arbeit MTA2 als Regulator von NF-ƙB vor, und stellt damit einen neuen Ansatz für Therapieentwicklung. Mehr Forschung ist dennoch erforderlich, um den biologischen Kontext und die genaue Kinetik der Regulation zu definieren.

9 Appendix

9.1 Appendix I: List of Antibodies

Table 9.1 Antibodies used for Western blotting (WB)

Antibody	Host	Dilution	Company (Catalogue Number)
CHD4	Mouse	1:1000	Abcam (ab70469)
Cyclin D1(92G2)	rabbit	1:1000	Cell Signalling (2978)
HDAC1	Rabbit	1:1000	Abcam (ab7028)
HDAC2	Rabbit	1:1000	Abcam (ab16032)
IκB (44D4)	Rabbit	1:1000	Cell Signalling (4812)
MTA2	Rabbit	1:200	Abcam (ab8106)
NF-κB p105/p50 [E381]	Rabbit	1:1000	Abcam (ab32360)
NF-κB p65 (C-20)	Rabbit	1:200	Santa Cruz (sc-372)
p300 (N-15)	Rabbit	1:200	Santa Cruz (sc-584)
RbAp46 (N-19)	Goat	1:200	Santa Cruz (sc-8272)
ß-actin [AC-15]	Mouse	1:3000	Abcam (ab6276)

Table 9.2 Antibodies used for Immunocytochemistry (ICC) & Proximity ligation assay (PLA)

Antibody	Host	Dilution	Company (Catalogue Number)
MTA2	Rabbit	1:200	Abcam (ab8106)
NF-κB p50 (NLS)	Rabbit	1:200	Santa Cruz (sc-114)
NF-κB p65 (C-20)	Rabbit	1:200	Santa Cruz (sc-372)
NF-κB p-p65 (A-8)	Mouse	1:200	Santa Cruz (sc-166748)
Surfactant protein C	Rabbit	1:1000	Millipore (AB3786)

Table 9.3 Antibodies used for Immunohistochemistry (IHC) & Immunofluorescence (IF)

Antibody	Host	Dilution	Antigen retrieval	Company (Catalogue Number)
CD11b [EP1345Y]	Rabbit	1:100	Trypsin	Abcam (ab52478)
CD3	Mouse	1:200	EDTA	Dako(M7254)
IKK2 (P-20)	Goat	1:200	Citrate	Santa Cruz (sc-34673)
MMP9 (C-20)	Goat	1:200	Citrate	Santa Cruz (sc-6840)
MTA2	Rabbit	1:200	Citrate	Abcam (ab8106)
NF-ƙB p50 (NLS)	Rabbit	1:200	Citrate	Santa Cruz (sc-114)
NF-ƙB p65 (C-20)	Rabbit	1:200	Citrate	Santa Cruz (sc-372)
NF-ƙB p-p65 (A-8)	Mouse	1:200	Citrate	Santa Cruz (sc-166748)
PCNA (FL-261)	Rabbit	1:200	Citrate	Santa Cruz (sc-7907)
Raf-1 (C-Raf; C-20)	Rabbit	1.200	Citrate	Santa Cruz (sc-227)

Table 9.4 List of Secondary antibodies

Antibody	Dilution	Application	Company (Catalogue Number)
Alexa Fluor® conjugates	1:1000	ICC, IF	Invitrogen, Molecular Probes
Anti-mouse IgG HRP conjugate	1:3000	WB	Promega (W4028)
Anti-rabbit IgG HRP conjugate	1:3000	WB	Promega (W4018)
Bovine anti-goat IgG HRP	1:3000	WB	Santa Cruz (sc-2378)
Normal rabbit IgG	1µg/0.2x10^6 cells	ChIP	Santa Cruz (sc-2027)

9.2 Appendix II: List of Primers

Table 9.5 List of primers used for quantitative real time PCR (Mus musculus)

Gene	Primer Sequence (5'-3')	Annealing temperature	Accession Number
Ccnd1	**FP:** ATGAACTTCACATCTGTGGCA **RP:** CCCCACGATTTCATCGAACA	58	NM_007631.2
Cdkn1a	**FP:** TGGTGTCTGAGCGGCCTGAA **RP:** GCCTCCTGACCCACAGCAGA	58	NM_001111099.1
Cdkn1b	**FP:** AATCCGGCTGGGTTAGCGGA **RP:** TCTTGGGCGTCTGCTCCACA	58	NM_009875.4
Chuk	**FP:** aTGCCTGTACACAGAGTTCTGCCC **RP:** TCACACATGTCAGAGGATGTTCACG	58	NM_001162410.1
Fn1	**FP:** TGGATAGCACCCAGTGTTCAG **RP:** CCTGTCTTCTCTTTCGGGTTCA	58	NM_010233.1
Hprt	**FP:** GCTGACCTGCTGGATTACAT **RP:** TTGGGGCTGTACTGCTTAAC	58	NM_013556.2
Ikbkb	**FP:** AGAAAAGTGAAGAACTGGTGGCCG **RP:** CCCTCAGGCGGTTACCGTGA	58	NM_001159774.1
Mmp9	**FP:** ACGGGTATCCCTTCGACGGC **RP:** AGTGGGGATCACGACGCCTTT	58	NM_013599.2
Mta1	**FP:** ACCAGTGGTATTCTTGGGGT **RP:** GTGGGGACTCATGTTACTGC	58	NM_054081.2
Mta2	**FP:** TCCCACCTACACTAAGCCAA **RP:** GTGGCAACTCTCACAAGTCA	58	NM_011842.3
Mta3	**FP:** TCCCAACCTACAAACCAAATCC **RP:** TTAGGTGGGCCCCAAGAATA	58	NM_001171053.1
Myc	**FP:** CCCACCCGCCCTTTATATTCC **RP:** GTCCTGGCTCGCAGATTGTA	58	NM_010849.4
Ncam1	**FP:** GCAGTTTACAATGCTGCGAA **RP:** CATCTCCTGCCACTTGACAC	58	NM_001081445.1
Nfkb1	**FP:** AGGGGTCACCCATGGCACCA **RP:** TGCCAAGGCGATGGGTTCCG	58	NM_008689.2
Nfkbia	**FP:** GCTACCCGAGAGCGAGGAT **RP:** GCCTCCAAACACACAGTCATCAT	58	NM_010907
Rela	**FP:** TGATAACCGGGCCCCCAA **RP:** CTGCACCTTGTCGCACAG	58	NM_009045.4
Tert	**FP:** CGGACAAAACATCCTCACCT **RP:** CGGTCACATCTGCCTTAACA	58	NM_009354.1
Tnf	**FP:** CAGGCGGTGCCTATGTCTC **RP:** CGATCACCCCGAAGTTCAGTAG	60	NM_013693.2
Twist1	**FP:** GGACAAGCTGAGCAAGATTCA **RP:** CGGAGAAGGCGTAGCTGAG	58	NM_011658.2
Vegfc	**FP:** ACCTCCATGTGTGTCCGTCT **RP:** TTCAAACAACGTCTTGCTGAGG	58	NM_009506.2

Table 9.6 List of primers used for quantitative real time PCR (Homo sapiens)

Gene	Primer Sequence (5'-3')	Annealing temperature	Accession Number
FN1	**FP:** ATTACTGGCCTGGAACCGGGA **RP:** ACCAGTTGGGGAAGCTCGTCT	60	NM_002026
HPRT	**FP:** TGACACTGGCAAAACAAT **RP:** GGTCCTTTTCACCAGCAA	58	
MMP9	**FP:** CGGAGCACGGAGACGGGTAT **RP:** GAGTTGGAACCACGACGCCC	58	NM_004994
MTA1	**FP:** ACCAGTGGTATTCTTGGGGT **RP:** GTGGGGACTCATGTTACTGC	58	NM_004689.3
MTA2	**FP:** TCCCACCTACACTAAGCCAA **RP:** GTGGCAACTCTCACAAGTCA	58	NM_004739.3
NFKB1	**FP:** GCCACCCGGCTTCAGAATGG **RP:** GGCCATCTGCTGTTGGCAGT	60	NM_003998.3
RELA	**FP:** GCAGTGTTGGGGGCACGATT **RP:** AGAGCAGCGTGGGGACTACG	58	NM_021975.3

Table 9.7 List of primers used for genotyping by qualitative PCR

Genotype	Primer Sequence (5'-3')	Annealing temperature	Amplicon size (bp)
SpC C-Raf BxB	**SPC S1:** GAG GAG AGG AGA GCA TAG CAC C **BXB :** ACA TCT CCG TGC CAT TTA CCC	60	400
SpC rtTA	**SPC USA:** GAC ACA TAT AAG ACC CTG GTC A **rtTA USA:** AAA ATC TTG CCA GCT TTC CCC	58	
Tet-O-IKK2EE ($IKK2^{CA}$)	**pBI5:** GGT ACC CGG GGA TCC TCT AGT CAG **IKK2-rev1:** GGT CAC TGT GTA CTT CTG CTG CTC CAG	63	672
Tet-O-IKK2DN ($IKK2^{DN}$)	**pBI5:** GGT ACC CGG GGA TCC TCT AGT CAG **IKK2-rev1**: GGT CAC TGT GTA CTT CTG CTG CTC CAG	63	822

Table 9.8 List of ChIP primers

Gene	Primer Sequence (5'-3')	Annealing temperature	Binding site
NFKB1	**Proximal FP:** GAC GTC AGT GGG AAT TTC C **Proximal RP:** GTG GCG AAA CCT CCT CTT C	58	-28
NFkB1	**Upstream FP:** TGC TGC ATG GAA TTA CAT CC **Upstream RP:** CAT CTT AAC TTG ATA ACA TTT GC	58	-2341
NFKBIA	**FP:** GAC GAC CCC AAT TCA AAT CG **RP:** TCA GGC TCG GGG AAT TTC C	58	-342

9.3 Appendix III: List of Buffers

Table 9.9 Buffers used for chromatin immunoprecipitation (ChIP)

Buffer	Composition
L1 lysis buffer	50 mM Tris.HCl pH 8 2 mM EDTA pH 8 0.1% NP40 (IGEPAL instead) 10% Glycerol
L2 nuclear resuspension buffer	50 mM Tris.HCl pH 8 5 mM EDTA pH 8 1% SDS
Dilution buffer (DB)	50 mM Tris.HCl pH 8 5 mM EDTA pH 8 0.5% NP40 0.2 M NaCl
Low salt washing buffer	20 mM Tris.HCl pH 8 2 mM EDTA pH 8 1% NP40 (IGEPAL instead) 0.1% SDS 0.15 M NaCl
High salt washing buffer	20 mM Tris.HCl pH 8 2 mM EDTA pH 8 1% NP40 (IGEPAL instead) 0.1% SDS 0.5 M NaCl
LiCl washing buffer	10 mM Tris.HCl pH 8 1 mM EDTA pH 8 1% NP40 (IGEPAL instead) 1% Na-deoxycholate 0.25 M LiCl
TE buffer	10 mM Tris.HCl pH 8 1 mM EDTA pH 8
C1 DNA elution buffer	10 mM Tris.HCl pH 8 1 mM EDTA pH 8 0.1 M NaHCO3 1% SDS
DNA elution TE buffer	25 mM Tris.HCl 1 mM EDTA pH 10

Table 9.10 Buffers used for immunoprecipitation (Co-IP) and nuclear fractionation

Buffer	Composition
Co-IP buffer	50mM Tris pH7.4 15mM EGTA 100mM NaCl 0.1% (v/v) TritonX-100
Modified cell lysis buffer	10mM Tris pH7.4 1.5mM MgCl2 10mM KCl 0.1% TritonX-100 1mM EDTA
2x SDS PAGE sample application buffer	150mM Tris pH6.8 1.2% SDS 30% glycerol 6.7% ß-mercaptoethanol 1.8mg bromophenol blue
Hypotonic lysis buffer	10mM Tris HCl pH 7.4 1.5 mM MgCl 10mM KC
Native nuclear lysis buffer	0.2% IGEPAL 100mM NaCl 50 mM Tris HCl pH 7.0 1mM EDTA

Table 9.11 Buffers used for SDS-PAGE & immunoblotting

Buffer	Composition
10x SDS PAGE running buffer	35mM SDS 250mM Tris 0.86M glycin
Blotting buffer	25mM Tris 192mM glycine 20% methanol
5x SDS PAGE sample application buffer	1.5M Tris-HCl pH 6.8 10% SDS 50% glycerol 25% ß-mercaptoethanol 0.01% bromophenol blue

10 References

1. World Cancer Report. *IARC* (2014).
2. Jemal, A. *et al.* Global cancer statistics. *CA Cancer J Clin* **61**, 69-90 (2011).
3. Travis, W.D. Pathology of lung cancer. *Clin Chest Med* **32**, 669-692 (2011).
4. Shames, D.S. & Wistuba, II The evolving genomic classification of lung cancer. *J Pathol* **232**, 121-133 (2014).
5. Davidson, M.R., Gazdar, A.F. & Clarke, B.E. The pivotal role of pathology in the management of lung cancer. *J Thorac Dis* **5 Suppl 5**, S463-478 (2013).
6. Chen, Z., Fillmore, C.M., Hammerman, P.S., Kim, C.F. & Wong, K.K. Non-small-cell lung cancers: a heterogeneous set of diseases. *Nat Rev Cancer* **14**, 535-546 (2014).
7. Devarakonda, S., Morgensztern, D. & Govindan, R. Genomic alterations in lung adenocarcinoma. *Lancet Oncol* **16**, e342-351 (2015).
8. Sutherland, K.D. & Berns, A. Cell of origin of lung cancer. *Mol Oncol* **4**, 397-403 (2010).
9. Xu, X. *et al.* Evidence for type II cells as cells of origin of K-Ras-induced distal lung adenocarcinoma. *Proc Natl Acad Sci U S A* **109**, 4910-4915 (2012).
10. Kloth, M. & Buettner, R. Changing histopathological diagnostics by genome-based tumor classification. *Genes (Basel)* **5**, 444-459 (2014).
11. Ferlay, J. *et al.* Estimates of worldwide burden of cancer in 2008: GLOBOCAN 2008. *Int J Cancer* **127**, 2893-2917 (2010).
12. Ding, L. *et al.* Somatic mutations affect key pathways in lung adenocarcinoma. *Nature* **455**, 1069-1075 (2008).
13. Slebos, R.J. *et al.* K-ras oncogene activation as a prognostic marker in adenocarcinoma of the lung. *N Engl J Med* **323**, 561-565 (1990).
14. Meister, M., Tomasovic, A., Banning, A. & Tikkanen, R. Mitogen-Activated Protein (MAP) Kinase Scaffolding Proteins: A Recount. *Int J Mol Sci* **14**, 4854-4884 (2013).
15. Blasco, R.B. *et al.* c-Raf, but not B-Raf, is essential for development of K-Ras oncogene-driven non-small cell lung carcinoma. *Cancer Cell* **19**, 652-663 (2011).
16. Rapp, U.R. *et al.* Structure and biological activity of v-raf, a unique oncogene transduced by a retrovirus. *Proc Natl Acad Sci U S A* **80**, 4218-4222 (1983).
17. Wellbrock, C., Karasarides, M. & Marais, R. The RAF proteins take centre stage. *Nat Rev Mol Cell Biol* **5**, 875-885 (2004).
18. Kerkhoff, E. *et al.* Lung-targeted expression of the c-Raf-1 kinase in transgenic mice exposes a novel oncogenic character of the wild-type protein. *Cell Growth Differ* **11**, 185-190 (2000).
19. Khazak, V., Astsaturov, I., Serebriiskii, I.G. & Golemis, E.A. Selective Raf inhibition in cancer therapy. *Expert Opin Ther Targets* **11**, 1587-1609 (2007).
20. Zhang, J., Gold, K.A. & Kim, E. Sorafenib in non-small cell lung cancer. *Expert Opin Investig Drugs* **21**, 1417-1426 (2012).
21. Baumann, B. *et al.* Raf induces NF-kappaB by membrane shuttle kinase MEKK1, a signaling pathway critical for transformation. *Proc Natl Acad Sci U S A* **97**, 4615-4620 (2000).
22. Sen, R. & Baltimore, D. Inducibility of kappa immunoglobulin enhancer-binding protein Nf-kappa B by a posttranslational mechanism. *Cell* **47**, 921-928 (1986).
23. Karin, M. & Greten, F.R. NF-kappaB: linking inflammation and immunity to cancer development and progression. *Nat Rev Immunol* **5**, 749-759 (2005).
24. Karin, M., Cao, Y., Greten, F.R. & Li, Z.W. NF-kappaB in cancer: from innocent bystander to major culprit. *Nat Rev Cancer* **2**, 301-310 (2002).
25. Oeckinghaus, A. & Ghosh, S. The NF-kappaB family of transcription factors and its regulation. *Cold Spring Harb Perspect Biol* **1**, a000034 (2009).
26. Hoesel, B. & Schmid, J.A. The complexity of NF-kappaB signaling in inflammation and cancer. *Mol Cancer* **12**, 86 (2013).
27. Ghosh, S., May, M.J. & Kopp, E.B. NF-kappa B and Rel proteins: evolutionarily conserved mediators of immune responses. *Annu Rev Immunol* **16**, 225-260 (1998).

28. Perkins, N.D. The diverse and complex roles of NF-kappaB subunits in cancer. *Nat Rev Cancer* **12**, 121-132 (2012).
29. Wong, D. *et al.* Extensive characterization of NF-kappaB binding uncovers non-canonical motifs and advances the interpretation of genetic functional traits. *Genome Biol* **12**, R70 (2011).
30. Strober, W., Fuss, I., Kitani, A. & Fichtner-Feigel, S. (Google Patents, 2006).
31. Chen, F.E. & Ghosh, G. Regulation of DNA binding by Rel/NF-kappaB transcription factors: structural views. *Oncogene* **18**, 6845-6852 (1999).
32. Israel, A. The IKK complex, a central regulator of NF-kappaB activation. *Cold Spring Harb Perspect Biol* **2**, a000158 (2010).
33. Jost, P.J. & Ruland, J. Aberrant NF-kappaB signaling in lymphoma: mechanisms, consequences, and therapeutic implications. *Blood* **109**, 2700-2707 (2007).
34. Hochrainer, K., Racchumi, G. & Anrather, J. Site-specific phosphorylation of the p65 protein subunit mediates selective gene expression by differential NF-kappaB and RNA polymerase II promoter recruitment. *J Biol Chem* **288**, 285-293 (2013).
35. Hou, S., Guan, H. & Ricciardi, R.P. Phosphorylation of serine 337 of NF-kappaB p50 is critical for DNA binding. *J Biol Chem* **278**, 45994-45998 (2003).
36. Hochrainer, K., Racchumi, G. & Anrather, J. Hypo-phosphorylation leads to nuclear retention of NF-kappaB p65 due to impaired IkappaBalpha gene synthesis. *FEBS Lett* **581**, 5493-5499 (2007).
37. Yang, F., Tang, E., Guan, K. & Wang, C.Y. IKK beta plays an essential role in the phosphorylation of RelA/p65 on serine 536 induced by lipopolysaccharide. *J Immunol* **170**, 5630-5635 (2003).
38. Duran, A., Diaz-Meco, M.T. & Moscat, J. Essential role of RelA Ser311 phosphorylation by zetaPKC in NF-kappaB transcriptional activation. *EMBO J* **22**, 3910-3918 (2003).
39. Bohuslav, J., Chen, L.F., Kwon, H., Mu, Y. & Greene, W.C. p53 induces NF-kappaB activation by an IkappaB kinase-independent mechanism involving phosphorylation of p65 by ribosomal S6 kinase 1. *J Biol Chem* **279**, 26115-26125 (2004).
40. Ju, J. *et al.* Phosphorylation of p50 NF-kappaB at a single serine residue by DNA-dependent protein kinase is critical for VCAM-1 expression upon TNF treatment. *J Biol Chem* **285**, 41152-41160 (2010).
41. Deng, W.G., Zhu, Y. & Wu, K.K. Up-regulation of p300 binding and p50 acetylation in tumor necrosis factor-alpha-induced cyclooxygenase-2 promoter activation. *J Biol Chem* **278**, 4770-4777 (2003).
42. Deng, W.G. & Wu, K.K. Regulation of inducible nitric oxide synthase expression by p300 and p50 acetylation. *J Immunol* **171**, 6581-6588 (2003).
43. Furia, B. *et al.* Enhancement of nuclear factor-kappa B acetylation by coactivator p300 and HIV-1 Tat proteins. *J Biol Chem* **277**, 4973-4980 (2002).
44. Perez-Nazario, N. *et al.* Selective ablation of lung epithelial IKK2 impairs pulmonary Th17 responses and delays the clearance of Pneumocystis. *J Immunol* **191**, 4720-4730 (2013).
45. Pannicke, U. *et al.* Deficiency of innate and acquired immunity caused by an IKBKB mutation. *N Engl J Med* **369**, 2504-2514 (2013).
46. Silva, A., Cornish, G., Ley, S.C. & Seddon, B. NF-kappaB signaling mediates homeostatic maturation of new T cells. *Proc Natl Acad Sci U S A* **111**, E846-855 (2014).
47. Ravi, R. & Bedi, A. NF-kappaB in cancer--a friend turned foe. *Drug Resist Updat* **7**, 53-67 (2004).
48. Tergaonkar, V., Pando, M., Vafa, O., Wahl, G. & Verma, I. p53 stabilization is decreased upon NFkappaB activation: a role for NFkappaB in acquisition of resistance to chemotherapy. *Cancer Cell* **1**, 493-503 (2002).
49. Beg, A.A. & Baltimore, D. An essential role for NF-kappaB in preventing TNF-alpha-induced cell death. *Science* **274**, 782-784 (1996).

50. Mantovani, A. Molecular pathways linking inflammation and cancer. *Curr Mol Med* **10**, 369-373 (2010).
51. Karin, M. NF-kappaB as a critical link between inflammation and cancer. *Cold Spring Harb Perspect Biol* **1**, a000141 (2009).
52. Ben-Neriah, Y. & Karin, M. Inflammation meets cancer, with NF-kappaB as the matchmaker. *Nat Immunol* **12**, 715-723 (2011).
53. Mantovani, A., Garlanda, C. & Allavena, P. Molecular pathways and targets in cancer-related inflammation. *Ann Med* **42**, 161-170 (2010).
54. Vlantis, K. *et al.* Constitutive IKK2 activation in intestinal epithelial cells induces intestinal tumors in mice. *J Clin Invest* **121**, 2781-2793 (2011).
55. Greten, F.R. *et al.* IKKbeta links inflammation and tumorigenesis in a mouse model of colitis-associated cancer. *Cell* **118**, 285-296 (2004).
56. Maxwell, P.J. *et al.* HIF-1 and NF-kappaB-mediated upregulation of CXCR1 and CXCR2 expression promotes cell survival in hypoxic prostate cancer cells. *Oncogene* **26**, 7333-7345 (2007).
57. Akca, H., Demiray, A., Tokgun, O. & Yokota, J. Invasiveness and anchorage independent growth ability augmented by PTEN inactivation through the PI3K/AKT/NFkB pathway in lung cancer cells. *Lung Cancer* **73**, 302-309 (2011).
58. Takeuchi, S. & Nawashiro, H. NFKBIA deletion in glioblastomas. *N Engl J Med* **365**, 276-277; author reply 277-278 (2011).
59. Yan, M. *et al.* Correlation of NF-kappaB signal pathway with tumor metastasis of human head and neck squamous cell carcinoma. *BMC Cancer* **10**, 437 (2010).
60. Kendellen, M.F., Bradford, J.W., Lawrence, C.L., Clark, K.S. & Baldwin, A.S. Canonical and non-canonical NF-kappaB signaling promotes breast cancer tumor-initiating cells. *Oncogene* **33**, 1297-1305 (2014).
61. Del Prete, A. *et al.* Molecular pathways in cancer-related inflammation. *Biochem Med (Zagreb)* **21**, 264-275 (2011).
62. Demchenko, Y.N. *et al.* Novel inhibitors are cytotoxic for myeloma cells with NFkB inducing kinase-dependent activation of NFkB. *Oncotarget* **5**, 4554-4566 (2014).
63. Jones, D.R., Broad, R.M., Madrid, L.V., Baldwin, A.S., Jr. & Mayo, M.W. Inhibition of NF-kappaB sensitizes non-small cell lung cancer cells to chemotherapy-induced apoptosis. *Ann Thorac Surg* **70**, 930-936; discussion 936-937 (2000).
64. Antoon, J.W. *et al.* Targeting NFkB mediated breast cancer chemoresistance through selective inhibition of sphingosine kinase-2. *Cancer Biol Ther* **11**, 678-689 (2011).
65. Rundall, B.K., Denlinger, C.E. & Jones, D.R. Combined histone deacetylase and NF-kappaB inhibition sensitizes non-small cell lung cancer to cell death. *Surgery* **136**, 416-425 (2004).
66. Singha, B. *et al.* IKK inhibition increases bortezomib effectiveness in ovarian cancer. *Oncotarget* **6**, 26347-26358 (2015).
67. Smits, A.H., Jansen, P.W., Poser, I., Hyman, A.A. & Vermeulen, M. Stoichiometry of chromatin-associated protein complexes revealed by label-free quantitative mass spectrometry-based proteomics. *Nucleic Acids Res* **41**, e28 (2013).
68. Lai, A.Y. & Wade, P.A. Cancer biology and NuRD: a multifaceted chromatin remodelling complex. *Nat Rev Cancer* **11**, 588-596 (2011).
69. Allen, H.F., Wade, P.A. & Kutateladze, T.G. The NuRD architecture. *Cell Mol Life Sci* **70**, 3513-3524 (2013).
70. Segre, C.V. & Chiocca, S. Regulating the regulators: the post-translational code of class I HDAC1 and HDAC2. *J Biomed Biotechnol* **2011**, 690848 (2011).
71. Torchy, M.P., Hamiche, A. & Klaholz, B.P. Structure and function insights into the NuRD chromatin remodeling complex. *Cell Mol Life Sci* **72**, 2491-2507 (2015).
72. Manavathi, B. & Kumar, R. Metastasis tumor antigens, an emerging family of multifaceted master coregulators. *J Biol Chem* **282**, 1529-1533 (2007).

73. Millard, C.J., Fairall, L. & Schwabe, J.W. Towards an understanding of the structure and function of MTA1. *Cancer Metastasis Rev* **33**, 857-867 (2014).
74. Baubec, T., Ivanek, R., Lienert, F. & Schubeler, D. Methylation-dependent and -independent genomic targeting principles of the MBD protein family. *Cell* **153**, 480-492 (2013).
75. Luo, J., Su, F., Chen, D., Shiloh, A. & Gu, W. Deacetylation of p53 modulates its effect on cell growth and apoptosis. *Nature* **408**, 377-381 (2000).
76. Toh, Y. & Nicolson, G.L. The role of the MTA family and their encoded proteins in human cancers: molecular functions and clinical implications. *Clin Exp Metastasis* **26**, 215-227 (2009).
77. Liu, S.L. *et al.* Expression of metastasis-associated protein 2 (MTA2) might predict proliferation in non-small cell lung cancer. *Target Oncol* **7**, 135-143 (2012).
78. Liu, Y.P., Shan, B.E., Wang, X.L. & Ma, L. Correlation between MTA2 overexpression and tumour progression in esophageal squamous cell carcinoma. *Exp Ther Med* **3**, 745-749 (2012).
79. Liu, J., Wang, H., Huang, C. & Qian, H. Subcellular localization of MTA proteins in normal and cancer cells. *Cancer Metastasis Rev* **33**, 843-856 (2014).
80. Tartey, S. *et al.* Akirin2 is critical for inducing inflammatory genes by bridging IkappaB-zeta and the SWI/SNF complex. *EMBO J* **33**, 2332-2348 (2014).
81. Ennen, M. *et al.* DDB2: a novel regulator of NF-kappaB and breast tumor invasion. *Cancer Res* **73**, 5040-5052 (2013).
82. Elsharkawy, A.M. *et al.* The NF-kappaB p50:p50:HDAC-1 repressor complex orchestrates transcriptional inhibition of multiple pro-inflammatory genes. *J Hepatol* **53**, 519-527 (2010).
83. Ziegler-Heitbrock, L. The p50-homodimer mechanism in tolerance to LPS. *J Endotoxin Res* **7**, 219-222 (2001).
84. Paz-Priel, I., Houng, S., Dooher, J. & Friedman, A.D. C/EBPalpha and C/EBPalpha oncoproteins regulate nfkb1 and displace histone deacetylases from NF-kappaB p50 homodimers to induce NF-kappaB target genes. *Blood* **117**, 4085-4094 (2011).
85. Corti, M., Brody, A.R. & Harrison, J.H. Isolation and primary culture of murine alveolar type II cells. *Am J Respir Cell Mol Biol* **14**, 309-315 (1996).
86. Ahlbrecht, K. *et al.* Spatiotemporal expression of flk-1 in pulmonary epithelial cells during lung development. *Am J Respir Cell Mol Biol* **39**, 163-170 (2008).
87. Unkel, B. *et al.* Alveolar epithelial cells orchestrate DC function in murine viral pneumonia. *J Clin Invest* **122**, 3652-3664 (2012).
88. Mercurio, F. *et al.* IKK-1 and IKK-2: cytokine-activated IkappaB kinases essential for NF-kappaB activation. *Science* **278**, 860-866 (1997).
89. Boyden, S. The chemotactic effect of mixtures of antibody and antigen on polymorphonuclear leucocytes. *J Exp Med* **115**, 453-466 (1962).
90. Badr, C.E. *et al.* Real-time monitoring of nuclear factor kappaB activity in cultured cells and in animal models. *Mol Imaging* **8**, 278-290 (2009).
91. Herrmann, O. *et al.* IKK mediates ischemia-induced neuronal death. *Nat Med* **11**, 1322-1329 (2005).
92. Jensen, M.M., Jorgensen, J.T., Binderup, T. & Kjaer, A. Tumor volume in subcutaneous mouse xenografts measured by microCT is more accurate and reproducible than determined by 18F-FDG-microPET or external caliper. *BMC Med Imaging* **8**, 16 (2008).
93. Krupnick, A.S. *et al.* Quantitative monitoring of mouse lung tumors by magnetic resonance imaging. *Nat Protoc* **7**, 128-142 (2012).
94. Irvin, C.G. & Bates, J.H. Measuring the lung function in the mouse: the challenge of size. *Respir Res* **4**, 4 (2003).
95. Baud, V. & Karin, M. Is NF-kappaB a good target for cancer therapy? Hopes and pitfalls. *Nat Rev Drug Discov* **8**, 33-40 (2009).
96. Fu, J. *et al.* The TWIST/Mi2/NuRD protein complex and its essential role in cancer metastasis. *Cell Res* **21**, 275-289 (2011).

97. Kampen, K.R. The discovery and early understanding of leukemia. *Leuk Res* **36**, 6-13 (2012).
98. Tang, X. *et al.* Nuclear factor-kappaB (NF-kappaB) is frequently expressed in lung cancer and preneoplastic lesions. *Cancer* **107**, 2637-2646 (2006).
99. Tobar, N., Villar, V. & Santibanez, J.F. ROS-NFkappaB mediates TGF-beta1-induced expression of urokinase-type plasminogen activator, matrix metalloproteinase-9 and cell invasion. *Mol Cell Biochem* **340**, 195-202 (2010).
100. Guan, X., Chance, M.R. & Barnholtz-Sloan, J.S. Splitting random forest (SRF) for determining compact sets of genes that distinguish between cancer subtypes. *J Clin Bioinforma* **2**, 13 (2012).
101. Kellar, A., Egan, C. & Morris, D. Preclinical Murine Models for Lung Cancer: Clinical Trial Applications. *Biomed Res Int* **2015**, 621324 (2015).
102. Kwon, M.C. & Berns, A. Mouse models for lung cancer. *Mol Oncol* **7**, 165-177 (2013).
103. Staudt, L.M. Oncogenic activation of NF-kappaB. *Cold Spring Harb Perspect Biol* **2**, a000109 (2010).
104. Daniluk, J. *et al.* An NF-kappaB pathway-mediated positive feedback loop amplifies Ras activity to pathological levels in mice. *J Clin Invest* **122**, 1519-1528 (2012).
105. Jourdan, M. *et al.* Targeting NF-kappaB pathway with an IKK2 inhibitor induces inhibition of multiple myeloma cell growth. *Br J Haematol* **138**, 160-168 (2007).
106. Deng, C. *et al.* The novel IKK2 inhibitor LY2409881 potently synergizes with histone deacetylase inhibitors in preclinical models of lymphoma through the downregulation of NF-kappaB. *Clin Cancer Res* **21**, 134-145 (2015).
107. Xia, Y. *et al.* Reduced cell proliferation by IKK2 depletion in a mouse lung-cancer model. *Nat Cell Biol* **14**, 257-265 (2012).
108. Lin, Y., Bai, L., Chen, W. & Xu, S. The NF-kappaB activation pathways, emerging molecular targets for cancer prevention and therapy. *Expert Opin Ther Targets* **14**, 45-55 (2010).
109. Kim, H.J., Hawke, N. & Baldwin, A.S. NF-kappaB and IKK as therapeutic targets in cancer. *Cell Death Differ* **13**, 738-747 (2006).
110. Chariot, A. The NF-kappaB-independent functions of IKK subunits in immunity and cancer. *Trends Cell Biol* **19**, 404-413 (2009).
111. Zheng, S., El-Naggar, A.K., Kim, E.S., Kurie, J.M. & Lozano, G. A genetic mouse model for metastatic lung cancer with gender differences in survival. *Oncogene* **26**, 6896-6904 (2007).
112. Zhou, J. *et al.* P300 binds to and acetylates MTA2 to promote colorectal cancer cells growth. *Biochem Biophys Res Commun* **444**, 387-390 (2014).
113. Zhang, B., Zhang, H. & Shen, G. Metastasis-associated protein 2 (MTA2) promotes the metastasis of non-small-cell lung cancer through the inhibition of the cell adhesion molecule Ep-CAM and E-cadherin. *Jpn J Clin Oncol* **45**, 755-766 (2015).
114. Ding, W., Hu, W., Yang, H., Ying, T. & Tian, Y. Prognostic correlation between MTA2 expression level and colorectal cancer. *Int J Clin Exp Pathol* **8**, 7173-7180 (2015).
115. Covington, K.R. *et al.* Metastasis tumor-associated protein 2 enhances metastatic behavior and is associated with poor outcomes in estrogen receptor-negative breast cancer. *Breast Cancer Res Treat* (2013).
116. Williams, C.J. *et al.* The chromatin remodeler Mi-2beta is required for CD4 expression and T cell development. *Immunity* **20**, 719-733 (2004).
117. Miccio, A. & Blobel, G.A. Role of the GATA-1/FOG-1/NuRD pathway in the expression of human beta-like globin genes. *Mol Cell Biol* **30**, 3460-3470 (2010).
118. Miccio, A. *et al.* NuRD mediates activating and repressive functions of GATA-1 and FOG-1 during blood development. *EMBO J* **29**, 442-456 (2010).
119. Zhang, H., Stephens, L.C. & Kumar, R. Metastasis tumor antigen family proteins during breast cancer progression and metastasis in a reliable mouse model for human breast cancer. *Clin Cancer Res* **12**, 1479-1486 (2006).

120. Matsusue, K., Takiguchi, S., Toh, Y. & Kono, A. Characterization of mouse metastasis-associated gene 2: genomic structure, nuclear localization signal, and alternative potentials as transcriptional activator and repressor. *DNA Cell Biol* **20**, 603-611 (2001).
121. Kravtsova-Ivantsiv, Y. *et al.* KPC1-mediated ubiquitination and proteasomal processing of NF-kappaB1 p105 to p50 restricts tumor growth. *Cell* **161**, 333-347 (2015).
122. Cai, Y. *et al.* The NuRD complex cooperates with DNMTs to maintain silencing of key colorectal tumor suppressor genes. *Oncogene* **33**, 2157-2168 (2014).
123. Lu, J. & Jin, M.L. Short-hairpin RNA-mediated MTA2 silencing inhibits human breast cancer cell line MDA-MB231 proliferation and metastasis. *Asian Pac J Cancer Prev* **15**, 5577-5582 (2014).
124. El-Nikhely, N., Larzabal, L., Seeger, W., Calvo, A. & Savai, R. Tumor-stromal interactions in lung cancer: novel candidate targets for therapeutic intervention. *Expert Opin Investig Drugs* **21**, 1107-1122 (2012).
125. Quail, D.F. & Joyce, J.A. Microenvironmental regulation of tumor progression and metastasis. *Nat Med* **19**, 1423-1437 (2013).
126. Laoui, D. *et al.* Tumor hypoxia does not drive differentiation of tumor-associated macrophages but rather fine-tunes the M2-like macrophage population. *Cancer Res* **74**, 24-30 (2014).
127. Zhong, H., May, M.J., Jimi, E. & Ghosh, S. The phosphorylation status of nuclear NF-kappa B determines its association with CBP/p300 or HDAC-1. *Mol Cell* **9**, 625-636 (2002).
128. Pacaud, R. *et al.* DNMT3L interacts with transcription factors to target DNMT3L/DNMT3B to specific DNA sequences: role of the DNMT3L/DNMT3B/p65-NFkappaB complex in the (de-)methylation of TRAF1. *Biochimie* **104**, 36-49 (2014).

11 Declaration

"I declare that I have completed this dissertation single-handedly without the unauthorized help of a second party and only with the assistance acknowledged therein. I have appropriately acknowledged and referenced all text passages that are derived literally from or are based on the content of published or unpublished work of others, and all information that relates to verbal communications. I have abided by the principles of good scientific conduct laid down in the charter of the Justus Liebig University of Giessen in carrying out the investigations described in the dissertation."

Bad Nauheim, January 2016 **Nefertiti El-Nikhely**

12 Acknowledgement

I would like to express my deep gratitude to **Prof. Ulf Rapp** and **Prof. Thomas Braun** for accepting me for the IMPRS graduate programme at the Max Planck Institute for Heart and Lung Research in Bad Nauheim. I highly appreciate their scientific dedication which will always stay an inspiration.

My PhD would not have been possible without the enormous support of **Prof. Werner Seeger** and **Dr. Rajkumar Savai**. I am deeply indebted to them and especially to **Dr. Rajkumar Savai** for accepting me in his group, for his continuous supervision, his patience and for playing an essential role in my career development. I am sincerely grateful to **Prof. Reinhard Dammann** from the Justus Liebig University for his co-supervision, his support and guidance especially at the beginning of my PhD and for his valuable suggestions.

During the period of my PhD, I encountered many treasured colleagues from whom I have learned a lot. In particular, I would like to thank **Dr. Anja Schmall** and **Dr. Alina Asafova** for their continuous support and useful discussions. The continuous interaction with my colleagues **Dr. Alexandra Tretyn, Poonam Sarode, Xiang Zheng** and **David Brunn** was a fruitful asset for my scientific development and a precious mental support. I am greatly thankful for their constant feedback and help. **Dr. Kati Turkowski** and **Dr. Hamza Al-Tamari** I would like to thank for their aid in formatting the thesis. I am greatly thankful to **Dr. Swati Dabral** for her time investment in thorough discussions, troubleshooting and revision of the thesis.

I would like to express my thanks to our collaborators, **Dr. Astrid Wietelmann** for her guidance with the MRI experiments, **Dr. Andreas Weigert** for the FACS analysis, and **Dr. Guillermo Barreto, Dr. Indrabahadur Singh** and **Julio Cordera** for their valuable support and rich scientific discussions.

Lab life wouldn't have been tolerable without **Marianne Hoeck, Yanina Knepper** and **Vanessa Golchert**. I would like to thank them for their superb technical support. **Marianne** was always there for me not only as technical support but as great mental support as well. Her work dedication is contagious. **Yanina** was of enormous help with the animal experiments, and **Vanessa** exerted excellent work with immunohistochemistry and immunofluorescence.

Acknowledgement

I would like to express my gratitude to all colleagues at the MPI for creating an encouraging work environment.

Despite the relatively huge geographic distance but my family was always there for me. To my soulmate sister and my father I am endlessly indebted for their never ending patience, inspiration, support and love.

13 Scientific Contributions

Poster Presentations

- **El-Nikhely N**, Ceteci F, Wietelmann A, Seeger W, Rapp UR, Savai R. "*The role of NFκB/IKK2 pathway in the pathogenesis of lung cancer*". IMPRS retreat, Kleinwalsertal, Austria (Poster Award), 2012
- **El-Nikhely N**, Ceteci F, Wietelmann A, Seeger W, Rapp UR, Savai R. "The role of NFκB/IKK2 pathway in the pathogenesis of lung cancer". AACR Annual Meeting, Chicago, USA, 2012

Scientific Talks

- "*MTA2: a potential p50/p65 regulator in lung cancer?*", MPI Retreat, Lohr am Main, Germany, 2014
- "*Nuclear Factor-kappa B in the pathogenesis of Non-Small Cell Lung Cancer, a link between inflammation and NSCLC*", GGL Conference, Gießen, Germany, 2012

Publications

1. Kiehl S, Herkt SC, Richter AM, Fuhrmann L, **El-Nikhely N**, Seeger W, Savai R, Dammann RH. ABCB4 is frequently epigenetically silenced in human cancers and inhibits tumor growth. Sci Rep. 2014 Nov 4;4:6899.
2. Kopp F, Hermawan A, Oak PS, Ulaganathan VK, Herrmann A, **Elnikhely N**, Thakur C, Xiao Z, Knyazev P, Ataseven B, Savai R, Wagner E, Roidl A. Sequential Salinomycin Treatment Results in Resistance Formation through Clonal Selection of Epithelial-Like Tumor Cells. Transl Oncol. 2014 Dec;7(6):702-11.
3. Zanucco E, **El-Nikhely N**, Götz R, Weidmann K, Pfeiffer V, Savai R, Seeger W, Ullrich A, Rapp UR. Elimination of B-RAF in oncogenic C-RAF-expressing alveolar epithelial type II cells reduces MAPK signal intensity and lung tumor growth. J Biol Chem. 2014 Sep 26;289(39):26804-16.
4. Larzabal L, **El-Nikhely N**, Redrado M, Seeger W, Savai R, Calvo A. Differential effects of drugs targeting cancer stem cell (CSC) and non-CSC populations on lung primary tumors and metastasis. PLoS One (2013) Nov 20;8(11):e79798.
5. Ceteci F, Ceteci S, Zanucco E, Thakur C, Becker M, **El-Nikhely N**, Fink L, Seeger W, Savai R, Rapp UR. E-cadherin controls bronchiolar progenitor cells and onset of preneoplastic lesions in mice. Neoplasia (2012) Dec;14(12):1164-77.
6. **El-Nikhely N**, Larzabal L, Seeger W, Calvo A, Savai R. Tumor-stromal interactions in lung cancer: novel candidate targets for therapeutic intervention. Expert Opin Investig Drugs (2012) Aug;21(8):1107-22.
7. Halla Thorsteinsdóttir, Christina C Melon, Monali Ray, Sharon Chakkalackal, Michelle Li, Jan E Cooper, Jennifer Chadder, Tirso W Saenz, Maria Carlota de Souza Paula, Wen Ke, Lexuan Li, Magdy A Madkour, Sahar Aly, **Nefertiti El-Nikhely**, Sachin Chaturvedi, Victor Konde, Abdallah S Daar & Peter A Singer. South-South entrepreneurial collaboration in health biotech. Nat Biotechnol (2010) May ; 28(5):407-416
8. Christina C. Melon, Monali Ray, Sharon, Chakkalackal, Michelle Li, Jan E. Cooper, Jennifer Chadder, Wen Ke, Lexuan Li, Magdy A. Madkour, Sahar Aly, **Nefertiti Adly**, Sachin Chaturvedi, Victor Konde, Abdallah S. Daar, Peter A. Singer, Halla Thorsteinsdóttir. A survey of South-North health biotech collaboration. Nat Biotechnol (2009) Mar;27(3):229-32
9. **El Nikhely, N**, Helmy, M., and Saeed, H., Abo Shamaa, L. and Abd El Rahman, Z. Ricin A chain from *Ricinus sanguienus*: DNA sequence, structure and toxicity. The Protein J (2007) Oct;26(7):481-9